PREFRONTAL CONTROL OF PREPARATORY ATTENTION AND COORDINATION WITH THE VENTRAL TEGMENTAL AREA

by

Nelson K. B. Totah

Bachelor of Science, Emory University, 2004

Submitted to the Graduate Faculty of

the Kenneth P. Dietrich School of

Arts and Sciences in partial fulfillment

of the requirements for the degree of

Doctor of Philosophy

University of Pittsburgh

2012

UNIVERSITY OF PITTSBURGH

DIETRICH SCHOOL OF ARTS AND SCIENCES

This dissertation was presented

by

Nelson K. B. Totah

It was defended on

December 14, 2011

and approved by

German Barrionuevo, M.D., Professor, Neuroscience

Bard Ermentrout, Ph.D., Professor, Mathematics, Computational Biology, and Neuroscience

Anthony A. Grace, Ph.D., Distinguished Professor, Neuroscience, Psychiatry, and Psychology

Carl R. Olson, Ph.D., Adjunct Professor, Neuroscience

Cyriel M. A. Pennartz, Ph.D., Cognitive and Systems Neuroscience, University of Amsterdam

Dissertation Advisor: Bita Moghaddam, Ph.D., Neuroscience and Psychiatry

PREFRONTAL CONTROL OF PREPARATORY ATTENTION AND COORDINATION WITH THE VENTRAL TEGMENTAL AREA

Nelson K. B. Totah, PhD

University of Pittsburgh, 2012

Preparatory attention selects upcoming stimuli that will be used to guide behavior. This cognitive faculty is controlled by the prefrontal cortex (PFC), which primes sensory cortex neurons that represent the stimulus. Lesion studies have implicated multiple PFC regions in the control of attention, including the rat prelimbic cortex (PL) and anterior cingulate cortex (ACC). The first aim of this dissertation was to characterize and compare neural activity in these regions during a preparatory attention task. The second aim was to assess interactions between these regions during preparatory attention. Coordinated activity between the PL and ACC was studied by measuring spike synchrony with local field potential (LFP) oscillations. The third aim was to study neural activity in the ventral tegmental area (VTA), which provides dopamine projections to the PFC that are known to modulate PFC control of attention. The nature of VTA neural activity during attention and its coordination with the PFC has not been characterized.

In order to study PFC and VTA neural activity during preparatory attention, we recorded single unit spiking and LFP and primarily focused analysis on the pre-stimulus period, when a preparatory attention control signal is generated by PFC neurons. The rat was trained to orient to a wall of three stimulus ports, expect a brief illumination at one of the ports, and make a response into the illuminated port. While the timing of stimulus onset was predictable, the location varied randomly. These task characteristics resulted in error trials in which the rat responded to an incorrect port. The analyses of pre-stimulus neural activity compared correct and error trials.

We observed a sustained change in PFC single unit firing rate during the pre-stimulus period. The sustained firing patterns were predictive of attentional accuracy, in that the sustained activity was reduced during error trials. Furthermore, we demonstrated that the PL and ACC interacted during preparatory attention. We also observed sustained activity in the VTA, which may stabilize sustained PFC activity during preparatory attention. VTA spiking correlated with ACC gamma (40 Hz) oscillations, which may be used to communicate the attention control signal from the PFC to sensory cortex.

TABLE OF CONTENTS

LIST OF TABLES

LIST OF FIGURES

1.0 INTRODUCTION

Successful stimulus-guided behavior requires that relevant stimuli be selected, while irrelevant stimuli are ignored. This ability to select relevant stimuli is called top-down attention. The term "top-down" describes using motivations and goals to selectively enhance communication of relevant stimuli through the sensory cortical hierarchy (Desimone and Duncan, 1995). Top-down attention can select a stimulus by affecting its sensory cortex representation with regard to location in space, location within an object, presence of a feature (e.g., color or shape), presence of an entire object, and moment in time (Schroeder et al., 2001; Olson, 2001; Nobre, 2001).

Top-down attention can also select a stimulus by affecting its representation in sensory cortices prior to the actual onset of the stimulus, which enhances perception and speed of stimulus-guided behavior upon stimulus onset (LaBerge, 1995; Driver and Frith, 2000). This instantiation of top-down attention, which has been termed "expectation" or "preparatory attention" has received comparably less neurophysiological study than the aforementioned forms. Borrowing an example conceived by LaBerge (1995), when a person driving a car expects to see a green light, the location of the green light and the color green become primed in visual cortical areas representing location and color, respectively. This preparation occurs on the order of seconds before the stimulus whereas, upon the onset of the green light, a much faster (~ 0.05 to 0.50 sec) attentional process selectively identifies the green light from the rest of the visual

scene by further enhancing its representation in the same visual cortical areas. The focus of this dissertation, however, is not on how attention affects the sensory cortices, but rather on how preparatory attention is generated and controlled using goals. The experiments contained within this dissertation use recordings of neural activity during preparatory attention to investigate the neurophysiological mechanisms that the brain may use to select a stimulus in pursuit of a goal.

1.1 THE PREFRONTAL CORTEX REPRESENTS EXPECTANCY OF BEHAVIORALLY RELEVANT STIMULI

A large body of evidence employing diverse methods has converged on the idea that top-down attention is controlled by a network of prefrontal cortex (PFC) areas, including the dorsolateral PFC and anterior cingulate cortex (ACC) in the monkey and the prelimbic cortex (PL) and ACC in the rat. Lesions or transient inactivation of PFC networks impair top-down attention and increase distractibility across a variety of behavioral tasks (Mesulam, 1981; Woods and Knight, 1986; Posner and Petersen, 1990; Rossi et al., 2007), including the task used in this dissertation (Passetti et al., 2002; Muir et al., 1996; Chudasama et al., 2003). PFC networks are also co-activated with sensory cortical areas during preparatory attention (Stokes et al., 2009; Sylvester et al., 2009; Kastner et al., 1999).

PFC networks could control preparatory attention because PFC neurons respond to the occurrence of stimuli that are relevant to goal-directed behavior and respond during expectancy of relevant stimuli. For instance, a phasic increase in firing rate can be recorded from PFC neurons upon the onset of a behaviorally relevant stimulus, and if the goal changes neurons will represent the newly relevant stimulus (Freedman et al., 2001; Rainer et al., 1998; Everling et al.,

2006). These studies support an influential theory of PFC function, which holds that single neurons throughout PFC networks respond to any stimuli that are behaviorally relevant and have the ability to use information about context, rules, and goals to select and filter relevant stimuli (Duncan, 2001). PFC neurons also respond during expectancy of behaviorally relevant stimuli (Pragay et al., 1987; Johnston et al., 2007; Niki and Watanabe, 1979; Rainer et al., 1999). Two of these studies are critical because they extended the duration of the pre-stimulus period (Pragay et al., 1987; Niki and Watanabe, 1979). When the pre-stimulus period was extended by 1 and 2 sec longer than that with which the animals had been trained, the pre-stimulus increase in firing rate continued until stimulus appearance. Furthermore, non-task related neurons became responsive during expectancy, and the longer pre-stimulus period correlated with faster reaction time and fewer behavioral errors. The authors refer to the pre-stimulus change as "orienting" of attention (Niki and Watanabe, 1979) and "directing attention in time" (Pragay et al., 1987), because the neurons responded in expectancy of a behaviorally relevant stimulus and neural activity reflected behavioral performance. This preparatory increase of firing rate has also been demonstrated in the premotor cortex, but the activity continued to follow the original temporal structure of the task after a variable duration pre-stimulus period was introduced (Mauritz and Wise, 1986). In summary, while a limited number of electrophysiology recording studies have implicated PFC networks in expectancy of behaviorally relevant stimuli, these studies do not explicitly test the idea that PFC networks control preparatory attentional selection of a stimulus.

1.2 THE NEUROPHYSIOLOGICAL BASIS OF CONTROLLING PREPARATORY ATTENTION

Few studies have recorded in the PFC during preparatory attention, but recordings in sensory cortex have demonstrated that neurons will increase firing rate during the pre-stimulus period (Luck et al., 1997; Chelazzi et al., 1993; Ghose and Maunsell, 2002). This pre-stimulus increase is thought to occur because PFC networks drive the firing of sensory neurons that represent the stimulus (Desimone and Duncan, 1995; Reynolds and Heeger, 2009). Support for this hypothesis was provided by simultaneously recording PFC and sensory cortex neurons during an attention task (Gregoriou et al., 2009). This study did not examine preparatory attention, but is important because it supports the top-down bias hypothesis that can be used to explain the neurophysiological control of preparatory attention. Gregoriou and colleagues recorded from a part of the PFC called the frontal eye field (FEF) and sensory cortex area V4 during a cued covert spatial attention task. PFC neurons and V4 neurons had overlapping receptive fields, which allowed a within-neuron comparison to be made between trials in which attention was inside or outside of the shared receptive field. The authors demonstrated that the firing rate of both PFC and V4 neurons was enhanced during attention and that the changes in PFC preceded those in V4. PFC population neural activity (measured by local field potential) led V4 with a delay that was consistent with the conduction time of the monosynaptic connection between the regions. Finally, Granger causality analysis, a statistical measure of directional causation, demonstrated that the PFC influenced V4 population neural activity just after the PFC single neurons became activated. The work by Gregoriou and colleagues provides strong evidence that the FEF produces an attentional bias signal that influences activity in the V4 via a monosynaptic connection.

During preparatory attention, pre-stimulus drive from PFC networks could influence sensory neurons by depolarizing them so that NMDA receptors become activated and the latency to encode a stimulus after its onset is reduced (Chawla et al., 2000; Schroeder et al., 2001). Additionally, preparatory attention could enhance perception by increasing effective connectivity between PFC networks and sensory cortical regions. Morishima and colleagues used trans-cranial magnetic stimulation (TMS) of the human frontal eye field to assess neuronal impulse transmission efficiency (Morishima et al., 2009). They measured the effects of a single TMS impulse on posterior cortical EEG activity evoked by a visual stimulus. When subjects were given a large time period to expect if the target stimulus would be motion or a face, the TMS pulse was reflected in sensory cortex area MT or fusiform face area, respectively. However, if subjects were not given time to expect the stimulus, then the effects of top-down control were not localized to particular regions of sensory cortex. Therefore, preparatory attention may enhance functional connectivity directed to sensory neurons that will represent the behaviorally relevant stimulus. In another experiment, stimulating the PFC using TMS of greater intensity impaired attention and attentional modulation of stimulus-evoked EEG potentials (Zanto et al., 2011). Critically, the degree of impairment was correlated with the subjects' degree of functional connectivity between the PFC and visual area V5.

The layers and long-range connectivity of the cortex are organized in a manner that would allow for the transmission of top-down signals carrying information about behavioral relevance and expectations (Mumford, 1992; Felleman and Van Essen, 1991; Mountcastle, 1997). The granular layer 4 contains excitatory stellate cells, which receive afferents from the thalamus and can be thought of as distributing information locally to other cells in the column. Pyramidal neurons are in 2 groups: the supragranular layers (2/3) and the infragranular layers

(5/6) and project beyond their column to other cortical regions. Finally, layer 1 contains dendrites of pyramidal neurons and some types of interneurons. In general, there is a tendency for higher-level cortical regions (i.e., PFC) to project from layer 5 pyramidal neurons to layers 1 and 6 in lower cortical regions (i.e., sensory cortex). In accordance with the anatomical connectivity data, neurophysiological experiments have demonstrated that top-down attention modulates neural activity primarily in sensory cortex supragranular layers (Mehta et al., 2000b) and that the modulation gradually propagates down to lower cortical areas (Mehta et al., 2000a; Buffalo et al., 2010). Preparatory attention could modulate supragranular sensory cortex neurons by activating PFC pyramidal neurons, which project directly to other cortical regions; notably, PFC pyramidal neurons increase firing rate in expectation of a behaviorally relevant stimulus, whereas local inhibitory interneurons do not (Hussar and Pasternak, 2009).

1.3 SYNCHRONY AND COMMUNICATION OF A PREPARATORY ATTENTION SIGNAL

Communication of a top-down signal from PFC pyramidal neurons may rely on phase synchrony and/or coherence of neuronal oscillations (Varela et al., 2001; Fries, 2005). Fries and colleagues have proposed that rhythmic gamma (30 – 80 Hz) oscillations in neuronal membrane potentials serve two important roles in affecting communication (Fries, 2005). First, by synchronizing groups of neurons (i.e., ensembles), the effectiveness of spike output is enhanced. Second, by synchronizing oscillations between ensembles, the sending neurons transmit spikes during time windows of receiving neurons' increased sensitivity to spike input. Increased gamma oscillation power and phase synchrony are observed in PFC networks during attention, which suggest that

gamma synchrony could be used to communicate preparatory attention signals to sensory cortices (Gruber et al., 1999; Gregoriou et al., 2009; Siegel et al., 2008).

I will briefly review the neurophysiological mechanism by which gamma synchrony may enhance communication between ensembles. The first idea is that gamma oscillations could organize local neurons into an ensemble with each member firing synchronously and thus having a greater impact on the post-synaptic potential (PSP) of the neurons' shared target. A post-synaptic neuron's action potential threshold was shown to decrease with increasing slope of its PSP during the 250 msec before the action potential, which suggests that spikes sent at the same time will have a greater effect on PSP (Azouz and Gray, 2000). Recordings in the awake, behaving rat PFC used cross-correlation of spiking to identify monosynaptically connected networks of pyramidal neurons and demonstrated that the effects of synchronous (< 5 msec apart) spikes had a supralinear effect on the probability that the post-synaptic neuron would spike (Fujisawa et al., 2008). Thus, via multiple neurons sending spikes with high temporal coincidence, a greater impact is made on the target neuron's PSP and firing rate.

Gamma oscillations synchronize a group of neurons into an ensemble by a process of enslavement (Whittington et al., 2000). Excitatory drive to a network of excitatory pyramidal neurons and inhibitory interneurons causes pyramidal neurons to fire irregularly and drives interneurons. A single interneuron may simultaneously inhibit many other interneurons, which will spike synchronously as a population, once the inhibition wears off. The interneuron population firing then inhibits the pyramidal neurons that will join as an ensemble. The most strongly driven pyramidal neuron will reach spike threshold first and drive the population of synchronized interneurons to start the next cycle. Therefore, many pyramidal neurons are only able to fire synchronously between windows of population inhibition (Whittington et al., 2000;

Börgers and Kopell, 2005). Through this process, the strong input to a pyramidal neuron initiates when the gamma oscillations will begin, while the interneurons produce the synchronized gamma cycles.

While neuron spiking as an ensemble would increase neuronal output, gamma oscillations also provide a means for enhancing target neurons' sensitivity to afferent input. Synchrony between the oscillations to which two ensembles are entrained enhances the sensitivity of the receiving group because oscillations provide predictable windows in which post-synaptic voltage-gated channels (i.e., NMDA receptors) are in an open state. If the phase of oscillations between the sending and receiving ensembles are synchronized by a phase offset equivalent to the monosynaptic conduction time, the spikes representing a top-down attention signal would arrive during windows of enhanced effectiveness on the PSP (Fries, 2005). A related hypothesis, with experimental and computational support, is that multiple bits of information could be selected or segregated by spiking at different phases of an oscillation (Tiesinga et al., 2008; Siegel et al., 2009; Buzsaki and Chrobak, 1995; Montemurro et al., 2008; O'Keefe and Recce, 1993). In this scenario, sensory stimuli selected by attention may be associated with neuronal firing at a specific phase of a gamma oscillation, whereas spiking related to unselected irrelevant stimuli could occur at other phases (Tiesinga et al., 2008). In summary, synchrony—by increasing the effectiveness of PFC output and the sensory neuron sensitivity to input—may allow PFC neurons to selectively drive sensory neurons in expectancy of a behaviorally relevant stimulus.

1.4 DOPAMINE NEUROTRANSMISSION MODULATES THE CONTROL OF PREPARATORY ATTENTION

It is generally assumed that the neuromodulator, dopamine, regulates the control of top-down attention. For instance, drugs that increase the amount of extra-synaptic dopamine in the PFC are effective in treating attention deficit disorders (Arnsten, 2011a; Nieoullon, 2002; Swanson et al., 2010) and enhance attentional accuracy in laboratory animals (Berridge et al., 2006). On the other hand, reducing dopamine neurotransmission in the PFC by blocking post-synaptic receptors with antagonists (Granon et al., 2000) or by selectively removing dopamine-containing terminals (Crofts et al., 2001) impairs top-down attention. However, the manner in which dopamine neurotransmission affects PFC control of attention is not well understood (Noudoost and Moore, 2011b). Additionally, the spiking activity of dopamine neurons during top-down attention is not characterized. Therefore, the studies contained in this dissertation attempt to characterize dopamine neuron activity and its effects on PFC network neural activity during preparatory attention.

The ventral tegmental area (VTA) in the midbrain contains neurons which use dopamine as their primary neurotransmitter and project to targets including PFC networks, the nucleus accumbens, lateral hypothalamus, and the amygdala (Sesack, 2002; Sesack et al., 2003). The projections of (non-local) VTA neurons are targeted to a single area such that neurons projecting to PFC networks do not project to the nucleus accumbens (Sesack et al., 2003; Fields et al., 2007). This segregation of projections is in line with finding that the attention enhancing effects of methylphenidate are due to increasing extra-synaptic dopamine in PFC networks and not in the nucleus accumbens (Berridge et al., 2006), which has been primarily associated with reward, reinforcement-related events, and learning (Fields et al., 2007; Schultz, 1998; 2007). Medial

VTA dopamine neurons project to PFC networks and target infragranular layers 5 and 6 (Berger et al., 1976; Descarries et al., 1987; Lindvall et al., 1978), thus allowing dopamine to modulate the neurons that communicate top-down signals to the sensory cortices (**Section 1.2**).

Dopamine neurotransmission in the PFC could affect cortical ensemble formation (O'Donnell, 2003), which is a critical component of communicating top-down attention signals (**Section 1.4**). Dopamine in the PFC may also stabilize recurrent activity (Williams and Goldman-Rakic, 1995; Durstewitz et al., 2000; Bandyopadhyay et al., 2005), which has been observed during expectancy of behaviorally relevant stimuli (Niki and Watanabe, 1979; Pragay et al., 1987). The neurophysiological mechanisms by which dopamine could affect ensemble formation or recurrent activity could involve modulating post-synaptic membrane conductance to reduce the effects of afferent input (Seamans and Yang, 2004), synchronizing membrane potential up states across a population of neurons (Peters et al., 2004), and modulating local inhibitory interneuron spike timing in response to excitatory afferent drive (Tierney et al., 2008). In summary, VTA dopamine neurons may provide a neuromodulatory effect that supports ensemble formation in the deep PFC layers that communicate top-down signals.

1.5 PURPOSE OF DISSERTATION

PFC networks are implicated in preparatory attention and the communication of a top-down attention signal. By examining the oscillatory frequencies and times of synchrony associated with preparatory attention, an understanding of ensemble formation across members of the PFC network can be gained. Finally, it is important to understand how dopamine may affect control preparatory attention by PFC networks.

The purpose of this dissertation was, first, to develop and characterize a preparatory attention task that was suitable for recording neural activity in the behaving rat (**Section 2**). Neural activity was recorded simultaneously in the PL and ACC. We assessed changes in firing rate during preparatory attention and related those changes to attentional accuracy (**Section 2**). The neural activity was compared between PFC areas for participation in detection of behavioral errors and expectancy of reward. Given that these PFC areas could control specific aspects of attention or work as a network, we studied how neurons interact across the entire network using oscillatory synchrony (**Section 3**). We also assessed network activity in relation to stimulus-guided behavior.

We recorded VTA neurons in order to characterize their activity during preparatory attention and its relation to attentional accuracy (**Section 4**). We recorded the ACC and the VTA simultaneously to examine how VTA neuronal firing was correlated with ACC neural activity. The goal of this work was to elucidate how the VTA might affect ensemble formation and oscillations in the ACC that are involved with communication of a top-down attention signal (**Section 4**). We not only characterized VTA-ACC network activity during preparatory attention but also during stimulus-guided behavior.

2.0 ANTERIOR CINGULATE CORTEX NEURONS REPRESENT PREPARATORY ATTENTION AND ERROR DETECTION WITHIN THE SAME BEHAVIORAL SEQUENCE

2.1 ABSTRACT

The anterior cingulate cortex (ACC) has been implicated in both preparatory attention (i.e., selecting behaviorally relevant stimuli) and in detecting errors. We recorded from the rat ACC and prelimbic cortex (PL), which is functionally homologous with the primate dorsolateral PFC, during an attention task. The 3-choice serial reaction time task requires a rat to orient toward and divide attention between 3 brief (300 msec duration) light stimuli presented in random order across nose poke holes in an operant chamber. In both the ACC and PL, we found that neural activity was related to the level of preparatory (pre-stimulus) attention and subsequent correct or incorrect choice, in that the magnitude of the single units' response to the stimulus was lower on incorrect trials and was not different from baseline on unattended trials. This preparatory neural activity consisted of both excitatory and inhibitory phasic responses. The number of units responding to the stimulus was similarly graded, in that fewer units exhibited phasic responses to the stimulus on incorrect and unattended trials, compared to correct trials. Although preparatory activity was found in both the ACC and PL, activity after incorrect nose pokes, which may be related to error detection, were only observed in the ACC. Thus, during the same behavioral

sequence, the ACC encodes both error-related events and preparatory attention, whereas the PL only participates in preparatory attention. The finding of substantial inhibitory activity during the preparatory period suggests a critical role for inhibition of pyramidal cells in PFC-mediated cognitive functions.

2.2 INTRODUCTION

Proper goal directed behavior requires that an organism internalizes behaviorally relevant stimuli, brings appropriate stimulus-response rules online, and monitors outcomes to adjust behavior accordingly. Preparatory attention or the selection of task-relevant stimuli is critical for the execution of proper goal-directed behavior. The dorsolateral prefrontal cortices (DLPFC) and the anterior cingulate cortex (ACC) have both been implicated in preparatory attention (Botvinick et al., 2004; Miller and Cohen, 2001). Views on the role of the ACC, however, differ. A leading theory suggests this region detects errors and then signals the DLPFC to adjust the level of preparatory attention (Botvinick et al., 2004). This view holds that ACC neurons should selectively respond to instances of error detection, which potentially represent a negative reward prediction error signal (Nieuwenhuis et al., 2004) or uncertainty, but ACC neurons should not necessarily respond during preparatory attention to upcoming goal-relevant stimuli. Another theory suggests that the ACC is involved in preparatory attention (Posner and Petersen, 1990; Roelofs et al., 2006; Weissman et al., 2005). This is supported by the observation of attentional impairments after lesions of the rat ACC (Chudasama et al., 2003; Ng et al., 2007; Passetti et al., 2002) and by primate single unit recordings demonstrating excitatory phasic activity during pre-stimulus periods (Johnston et al., 2007; Roelofs et al., 2006; Shidara and Richmond, 2002).

To elucidate the neurophysiological and anatomical basis of preparatory attention we conducted single unit recordings in the rat ACC and prelimbic cortex (PL) during an attention task. The rat PL and ACC may be functionally analogous to the human and primate DLPFC and ACC, respectively, although this homology is largely based on functionality (Uylings et al., 2003). During the task rats were required to wait on a brief stimulus and then respond quickly. Stimulus and response conflict were not employed; thus, we assumed that pre-stimulus neuronal activity reflected preparatory attention to select the upcoming stimuli, rather than conflict resolution. Another feature of the task was that the rat had the opportunity to make incorrect response choices. Thus, we could test if detection of errors and upcoming goal-relevant stimuli during a single trial are represented differently in the ACC versus the PL.

We found that error-related phasic responses were selective for the ACC whereas both regions exhibited preparatory activity. This suggests a dual role for the ACC; in addition to signaling error-related events, it is involved in selection of goal-relevant stimuli along with the PL. In addition, the preparatory phasic responses were both inhibitory and excitatory suggesting that different afferent regulation of putative PFC pyramidal neurons is important for preparatory attention. The inhibition of PFC pyramidal units during attention may be due to excitation of PFC interneurons via thalamic inputs (Rotaru et al., 2005).

2.3 METHODS

2.3.1 SUBJECTS AND BEHAVIORAL METHODS

Male Sprague-Dawley rats were used. Twenty-four rats were used for the task characterization experiments and 10 were used for the electrophysiology experiments. All rats were housed on a reverse light cycle and trained and tested in dark red light during the rats' active phase (0700 to 1400 hours). Both task characterization and recording studies used 2 different cohorts of rats for each study. All experiments were carried out in compliance with the University of Pittsburgh Institutional Care and Use Committee (IACUC).

The task is based on the 5-choice serial reaction time task (Carli et al., 1983), except that 3 choice operant chambers were used to accommodate the existing behavioral electrophysiology setup. Experiments were carried out in operant chambers with a house light on the ceiling, 3 stimulus holes with internal LED lights on one wall, and an illuminated food magazine on the wall opposite the stimulus holes. Nose pokes into the stimulus holes and food magazine were registered by photosensors. Training began after 1 wk of handling and chamber habituation. A correct response, consisting of a nose-poke into a lit stimulus, was rewarded with 2 sucrose pellets. Incorrect responses into an unlit stimulus or not responding within 5 sec after stimulus presentation (an omission) were punished with a house-light off "time out." The rat initiated the next trial with a poke into the empty food magazine; thus allowing the rat to reduce the duration of the timeout. An 8 sec intertrial interval (ITI) passed before the next stimulus presentation. Premature responses during the ITI were repeatedly punished with 5 sec time-outs before restarting the ITI.

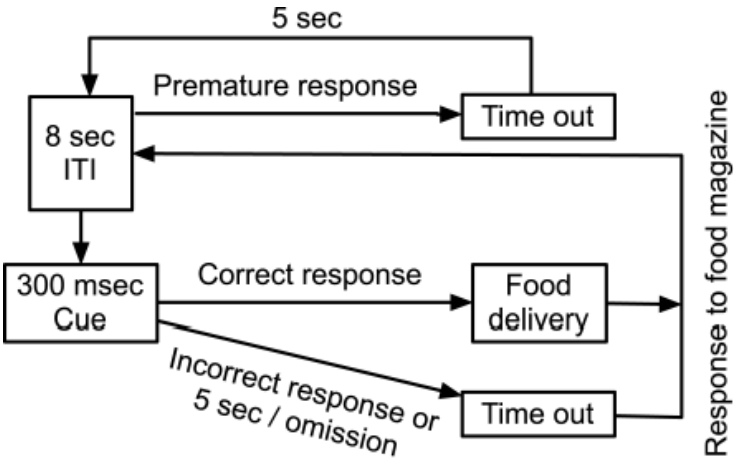

Figure 2.1. The 3-choice serial reaction time task.

A recording session lasted 30 min. After an 8 sec inter-trial interval (ITI), one of three stimulus locations was randomly illuminated for 300 msec. If the rat made a premature stimulus hole nose poke prior to stimulus illumination, the house light was extinguished for 5 sec and then a new trial was started. The rat had 5 sec to respond into one of the stimulus holes. A correct response led to reward delivery into the food magazine on the wall opposite from the stimulus holes. An incorrect response or omission of response led to house light extinguishment. After an error, a new trial was begun and the house light was illuminated again after the rat nose poked into the empty food magazine.

See **Figure 2.1** for the task layout. Rats were trained in 6 successive "levels" which used reduced stimulus durations at each level (15 sec, 5 sec, 2 sec, 1 sec, 500 msec, and 300 msec). Each individual rat progressed through training levels after meeting performance criterion. The first 4 training levels used the following criterion: > 80% accuracy and < 20% omissions for 3 consecutive sessions. At the 500 msec level, rats had to perform at > 75% accuracy for 6 consecutive sessions and < 20% omissions. Rats were deemed ready for testing (or surgical implantation) at the 300 msec level once they met performance criterion of > 70% accuracy and < 20% omissions for 6 consecutive sessions. Sessions consisted of either 30 min or 150 rewards, whichever occurred first. At the 300 msec stimulus duration the session lasted 30 min regardless of reward obtained. Percent accuracy [100*(# of correct responses / # of total responses)] was

taken as the measure of attentional performance. Rats exhibited attentive behavior, whereby they oriented to the stimulus and waited for the signal; it was extremely rare (approximately <1 % of trials across many 30 min sessions) for rats to orient away from the stimulus once they had begun orienting to them.

2.3.2 ELECTROPHYSIOLOGY PROCEDURE

Upon completion of training, rats (n=10) were implanted under isoflurane anesthesia with 2 microelectrode arrays each consisting of 8 Teflon-insulated stainless steel wires in a 2-by-4 pattern measuring 0.25 mm by 0.70 mm with an impedance of 300 – 700 kΩ (NB Labs, Denison, TX). One array was placed spanning the ACC: –0.2 to –1.0 mm anterior to bregma, –0.4 to –0.7 mm lateral to bregma, and –2.5 mm ventral from the dura surface and one array was placed spanning the contralateral PL (prelimbic cortex): +2.4 to +3.4 mm anterior to bregma, +0.5 to +0.8 mm lateral to bregma, and –3.8 mm ventral from the dura surface.

After 1 week of recovery, rats were acclimated to attachment of the electrode cable in the operant box over 4 days. Single units were recorded via a unity-gain field effect transistor headstage and lightweight cabling which passed through a commutator to allow freedom of movement. Single units were amplified using a 1000X gain and 300 – 8,000 Hz band pass filter and were digitized at a rate of 40 kHz. Recorder software (Plexon, Inc.) was used to record waveforms crossing a channel-specific voltage threshold and signals from the operant box were used as event markers to coordinate behavioral events with the signal from the microelectrode array. Units were isolated in Off-Line Sorter software (Plexon, Inc.) using a 3-dimensional space generated from the first 3 principle components of the data, as well as 2-dimensional spaces generated from peak and valley amplitudes. Stability of units over time was confirmed by

viewing the waveform clusters in a 3-dimensional space of the first 2 principle components and time. Units were rejected if the interspike interval histogram was inconsistent with a refractory period of <1.1 msec. In general, 2 – 3 units were clearly isolated per electrode. In 10 rats, the mean number of units recorded in the ACC was 10.6 and the range was 20. In the PL, the mean number of units recorded was 15.3 and the range was 25.

Neural activity was recorded during three 30 min sessions using the 300 msec stimulus duration and the session with the best behavioral performance was chosen for analysis. An 8 sec ITI was used in the recording sessions to provide sufficient time for the rat to retrieve reward from the food magazine, initiate the next trial, and turn to orient to the stimulus. Sessions were video taped and reviewed in order to eliminate trials on which the rat faced a side wall because those were not stereotypical task behaviors (see **Table 2.1** for frequency of these trials). Video analysis also demonstrated that grooming occurred rarely and thus did not affect single unit activity (see **Table 2.1**). Review of task performance on video was used to select omission trials during which the rat was oriented away from the stimulus and not behaviorally engaged in waiting for the brief stimulus illumination.

Table 2.1. Timing and occurrence of critical behavioral events.

Times and latencies in sec. All data presented as mean and standard error.

Timing and Occurance of Critical Behavioral Events	
Time of orientation to the cues*	2.30±0.09 sec
Cue presentation to cue hole nose poke latency (correct trials)	0.65±0.03 sec
Cue presentation to cue hole nose poke latency (incorrect trials)	1.39±0.08 sec
Cue hole nose poke to food magazine nose poke latency (reward)	2.20±0.03 sec
Cue hole nose poke to food magazine nose poke latency (error)	3.87±0.20 sec
Number of trials with grooming during pre-cue period	1.80±0.70
Number of correct trials not stereotypically oriented to the cue	4.60±1.66
Number of incorrect trials not stereotypically oriented to the cue	3.30±1.07
Number of error trials ended automatically (i.e., not by food magazine nose poke)	1.10±0.35

2.3.3 ELECTROPHYSIOLOGICAL DATA ANALYSIS

Peri-event firing rate time histograms (PETH) were used to analyze neuronal responses to behavioral events (stimulus onsets; correct, incorrect, and premature stimulus hole nose pokes; and food magazine nose pokes). Neural activity was analyzed in peri-event windows with the behavioral event of interest at time = 0. Windows were chosen that correlated with the behavior of interest. A -1 to +1 sec window was used for analysis of all behavioral events, except the pre-stimulus window, which was -4 to 0 sec in relation to stimulus onset. The larger pre-stimulus window was chosen because, on average, the rats began facing the stimulus and remained in an oriented posture starting 6 sec prior to stimulus onset. Details of orientation times are provided in **Table 2.1**. Pre-stimulus neural activity was compared between the 3 trials types, determined by the subsequent stimulus hole nose poke response (or lack of nose poke response) following the stimulus onset. Phasic changes in firing rate were measured by calculating a z-score using the firing rate during -6 to -4 sec before stimulus onset; the baseline was calculated on a cell-by-cell basis.

Analysis of electrophysiological data was carried out in Matlab. The z-score was calculated from an approximate Poisson distribution of the expected firing rate, where Z = ((observed # of spikes per bin) – (expected # of spikes)) / (√expected # of spikes) and the expected # of spikes = ((total # of spikes during baseline time period) / (baseline time duration)) * (time bin size). A z-score $\geq$ 2.36 for x consecutive time bins was used to determine a unit's significant ($p < 0.01$) phasic response to a behavioral event. For correct, incorrect, and premature stimulus hole nose poke events and for food magazine nose pokes, $x = 4$ and a 50 msec time bin was used for analysis in small peri-event time windows. For pre-stimulus activity, $x = 3$ and a 200 msec bin was used; the larger bin size was used to reduce variability over the larger peri-

event time window. Population activity was constructed by averaging the firing rate of all significantly responding units. A two-way repeated measures ANOVA was performed with time (repeated measure) and trial type or brain region as main factors to assess differences in population activity.

2.3.4 HISTOLOGY

At the completion of recordings, rats were anesthetized with chloral hydrate, a 30uA current was passed through the recording array for 10 seconds, and the rats were perfused with normal saline for 10 min and 10% buffered formalin for 10 min. After fixation, brains were sectioned and stained using cresyl violet. Placement of electrode tips was confirmed under a light microscope and single units recorded from improperly placed electrodes were excluded from analysis (**Figure 2.2**).

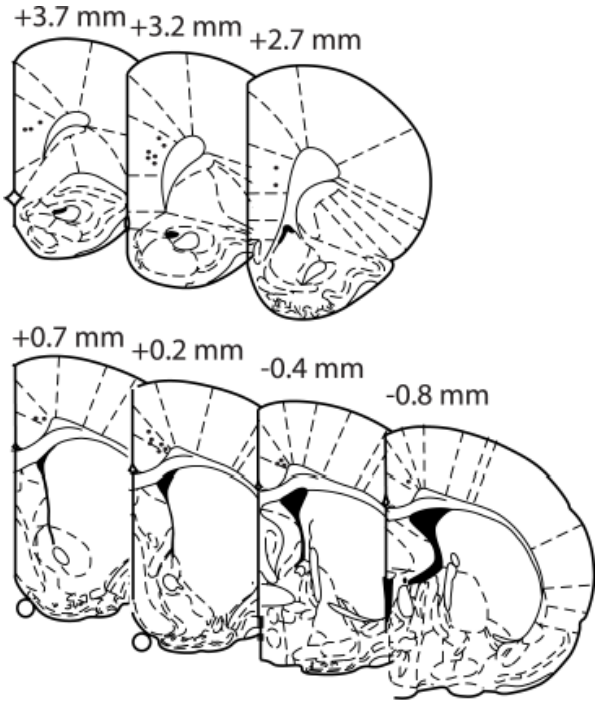

Figure 2.2. Electrode placements in the PL and the ACC.

Tissue was stained with cresyl violet and the placement of electrode tips were visualized from electrode tracks and electrolytic lesion markings.

2.4 RESULTS

2.4.1 PREPARATORY ATTENTION TASK ACQUISITION AND PERFORMANCE

For the task characterization study (N=48 from 2 equally sized cohorts), 96% of rats reached criterion performance at the testing level (300 msec stimulus duration) after approximately 41 training sessions. Accuracy was reduced as stimulus duration decreased and, at the 300 msec stimulus duration, accuracy reached 78.8±0.6% (**Figure 2.3**). Furthermore, all behavioral measures (only accuracy shown) remain stable after training ($p>0.05$), which indicates that the task is well learned. Omissions reached 5.9±0.5% and the number of premature responses reached 16.5±1.6. Performance at each task level was calculated from the last 3 sessions of each stimulus duration level. Similar levels of performance were observed during the electrophysiology recording sessions (**Figure 2.4**), with slight decreases in performance being due to behaving with a recording cable attached.

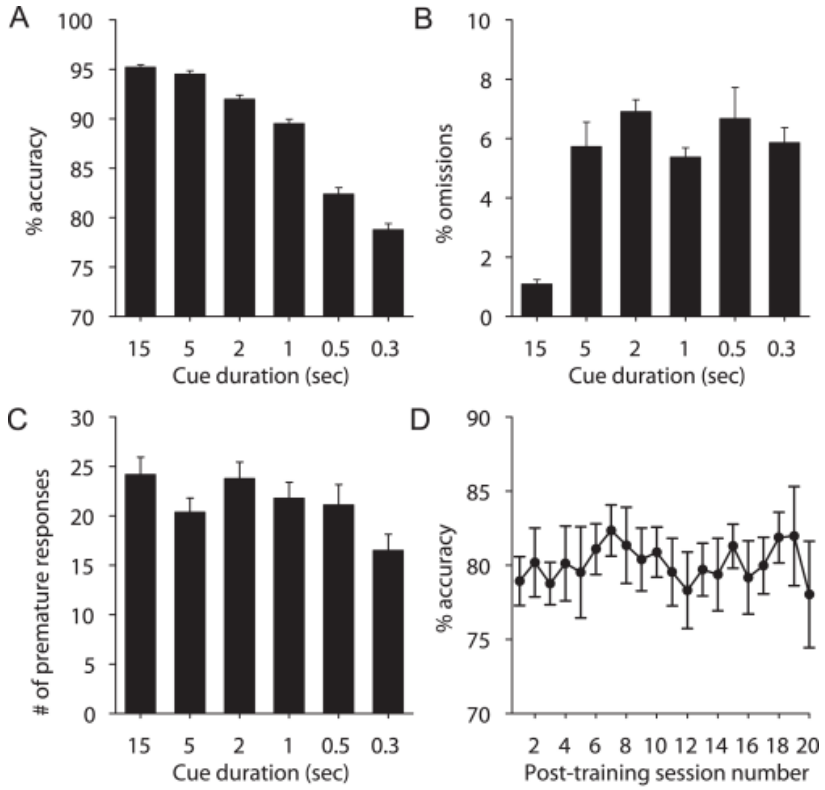

Figure 2.3. Behavioral task characterization.

Rats were trained in the task using an initial stimulus duration of 15 sec. Stimulus duration was shortened at each training level until the rat met performance criterion using a 300 msec stimulus duration. Performance criterion were used to move the rat to the next level (see methods). For figures A, B, and C, the mean and standard error were calculated from the final 3 sessions of each training level. (A) Percent accuracy, the measure of attention, at each training level. Accuracy decreased with shortening stimulus duration. (B) Percent omissions at each training level. (C) The number of premature responses at each training level. (D) Accuracy for 20 sessions (300 msec stimulus duration) after rats met performance criterion at the 300 msec stimulus duration.

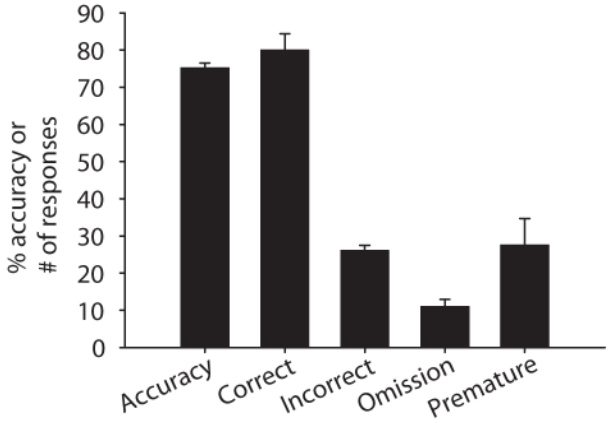

Figure 2.4. Behavioral task performance for the 10 rats used for electrophysiology.
Accuracy refers to the % accuracy and correct, incorrect, omission, and premature refer to the number of responses for each trial type.

2.4.2 PRE-STIMULUS NEURAL ACTIVITY IS RELATED TO PREPARATORY ATTENTION

A total of 106 units in the ACC and 153 units in the PL were recorded from 10 animals. Significant excitatory or inhibitory phasic changes in firing rate were observed prior to the stimulus. These responses were divided into 3 groups depending on whether a correct response, an incorrect response, or an omission of response followed.

Stimulus related phasic responses were observed on correct and incorrect trials, but the response magnitude was reduced on incorrect trials. **Figure 2.5** shows example peri-event time histograms of single units with significant pre-stimulus responses on correct trials and the activity of the *same* unit on incorrect and omission trials. Although stimulus-related responses were observed in both the ACC and PL, more units in the ACC were responsive to the stimulus. In the ACC, 27 (25.4%) out of the total number of recorded units were stimulus responsive on correct trials, whereas in PL cortex only 19 (12.4%) were stimulus responsive on correct trials (**Figure 2.5B, E**). In both brain regions, the number of stimulus responsive units was different

depending on response outcome, with fewer units phasically responding with excitation or inhibition before the stimulus on incorrect and omission trials. **Table 2.2** lists the number and percentage of units that responded during the pre-stimulus period on each trial type. Notably, inhibitory phasic responses to the stimulus were observed mostly on trials where a subsequent correct response was made, whereas fewer inhibitory responses were observed on incorrect and omission trials.

Table 2.2. The number of units that responded to each behavioral event.

The percentage out of the total number of units recorded is given in parentheses. The total number of units is listed in the brain region heading.

	Responsive units in ACC (n=106)		Responsive units in mPFC (n=153)	
	Increase	Decrease	Increase	Decrease
Pre-cue period				
Correct trials	16 (15.1%)	11 (10.3%)	8 (5.2%)	11 (7.2%)
Incorrect trials	5 (4.7%)	5 (4.7%)	2 (1.3%)	2 (1.3%)
Omission trials	3 (2.8%)	3 (2.8%)	2 (1.3%)	2 (1.3%)
Cue hole nose poke				
Correct trials	7 (6.6%)	6 (5.7%)	9 (5.9%)	6 (3.9%)
Incorrect trials	3 (3.0%)	1 (0.9%)	7 (4.6%)	0 (0%)
Premature Trials	6 (5.7%)	0 (0%)	6 (3.9%)	0 (0%)
Food magazine nose poke				
Food Consumption	13 (12.3%)	12 (11.3%)	14 (9.2%)	6 (3.9%)
Error resolution	8 (7.6%)	5 (4.7%)	5 (3.3%)	0 (0%)

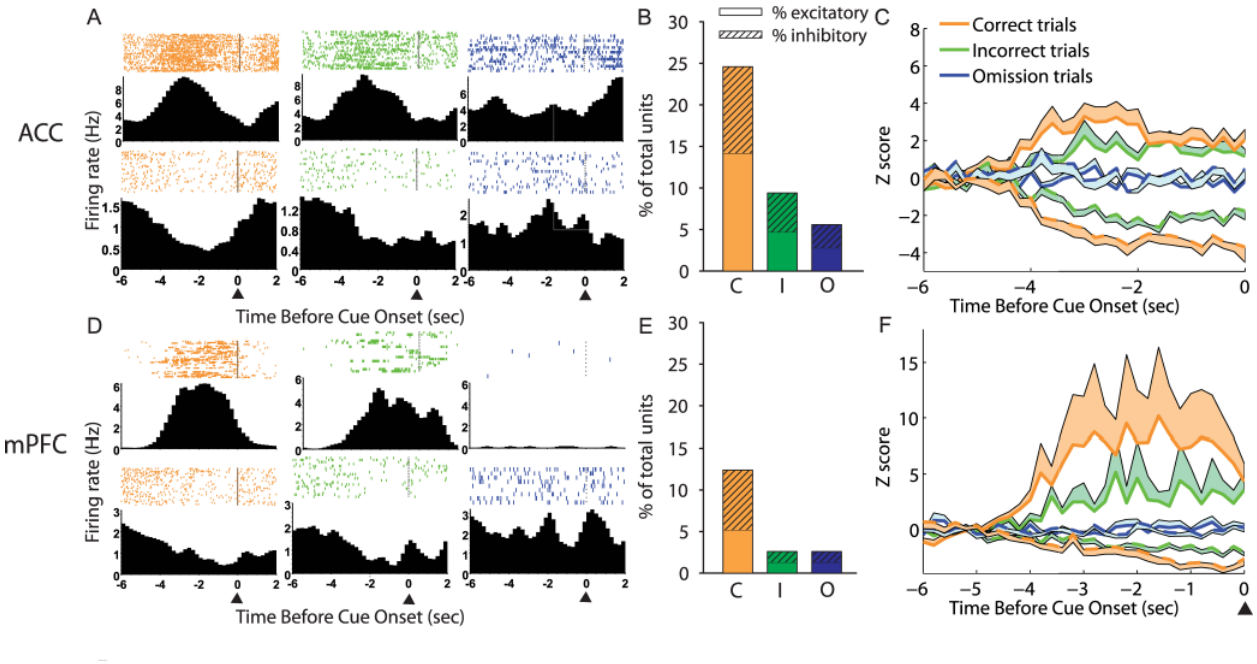

Figure 2.5. Pre-stimulus PFC single unit activity.

ACC (A, B, and C – top panel) and PL (D, E, and F – bottom panel). (A) Histograms aligned to stimulus onset (arrow) are shown from an example excitatory unit (top) and an example inhibitory unit (bottom). The unit's phasic response before the stimulus on correct trials (red) and the activity of the *same* unit on incorrect trials (green) and omission trials (blue). (B) The percent of total units which responded before the stimulus on correct trials (red), incorrect trials (green), and omission trials (blue). Excitatory units are shown as solid bar and inhibitory units are shown as hashed bar. (C) The population activity (excitatory – solid line and inhibitory – dashed line) of pre-stimulus responsive units on correct trials and the activity of those same units on incorrect and omission trials. (D), (E), and (F) PFC, same as above.

Figure 5C and F show the population activity of single units responsive on correct trials and the activity of those *same* units on incorrect and omission trials. Similar to the number of stimulus responsive units, the population response patterns were graded in that the magnitude of response to the stimulus was lower on incorrect trials and was not different from baseline on omission trials. For excitatory units (solid lines), there was a significant interaction between trial type (correct, incorrect, and omission) and time in both ACC ($F_{(58,1305)}$=6.76, p<0.0001) and PL ($F_{(58,\ 696)}$=1.77, p<0.001). A significant interaction between trial type (correct, incorrect, and

omission) and time was also observed for inhibitory units (dashed lines) in both ACC ($F_{(58,870)}$=3.69, p<0.0001) and PL ($F_{(58,870)}$=3.87, p<0.0001). When only correct and incorrect trial types were compared for units responding with excitation, there were significant differences in the magnitude of the Z score in the ACC (trial type, $F_{(1,30)}$=5.98, p<0.05; time, $F_{(29,870)}$=8.22, p<0.0001; trial X time interaction, p>0.05), but not in the PL (trial type, p>0.05; time, $F_{(29,464)}$=4.03, p<0.0001; trial X time interaction, p>0.05). However, when correct and incorrect trial types were compared for units responding with inhibition, there was a trend for a trial type and time interaction in the ACC ($F_{(29,580)}$=1.43, p=0.067) and a significant interaction in the PL (trial X time interaction, $F_{(29,580)}$=1.89, p<0.01). Although the interaction between trial type and time for correct and incorrect trials are not consistently significant, the results clearly support the finding of preparatory activity on trials with attention engaged (correct and incorrect trials) in comparison to unattended trials (omission trials). Review of behavior videos demonstrated that the preparatory behavior was similar for both correct and incorrect trials. While the latency to respond to the stimulus nose poke hole is longer for incorrect trials (**Table 2.1**), this is likely a correlate of increased decision-making time.

The activity (z-score) of the pre-stimulus responsive units on each trial does not correlate with the latency to nose poke into the stimulus hole on that trial (**Figure 2.6**). This may be because other non-attention related processing (i.e., motor preparation and response selection) occurs during the time between stimulus illumination and stimulus hole nose poke or because our measurement of phasic changes in single unit firing rate is not sensitive enough to correlate with behavioral latencies. Furthermore, given that rats are active and unconstrained in this task, there is considerable variability in body position and movement toward the stimulus between trials. This may diminish the possibility that a correlation is found between behavioral response

latencies and single unit phasic responses on each trial. Measures of large-scale neural activity, such as local field potential oscillations may correlate better with behavioral response latency.

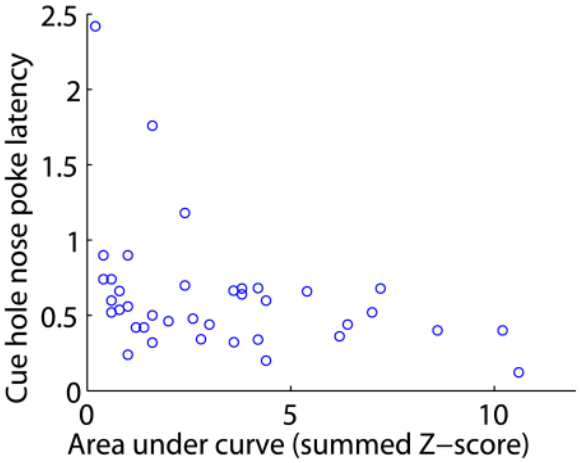

Figure 2.6. Lack of correlation between pre-stimulus activation and behavioral reaction time.
All units that were significantly responsive (here excitatory units are shown), within a rat and session were averaged together on a trial-by-trial basis. The summation of the z-scores from the resulting PETH for each trial was plotted against the behavioral latency on that trial. The y-axis shows the behavioral latency and the x-axis shows the area under the PETH curve. Data shown are an example from the ACC of one rat. No significant correlation was observed for any excitatory or inhibitory units in any rat.

Because the food magazine nose poke to either consume reward or end the house light extinguishment also initiated the next trial and 8 sec intertrial interval, pre-stimulus neural activity was potentially affected by reward or error processing, rather than attention. However, we found that pre-stimulus activity compared between trials after food consumption and trials after errors did not differ (**Figure 2.7**). For excitatory and inhibitory units, there was no interaction between previous reward or error and time in either the ACC ($p>0.05$) or the PL ($p>0.05$). Thus, pre-stimulus phasic changes in firing represent preparatory attention.

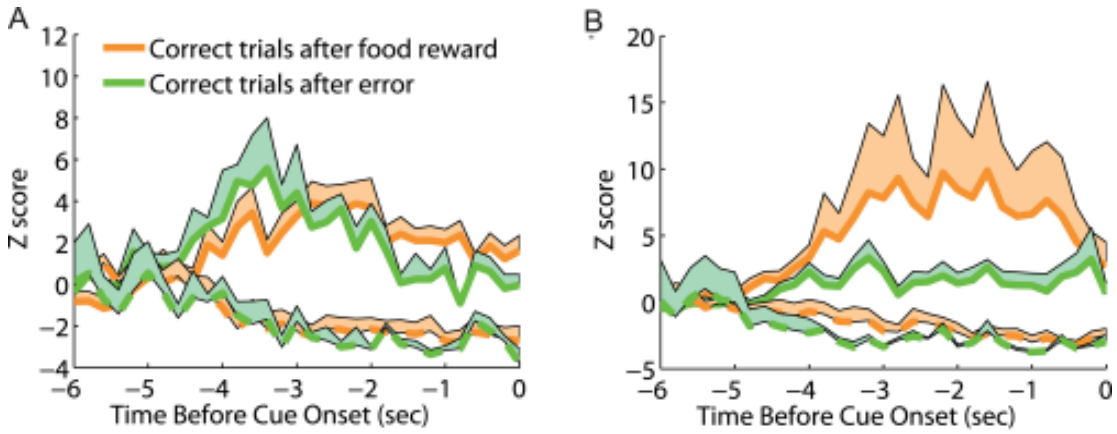

Figure 2.7. Activity of pre-stimulus responsive units on correct trials grouped by trials following previous rewards or errors.

The population activity (excitatory – solid line and inhibitory – dashed line) of pre-stimulus responsive units in the ACC (A) or PL (B).

Stimulus related phasic responses were only related to whether the response choice was correct or incorrect and not to the spatial location of the stimulus (**Figure 2.8**). The population activity of stimulus responsive units on correct trials according to which stimulus location (left, right, or center) was presented on each trial was not significantly different between stimulus locations for excitatory or inhibitory units in the ACC ($p>0.05$) or the PL ($p>0.05$).

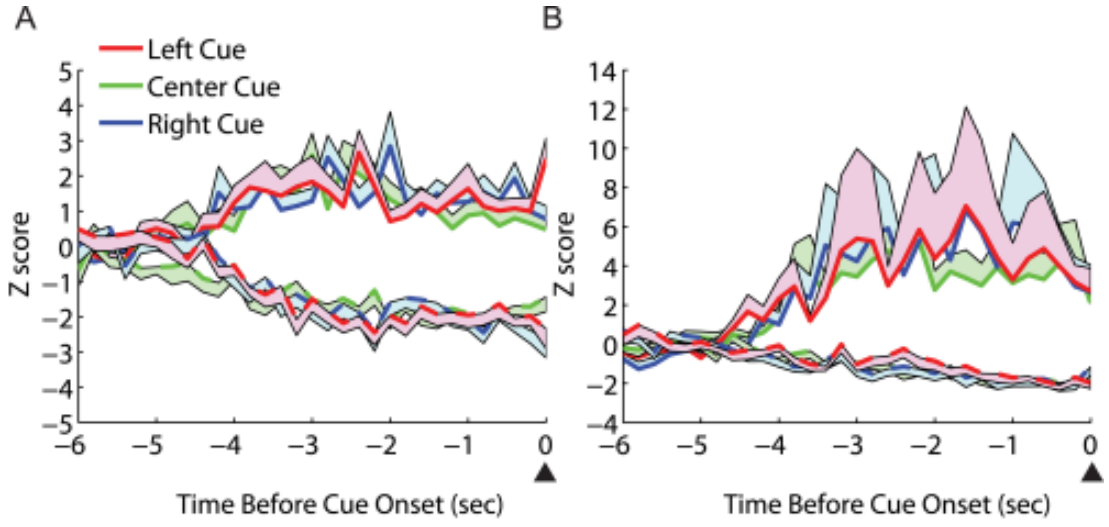

Figure 2.8. Pre-stimulus activity for each stimulus port location.

(A) ACC and (B) PL. Pre-stimulus responsive cells were divided into 3 groups depending on which of the 3 stimulus holes illuminated during that trial. No difference in excitatory or inhibitory responses was observed between stimulus locations (stimulus location X time interaction p=n.s.).

2.4.3 PHASIC NEURONAL RESPONSES RELATED TO ERROR FEEDBACK

Significant phasic responses related to motor execution and error processing were observed in the PL and ACC, respectively (**Figure 2.9**). Phasic responses related to stimulus hole nose poke onset were divided into 3 groups: correct, incorrect, and premature nose poke types. The percent of total units recorded that responded with excitation to the 3 stimulus hole nose poke events was similar between brain regions (see **Table 2.2**). Although the number of responsive units is small, our criteria for considering a unit responsive (4 consecutive time bins) is sufficiently stringent such that it is unlikely that a unit would be significant by chance. Phasic inhibitory responses were associated with correct stimulus hole nose pokes in both the ACC and PL (**Figure 2.9B and E**). These inhibitory units remained inhibited during the entire window of analysis around the correct stimulus hole nose poke (-1 to +1 sec) and did not return to baseline (**Figure 2.9C and F**).

In the PL, phasic excitations were observed for all 3 stimulus hole nose poke response types. However, the activity patterns related to each stimulus hole nose poke type were not significantly different from one another (nose poke type X time interaction, $p>0.05$). Error related activity was observed in the ACC only (**Figure 2.9C**). The error activity consisted of a phasic excitation after the incorrect stimulus hole nose poke. A significant interaction between trial type and time was observed ($F_{(78,585)}=2.90$, $p<0.0001$). It is important to note that a large phasic neural response after premature stimulus hole nose pokes, which were also errors, was not found in the ACC or PL. A premature stimulus hole nose poke is a different type of error than an

incorrect stimulus hole nose poke in that it occurs before stimulus onset and results in a timeout that cannot be resolved by the rat. On incorrect trials, an incorrect action has been made to the stimulus that must be dealt with by nose poking into the food magazine; thus, other actions need to be planned to continue the task.

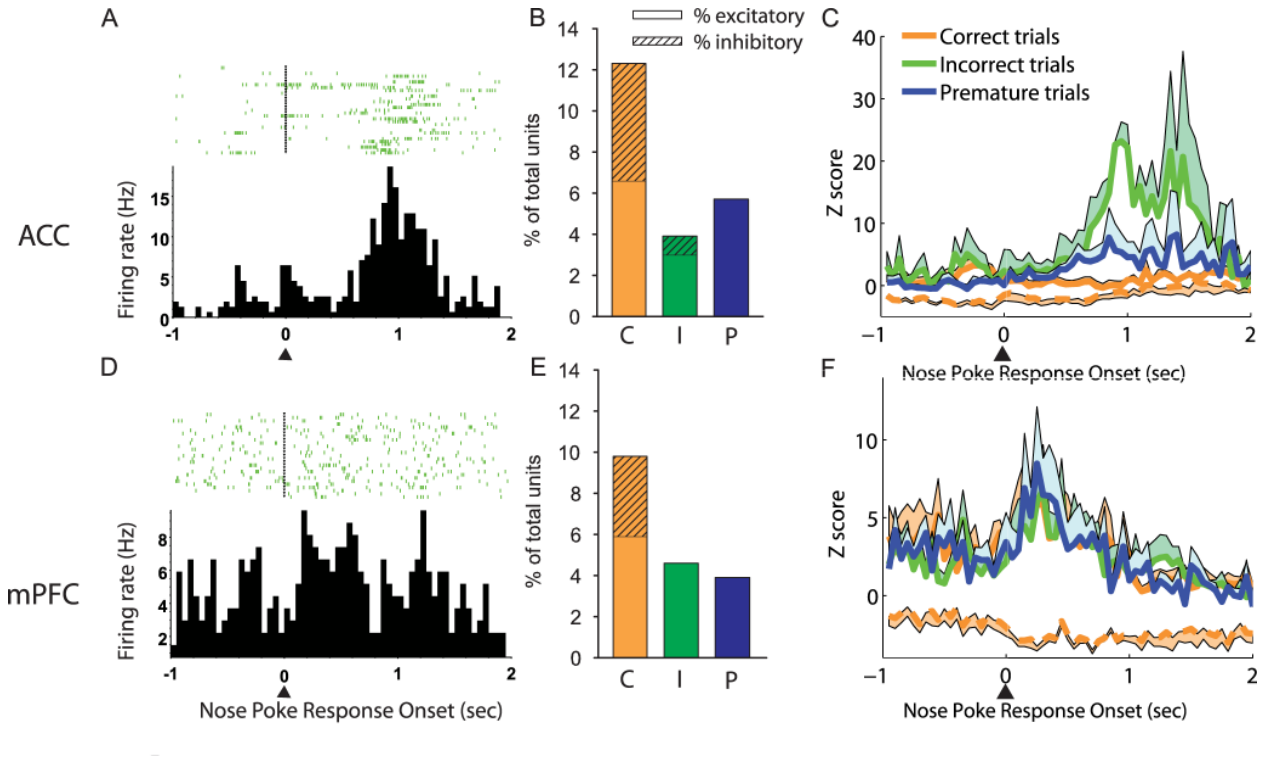

Figure 2.9. Stimulus port nose poke response related single unit activity in the PFC.

ACC (A, B, and C – top panel) and PL (D, E, and F – bottom panel). Nose pokes into the stimulus holes were divided into 3 groups: correct, incorrect, and premature (before the stimulus light). (A and D) Single unit examples of excitatory units that responded on incorrect stimulus hole nose pokes. (B and E) The percent of total units which responded during a -1 to +1 window around stimulus hole nose poke onset. Excitatory units are shown as solid bar and inhibitory units are shown as hashed bar. A similar proportion of units responded in each region. Correct stimulus hole nose pokes were associated with a significant number of inhibitory responses. (C and F) The population activity (excitatory – solid line and inhibitory – dashed line) of stimulus hole nose poke responsive units. Neural activity is aligned with nose poke entry into the stimulus hole (arrow). No difference was found between activity in the PFC (trial type X time interaction, p=n.s.), but a phasic response to incorrect stimulus hole nose pokes was observed in the ACC ($p<0.01$).

2.4.4 PHASIC NEURONAL ACTIVITY RELATED TO RESOLVING ERROR

In addition to the error related activity after incorrect stimulus hole nose pokes observed exclusively in the ACC, there was a larger number of single units in the ACC that were responsive to resolving errors, that is, the intentional action of the rat to end the timeout and initiate the next trial (**Figure 2.10**). In the ACC, 12.3% of the total units recorded responded with either excitation or inhibition to food magazine nose pokes on error trials, while in the PL only 3.3% responded (**Table 2.2**). Furthermore, in the ACC only, the population response patterns of inhibitory units discriminated food magazine nose pokes that resolved errors from food magazine nose pokes for consuming reward (**Figure 2.10B**). A significant interaction between food magazine nose poke type and time was observed for inhibitory units in the ACC ($F_{(39,585)}$=3.60, $p<0.0001$). The inhibitory response related to nose poking for resolving an error returned to baseline, while inhibition to reward consumption remained inhibited. For excitatory units, there was no significant interaction between food magazine nose poke type (reward or ending punishment) and time in the ACC ($p>0.05$) or the PL ($p>0.05$).

A larger number of single units in the ACC were also responsive to food magazine nose pokes for reward consumption. In the ACC, 23.6% of the total units recorded responded with either excitation or inhibition to food magazine nose pokes on reward consumption trials, while in the PL only 13.1% responded (**Table 2.2**). Furthermore, a large phasic excitation before food magazine nose poke for reward consumption was observed only in the ACC (**Figure 2.10A**).

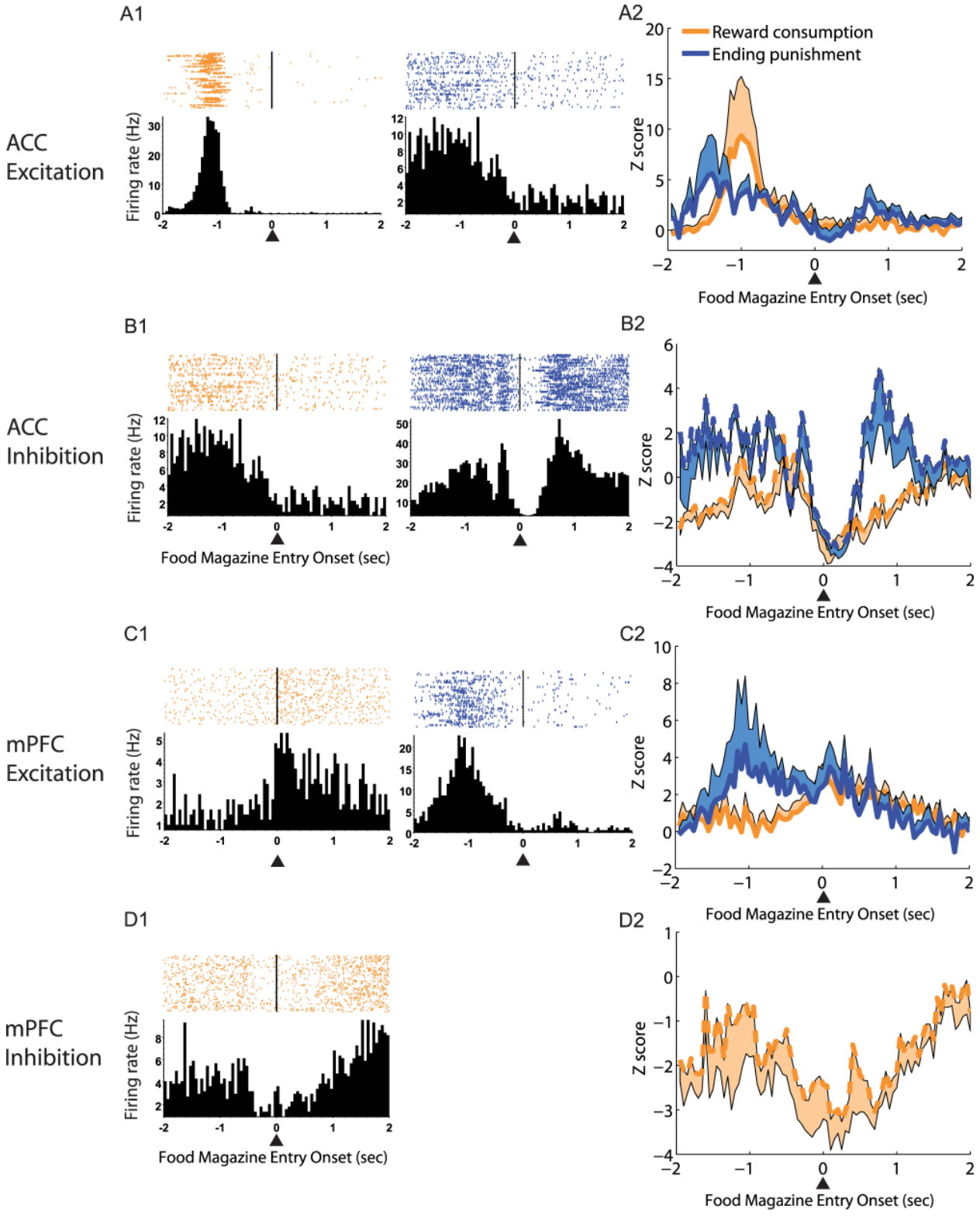

Figure 2.10. Reward consumption and error resolution related single unit activity in the PFC.

ACC (A – excitatory responses and B – inhibitory responses) and PL (C – excitatory responses and D – inhibitory responses). Nose pokes into the food magazine were divided into 2 groups: nose pokes that consumed reward and nose pokes that resolved an error. Both types of food magazine nose pokes began a new trial. (A1 and B1) Single unit examples of units in the ACC that responded to food consumption (orange) and error resolution (blue). Examples are shown for excitation (A1) and inhibition (B1). Population activity (A2 – excitatory response and B2 – inhibitory response) aligned to nose poke entry into the food magazine (arrow) are shown for food consumption (orange) and error resolution (blue). Neural activity is shown in the same scheme for the PL (excitatory units: C1, C2 and inhibitory units: D1, D2).

2.5 DISCUSSION

During the same behavioral sequence, error-related signals and the preparatory period were represented by ACC. The PL only responded to the preparatory period. On incorrect trials, the number of responsive units and the magnitude of pre-stimulus activity were reduced in both regions suggesting that these phasic responses are related to the degree of preparatory attention and subsequent correct or incorrect choice. The same relationship between pre-stimulus activity and subsequent performance was found for inhibitory phasic responses in both brain regions, suggesting that phasic inhibition contributes to preparatory attention. ACC units discriminated food magazine nose pokes to retrieve reward from those which resolved error when the rat ended the timeout, suggesting that these neurons represent action-outcome related information and aid in resolving the error.

2.5.1 ERROR-RELATED SIGNALING AND OUTCOME MONITORING IN THE ACC

Consistent with previous studies (Ito et al., 2003; Quilodran et al., 2008; Ruchsow et al., 2002) a phasic excitatory error-related response was observed after an incorrect stimulus hole nose poke in the ACC. This error signal could be used by the brain for conflict monitoring (Botvinick et al., 2004) or as a reinforcement learning signal (Nieuwenhuis et al., 2004), both of which are currently debated using studies which directly test those questions. Inhibitory units in the ACC discriminated between food magazine nose pokes for food reward and nose pokes to resolve error (i.e., end the timeout). Additionally, a larger percentage of units in the ACC responded to food magazine nose pokes for reward consumption and for error resolution compared to the PL. These data suggest that the ACC is more sensitive to outcome related information, in comparison to the PL. Thus, the ACC may represent outcome-related information, in addition to detecting errors.

2.5.2 THE ANTERIOR CINGULATE CORTEX AND PRELIMBIC CORTEX BOTH PARTICIPATE IN PREPARATORY ATTENTION

One theory of preparatory attention predicts that the PL/DLPFC should activate during preparatory periods, while the ACC should represent errors (Botvinick et al., 2004). Our recordings in the rodent PL are similar to the anticipatory single unit responses that have been recorded in the monkey DLPFC (Niki and Watanabe, 1979; Pragay et al., 1987). Thus, our results are consistent with a role for the PL/DLPFC in preparatory attention.

On the other hand, the demonstration of preparatory activity in the ACC is consistent with the view that this brain region plays a direct role in preparatory attention (Posner and

Petersen, 1990; Roelofs et al., 2006; Weissman et al., 2005). Pre-stimulus preparatory activity has been shown previously in the monkey ACC (Johnston et al., 2007; Koyama et al., 2001; Niki and Watanabe, 1979). Furthermore, our finding of reduced preparatory activity in the ACC (and PL) on incorrect trials is consistent with reduced human ACC event-related potentials, on trials with reduced preparatory attention (Padilla et al., 2006). Thus, the ACC has a dual role in goal-directed behavior, both detecting errors and responding during preparatory periods.

It is important to note that the preparatory activity could reflect reward prediction or expectation (Shidara and Richmond, 2002), rather than selection of stimuli *per se*. Thus, fluctuations in internal motivations may lead to reduced expectancy of reward and subsequent incorrect performance. However, preparatory activity on incorrect trials was reduced compared to correct trials, even though, the same information, or lack of information, about reward is available to the rat on both trial types. This strongly suggests that the preparatory activity reflects attention to a stimulus, rather than expectation of reward.

2.5.3 INHIBITION OF ANTERIOR CINGULATE CORTEX AND PRELIMBIC CORTEX UNITS DURING ATTENTION AND GOAL-DIRECTED BEHAVIOR

The finding of substantial inhibition during the preparatory period and a reduction of this inhibition on incorrect trials suggests that excitation of local inhibitory interneurons and/or inhibitory afferents are brought online during attention and goal-directed behavior. Local interneurons in the PFC modulate the firing of pyramidal cells and abnormalities in interneurons are present in schizophrenia, which suggests that interneurons play a critical role in PFC neural activity patterns and in its control of cognition (Ford et al., 2007; Lewis et al., 2003). The

inhibition of putative pyramidal cells during the pre-stimulus period may be due to the excitation of local PFC interneurons via thalamic inputs (Rotaru et al., 2005).

2.5.4 THE ANTERIOR CINGULATE CORTEX AND PRELIMBIC CORTEX MAY PROVIDE PREPARATORY ATTENTION FOR DIFFERENT ASPECTS OF BEHAVIOR

The preparatory attention signal in the ACC may relate selection of stimuli to trial outcomes, while the preparatory attention from the PL may select stimuli for use in stimulus-response rules. Preparatory ACC unit activity is related to the degree of reward expectancy (Shidara and Richmond, 2002). In the multi-trial stimulus reward task used by Shidara & Richmond (2002), the monkey's expectancy of reward and its motivation increases. Preparatory attention is increased when motivation to select a stimulus is increased (Sarter et al., 2006). Thus, as the organism experiences increased motivation, its preparatory attention is also increased, as represented by pre-stimulus activity. The preparatory signal in the ACC may link the selected stimulus with ACC processing of motivation and trial outcomes.

On the other hand, given the well demonstrated role of the PL/DLPFC in representing stimulus-response associations (Asaad et al., 1998; Passingham et al., 2000; Quintana and Fuster, 1992; Rainer et al., 1998; Sakagami and Niki, 1994) and selecting stimulus-response mappings (Miller and Cohen, 2001), the preparatory activity in the PL may be important for linking a selected stimulus with stimulus-response rules and holding that information in working memory. Indeed, once a task is well learned, the rat PL is not necessary for action-outcome associations, only stimulus-response associations (Corbit and Balleine, 2003; Ostlund and Balleine, 2005).

Thus, the ACC and PL may both participate in preparatory attention, with the former relating the trial outcome and motivation and the latter relating to stimulus-response rules.

2.5.5 GENERAL CONCLUSIONS

We demonstrate that the ACC responds to error-related events and, along with the PL, encodes preparatory attention. These results are consistent with the theory that the PL plays a role in preparatory attention but that the ACC plays a dual role in both preparatory attention and representing error-related events during the same task. We also propose that both ACC and PL regulate preparatory attention, but focus that control on linking selected stimuli to trial outcomes and stimulus-response rules, respectively.

3.0 PREPARATORY ATTENTION RELIES ON DYNAMIC INTERACTIONS BETWEEN PRELIMBIC CORTEX AND ANTERIOR CINGULATE CORTEX

3.1 ABSTRACT

An emerging view of prefrontal cortex (PFC) function is that multiple PFC areas process information in parallel, rather than as distinct modules. Two key functions assigned to the PFC are the regulation of top-down attention and goal-directed action. Electrophysiology and lesion studies indicate the involvement of both the anterior cingulate cortex (ACC) and prelimbic cortex (PL) in these functions. Little is known however, about how these cortical regions interact. We recorded single unit spiking and local field potential (LFP) simultaneously in rodents during a sustained attention task and assessed interactions between the ACC and PL by measuring spike-LFP phase synchrony and LFP-LFP phase synchrony between both PFC areas. We demonstrate that the magnitude of synchrony between the ACC and PL, before stimulus onset, predicts the subjects' behavioral choice after the stimulus. Furthermore, neurons switched from a state of beta synchrony during attention to a state of delta synchrony before the instrumental action. Our results indicate that multiple PFC areas interact during attention, and that the same neurons may participate in segregated assemblies that support both attention and action.

3.2 INTRODUCTION

It is widely accepted that a top-down attention signal originates from the prefrontal cortex (PFC) (Egner et al., 2008; Desimone and Duncan, 1995; Fuster, 2001; Miller and Cohen, 2001; Lebedev et al., 2004; Roelofs et al., 2006; Gregoriou et al., 2009; Posner and Petersen, 1990; Orr and Weissman, 2009). Human imaging and behaving animal electrophysiology studies have implicated various PFC modules, such as the anterior cingulate cortex (ACC), the frontal eye fields (FEF), and the dorsolateral PFC (dlPFC) as being responsible for priming the representation of an expected stimulus in sensory cortex (Kastner et al., 1999; Johnston et al., 2007; Coull et al., 2000; Egner et al., 2008; Stokes et al., 2009; Summerfield et al., 2006; Sylvester et al., 2009; Noudoost et al., 2010; Totah et al., 2009). An emerging view of PFC function is that discrete areas process information in a coordinated manner rather than as distinct modules (Moghaddam and Homayoun, 2007; Duncan, 2001). Coordinated activity between neurons in different networks and brain regions may be mediated by spike synchrony with local field potential (LFP) oscillations (Fries, 2005; Varela et al., 2001) as well as synchrony of LFP oscillations, which provides windows of time when the effectiveness of a proximal spike on a distal neuron's post-synaptic potential is enhanced (Buzsaki, 2004; Canolty et al., 2010; Womelsdorf et al., 2007). Although the effects of engaging top-down attention on synchrony between multiple visual cortex areas have been studied (Fries et al., 2008; Stein et al., 2000), less is known about synchrony-mediated communication between PFC areas during top-down attention.

In order to study the interactions between PFC areas during top-down attention, we recorded single unit spiking and LFP from two rat PFC areas during a rodent attention task. The regions included the ACC and the prelimbic cortex (PL), both of which have been implicated in

attention and goal-directed action (Chudasama et al., 2003; Ng et al., 2007; Passetti et al., 2002; Peters et al., 2005; Narayanan and Laubach, 2009; 2006). In the task, rats were trained to anticipate a brief visual stimulus, which appeared at one of three randomly selected locations, and to make an instrumental response to the perceived location. We focused the analysis on phase synchrony between the two PFC areas before stimulus onset (i.e., during top-down attention) and before the instrumental response (i.e., before the stimulus-guided response). Prior to the onset of a behaviorally-relevant stimulus, preparatory attention improves selection of an expected stimulus by enhancing the firing rate of sensory cortex neurons that will represent the stimulus (Chelazzi et al. 1993; Luck et al. 1997; Chawla, Rees, and Friston 1999; Chawla, Lumer, and Friston 2000; Driver and Frith 2000; Bressler et al. 2008; Stokes et al. 2009; Sylvester et al. 2009). Accordingly, we focused our analysis of preparatory attention on the pre-stimulus period, when the rat orients to and waits for the upcoming stimulus. The analyses compared correct trials with error trials, when the rat responded to one of the non-illuminated stimulus locations. We interpreted incorrect trials as being indicative of a preparatory attention signal that is inadequate for selecting the correct stimulus location. While we cannot eliminate the possibility that incorrect selection of stimulus location is due to deficient planning or stimulus expectation, these cognitive abilities are related in that they rely on PFC neural activity before onset of a behaviorally relevant stimulus and have similar effects on sensory cortex neural activity (Niki and Watanabe 1979; Pragay, Mirsky, and Nakamura 1987; Fuster 1995; Luck et al. 1997; Kastner et al. 1999; Rainer, Rao, and Miller 1999; Driver and Frith 2000; Ghose and Maunsell 2002; LaBerge 2002; Johnston et al. 2007; Hussar and Pasternak 2009; Stokes et al. 2009; Sylvester et al. 2009; Totah et al. 2009). In addition to studying preparatory attention, we assessed synchrony between the ACC and PL before the stimulus-guided instrumental response

in order to characterize how these PFC areas interact during action preparation and execution. We hypothesized that if multiple PFC areas need to coordinate their activity to generate preparatory attention and stimulus-guided behavior, then synchrony would predict performance accuracy.

3.3 METHODS

3.3.1 SUBJECTS AND BEHAVIORAL METHODS

Four male Sprague-Dawley rats were used in this study. All rats were housed on a reverse light cycle and trained and tested during the rats' active phase. All experiments were carried out in compliance with the University of Pittsburgh Institutional Animal Care and Use Committee (IACUC). The behavioral task has been described in detail in our previous work (Totah et al., 2009). Briefly, rats were trained and tested in operant chambers with a house light on the ceiling, three stimulus ports with internal LED lights on one wall, and an illuminated food magazine on the wall opposite from the stimulus ports. Nose pokes into the stimulus ports and the food magazine were registered by photosensors. A correct response, consisting of a nose poke into an illuminated stimulus port, was rewarded with sucrose. An incorrect response into an unlit stimulus port resulted in an extinguished house light. The rat was required to nose poke into a stimulus port within 5 sec after stimulus onset; otherwise, the house light was extinguished (i.e., an omission trial). The rat initiated each trial with a poke into the food magazine, which either contained sucrose pellets or was empty depending on whether the previous trial was correct or an error (i.e., an incorrect or omission trial).

At the start of a trial, an 8 sec pre-stimulus period passed before the stimulus onset. On each trial, one of the three stimulus ports would illuminate. The location of the stimulus was selected at random from the three stimulus ports. There was a balanced distribution of the selection of the three ports, but the order of presentation was random. Rats initially were trained to respond to a 15 sec duration stimulus and could respond during the stimulus or within 5 sec after the stimulus was extinguished. Each session lasted 30 minutes. Based on satisfying performance criteria (see previous work for detailed information regarding training, (Totah et al., 2009), the stimulus duration was gradually reduced to 300 msec. Rats were deemed ready for electrode implantation when they met the performance criterion of > 70% accuracy (i.e., # of correct responses / (# of correct responses + # of incorrect responses) and < 20% omissions (i.e., # of omitted responses / # of total trials) for six consecutive sessions using the 300 msec cue duration. The mean number of sessions needed to complete training was 42 sessions. Rats exhibited attentive behavior, whereby they oriented to the operant chamber wall that contained the stimulus ports and waited for the stimulus. Orientation to the wall of stimulus ports began approximately 2 seconds before stimulus onset and was maintained throughout the pre-stimulus period. It was extremely rare (approximately <1 % of trials across many 30 min sessions) for rats to orient away from the stimulus ports once they had begun orienting. Sessions were videotaped and reviewed in order to eliminate trials on which the rat did not directly face the stimulus ports because those were not stereotypical task behaviors.

3.3.2 ELECTROPHYSIOLOGY PROCEDURE

Rats were implanted under isoflurane anesthesia with two microelectrode arrays each consisting of eight Teflon-insulated stainless steel wires in a 2-by-4 pattern measuring 0.25 mm

by 0.70 mm with an impedance of 300 – 700 kΩ (NB Labs, Denison, TX). One array was placed spanning the ACC: –0.2 to –1.0 mm posterior to bregma, –0.4 to –0.7 mm lateral to bregma, and –2.5 mm ventral from the dura surface and one array was placed spanning the contralateral PL (prelimbic cortex): +2.4 to +3.4 mm anterior to bregma, +0.5 to +0.8 mm lateral to bregma, and –3.8 mm ventral from the dura surface. At the completion of recordings, rats were anesthetized with chloral hydrate, and the rats were perfused with normal saline for 10 min and 10% buffered formalin for 10 min. After fixation, brains were sectioned and stained using cresyl violet. Placement of electrode tips was confirmed under a light microscope and subjects' neural activity recorded from improperly placed electrodes was excluded from analysis.

After 1 week of recovery, rats were acclimated to attachment of the electrode cable in the operant box for four 30-min sessions and re-trained to criterion performance at the 300 msec stimulus duration. Once behavioral performance was stable and above criterion, a 30 min session was recorded. Single units and LFP were recorded via a unity-gain FET headstage and lightweight cabling, which passed through a commutator to allow freedom of movement. Neural activity was amplified using a 1,000X gain and single unit activity was band pass filtered at 300 – 8,000 Hz and LFPs were band pass filtered at 0.7 – 170 Hz. Neural activity was digitized at a rate of 40 kHz and LFPs were down sampled to 1 kHz using Recorder software (Plexon, Inc.). Single-unit activity was digitally high-pass filtered at 300 Hz and LFPs were digitally low-pass filtered at 125 Hz. Signals from the operant box were used as event markers to coordinate behavioral events with neural activity. Units were isolated in Off-Line Sorter software (Plexon, Inc.). Stability of units over time was confirmed by viewing the waveform clusters in a 3-dimensional space of the first two principal components and time. Units were rejected if the interspike interval histogram was inconsistent with a refractory period of <1.1 msec.

3.3.3 ELECTROPHYSIOLOGICAL DATA ANALYSIS

Electrophysiological data were analyzed with custom scripts written in Matlab (Mathworks, Natick, MA). An LFP signal was collected from one electrode in each brain region. The signal was aligned to the behavioral event of interest and trials with LFP clipping in either brain region were removed from analysis. The LFP signal was convolved with a complex Morlet wavelet, resulting in a complex number, W(*f*,*t*), at each scale (converted to a frequency for simplicity), *f*, and time, *t*. The conversion from scale to frequency resulted in all plots of frequency space appearing non-uniform because wavelet transformation results in higher resolution at lower frequency. Power spectra were calculated as $|W(f,t)|^2$ for each time-frequency bin on each trial. Each time-frequency bin was normalized to % maximum power on a trial-by-trial basis. Normalized power spectra then were averaged across trials. The presented spectrograms are the average across all four animals.

Phase synchrony between LFP signals was measured as a phase locking value (PLV) over time in each trial and averaged across trials within animals. The constancy of the difference in phase between the LFP signals at electrodes, *j* and *k*, was calculated as a PLV such that,

$$PLV_{j,k}(f,t) = \frac{1}{N}\left|\sum_{N} e^{i(\varphi_i - \varphi_j)}\right|$$

where N is the number of samples in the time window, φ is phase, and | | is the complex modulus (Lachaux et al. 1999; Rodriguez et al. 1999). PLV ranges from 0 to 1 (constant phase difference). The PLV is equivalent to one minus the circular variance of the phase differences. Phase angle was extracted from W(*f*,*t*) using,

$$\theta(f,t) = \tan^{-1}\frac{\Im\{W(f,t)\}}{\Re\{W(f,t)\}}$$

where $\theta(f,t)$ is phase angle at a time and frequency point and $\Im$ and $\Re$ are the imaginary and real components of the wavelet coefficient, respectively. For each frequency of interest, PLV was calculated using a time window consisting of 10 cycles and slid in steps of 1/20th of a time window. Because synchrony between two oscillatory signals can occur by chance, we used a surrogate data set to determine if the occurrence of synchrony was greater than expected by chance. We computed a distribution of PLVs that would be expected if the two LFP signals were independent of one another by computing 200 surrogate PLV values with a random trial selected for one of the electrodes (see above references). If the observed PLV was higher than the upper limit of the 95% confidence interval of the distribution of surrogate PLV values, then the PLV was not spurious.

Spike-LFP phase synchrony was calculated in 2 sec time windows slid in 200 msec steps (pre-stimulus period) and in 1 sec time windows slid in 100 msec steps (instrumental nose poke period). To assess the phase locking characteristics of a neuron, we collected the LFP phase angles that corresponded to the spike times for all spikes within a time window, across all trials (**Figure 3.1**).

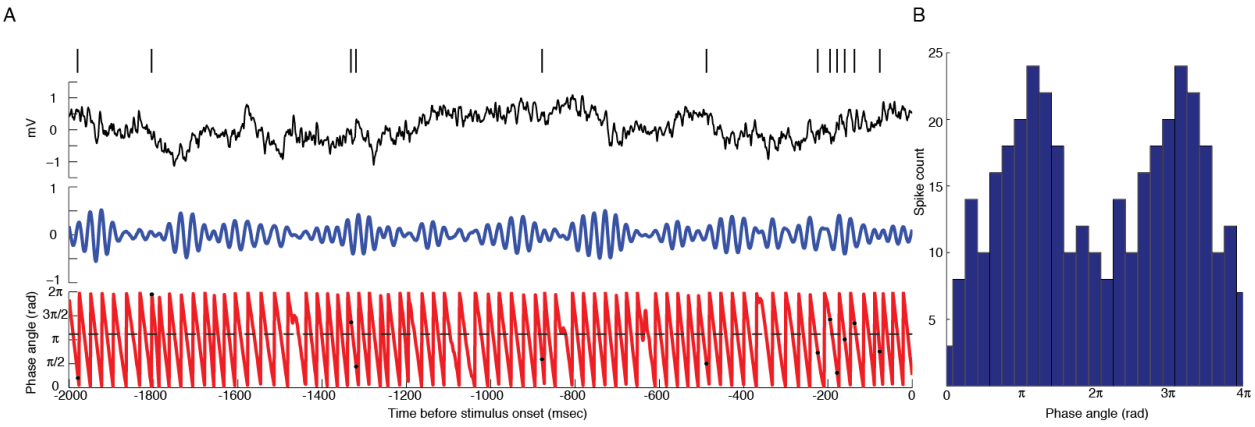

Figure 3.1. Summary of the method of analysis of spike-LFP phase locking.

Spike times (A, top) and LFP (A, black) were recorded simultaneously. (A) Data are plotted for a single example trial during the 2 sec before stimulus onset (t=0). The LFP was convolved with a complex Morlet wavelet. The

amplitude (blue) and phase angle (red) at 40 Hz are plotted below the raw data. Spike times are indicated by black dots on the plot of phase angle (red). In this trial, the spikes tend to occur around the mean resultant angle (dotted black line), which was calculated using spike times from all trials for this neuron. (B) Spikes from the 2 sec before stimulus onset combined across all trials, for the same neuron as in A. The neuron was significantly phase locked (Rayleigh's test for circular uniformity, Z = 8.936, p<0.0001) and the mean phase angle was 3.504 radians.

A neuron was considered significantly phase locked if the distribution of spike phase angles departed from a uniform circular distribution (Rayleigh's test for circular uniformity, p<0.05). The circular statistics toolbox (MATLAB) was used for statistical analyses of spike-LFP phase synchrony (Berens 2009). If any time window had <6 spikes, we could not rely on Rayleigh's test (Fisher 1996) and we chose to remove that neuron from analysis. The value of Rayleigh's Z statistic for a neuron was used as a measure of phase consistency or the strength of spike-LFP phase locking. Rayleigh's Z was calculated by

$$Z = nR^2$$

where *R* is the mean resultant phase vector length of *n* spikes. The p-value for Rayleigh's test for circular uniformity is calculated as:

$$p = e^{-Z} * (1 + \frac{2Z - Z^2}{4n} - \frac{24Z - 132Z^2 + 76Z^3 - 9Z^4}{228n^2})$$

Neurons were considered significantly phase locked if p<0.05. We controlled for spurious spike-LFP phase locking, while keeping the timing of behavioral events intact, by computing spike-LFP phase locking between spikes from a trial and the LFP signal from a different, randomly selected trial (without replacement). A distribution of the expected spurious phase locking was formed by calculating Rayleigh's Z values on 200 sets of trial shuffled data. For each time-frequency bin, the upper limit of the 95% confidence interval of the distribution was selected as the expected spurious Rayleigh's Z for that particular neuron in that particular time-frequency bin. Rayleigh's Z values were compared between the original data (correct trials)

and the shuffled data using a 2-way repeated measures ANOVA (with factors data type and time).

We were particularly interested in comparing the phase locking of neurons on correct and incorrect trials; however, there are fewer incorrect trials and, accordingly, a smaller sample size of spikes with which to calculate R. To equalize any bias due to unequal sample sizes, we employed a resampling procedure. For a given neuron with *x* number of spike times in the correct condition and *y* number of spike times in the incorrect condition (where $x > y$), we removed *y* number of spikes (selected randomly without replacement) from the correct condition and replaced them with all of the *y* number of spikes from the incorrect condition. We calculated Rayleigh's Z for the new group with replaced spike times. We repeated this resampling procedure 5,000 times and calculated Rayleigh's Z on each iteration. We then used the mean of the Z distribution to calculate a p value for that neuron. Thus, the same number of spikes per neuron is present in both correct and incorrect conditions. Accordingly, conditions labeled as "incorrect" in the spike-LFP phase locking analysis reflect the degree to which the insertion of the spike times from incorrect trials degrades or enhances spike-LFP phase locking observed on correct trials. This is similar to the method employed by Siegel et al. (2009) to control for the same sample size bias (Siegel et al. 2009). We also tried a bootstrapping procedure to control for the sample size bias, whereby we randomly sub-sampled *y* random spikes (with replacement) from the full sample in the correct condition (5,000 iterations). However, we found that this reduced the power of the Rayleigh's Z test for neurons with a large sample of spikes, which is in line with the findings of others (see supplemental materials, Sirota et al. 2008).

3.4 RESULTS

3.4.1 BROADBAND LFP OSCILLATION POWER DURING PREPARATORY ATTENTION

Across four rats, there were 37.5±4.2 correct choice trials and 12.8±3.4 incorrect choice trials (after removal of trials with LFP artifacts). **Figure 3.2** shows mean power spectrograms averaged across all animals. We examined the 2 sec window before stimulus onset, which corresponds to the approximate time of orientation to the wall of stimulus ports (Totah et al., 2009). We found that power was reduced on incorrect trials across a range of frequencies (t-test for each time-frequency bin, **Figure 3.2**, right panel). Additionally, the alpha power had a typical "waxing and waning" rhythm that has been observed previously (Linkenkaer-Hansen et al., 2001; 2004). The remaining analyses were focused on studying phase synchrony and excluded LFP amplitude from the analysis (Le Van Quyen and Bragin, 2007; Lachaux et al., 1999; Varela et al., 2001).

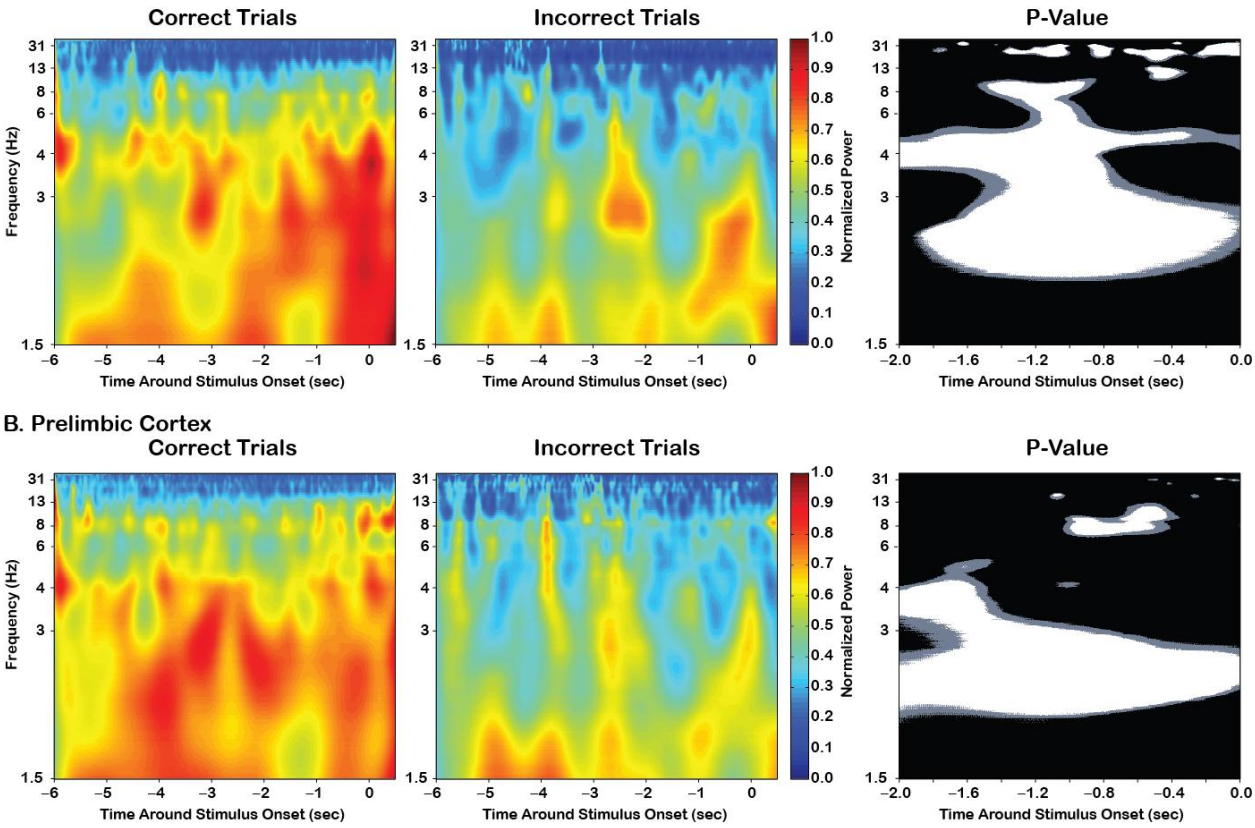

Figure 3.2. Pre-stimulus broadband LFP power is correlated with trial type in the PFC.

The spectrogram shows the mean normalized LFP power averaged across 4 rats. Stimulus onset is at t = 0 sec. Power was normalized within trial and then averaged across trials, within subject. Data are shown for correct trials (left) and incorrect trials (middle) for both the ACC (A) and PL (B). A t-test was used to compare each time-frequency bin between trial types. The results are plotted (right) using black if p=n.s., grey if 0.05<=p<0.08, and white if p<0.05. In both brain regions, delta (1 – 4 Hz), alpha (8 – 12 Hz), and beta (13 – 30 Hz) powers are greater on correct trials. However, the time course and frequency spread is not the same in both brain regions. Although not different between trial types, the power of alpha oscillations fluctuated over time in a periodic manner.

3.4.2 WITHIN-REGION SPIKE-LFP PHASE LOCKING DURING PREPARATORY ATTENTION

We recorded 32 neurons in the ACC and 61 neurons in the PL. During the 2 sec period preceding stimulus onset, neurons in both PFC areas were phase locked across a wide range of frequencies (Rayleigh's test for circular uniformity, $p<0.05$). Compared to incorrect trials, a larger proportion of neurons phase locked to various frequencies (between 1.5 Hz and 50.0 Hz) on correct trials (**Table 3.1**).

Table 3.1. The number and percent of PFC single units that were phase locked to any frequency during -2 to 0 sec before stimulus onset.

During incorrect trials, a larger proportion of neurons did not phase lock to LFP oscillations. In the case of between-region phase locking, the effect reached a trend (ACC spikes / PL LFP) and significance (PL spikes / ACC LFP). *$p<0.05$, $^{t}p<0.07$.

	Within Region		**Between Region**	
	ACC (n=32)	PFC (n=61)	ACC spikes PL LFP (n=32)	PL spikes ACC LFP (n=61)
Correct Trials, Pre-Stimulus	25 (78%)	41 (67%)	24 (75%) ^{t}	40 (66%) *
Incorrect Trials, Pre-Stimulus	21 (66%)	36 (59%)	17 (53%)	28 (46%)

At many frequencies, a similar proportion of neurons were phase locked on correct and incorrect trials (**Figure 3.3**). In the ACC, within-region delta band phase locking was reduced during incorrect trials ($\chi^2=4.27$, $p<0.05$; **Figure 3.3A**), whereas in the PL, within-region beta band phase locking was reduced during incorrect trials ($\chi^2=4.14$, $p<0.05$, **Figure 3.3B**). The reduced proportion of phase locked neurons was centered at 1.6 Hz in the delta band (ACC) and 17 Hz in the beta band (PL).

To study how phase locking strength varied over the pre-stimulus time period, we compared time-resolved Rayleigh's Z for ACC neurons that were phase locked at 1.6 Hz and PL neurons that were phase locked at 17 Hz during the 2 sec window before stimulus onset. The mean, time-resolved Rayleigh's Z across delta band phase locked ACC neurons was reduced on incorrect trials (**Figure 3.3C**) (ANOVA; main effect of trial: $F_{(1,3)}$=21.88, p=0.019; main effect of time: $F_{(30,90)}$=3.32, p<0.001; interaction: $F_{(30,90)}$=1.32, p=0.158). Comparing individual time points during the pre-stimulus period show that the difference between trial types is during the final 2 sec window before stimulus onset (t(6)=3.91, p=0.008). Although Rayleigh's Z in the theta band in the window ranging from -6 to approximately -3.5 sec before stimulus onset appeared to be higher magnitude on correct trials, this increase was not significant over time (ANOVA; main effect of trial: $F_{(1,3)}$=10.12, p=0.050; main effect of time: $F_{(30,90)}$=0.80, p=0.748; interaction: $F_{(30,90)}$=0.725, p=0.757). Furthermore, phase locked neurons did not exhibit changes in firing rate nor did they differ between trial types (ANOVA; main effect of trial: $F_{(1,3)}$=8.51, p=0.062; main effect of time: $F_{(39,117)}$=0.89, p=0.671; interaction: $F_{(39,117)}$=1.194, p=0.233).

There was a trend for the mean, time-resolved Rayleigh's Z across beta band phase locked PL neurons to be reduced on incorrect trials (**Figure 3.3D**) (ANOVA; main effect of trial: $F_{(1,6)}$=4.22, p=0.086; main effect of time: $F_{(30,180)}$=1.988, p=0.003; interaction: $F_{(30,180)}$=1.30, p=0.151). The difference between trial types occurred during the 2 sec window before stimulus onset (t(12)=3.99, p=0.002). However, phase locked neurons did not modulate their firing rate over time, nor did they have a difference in firing rate between trial types (ANOVA; main effect of trial: $F_{(1,6)}$=1.19, p=0.316; main effect of time: $F_{(39,234)}$=0.519, p=0.992; interaction: $F_{(39,234)}$=0.889, p=0.660). Therefore, within-region delta (within ACC) and beta frequency (within PL) phase locking strength before the stimulus predicted the animals' correct or incorrect

choice after stimulus onset. Critically, the higher magnitude phase locking on correct trials was not spurious because it was eliminated when the trials were randomly shuffled (Within-region ACC ANOVA; main effect of data type: $F_{(1,3)}$=19.32, p=0.043; main effect of time: $F_{(30,90)}$=2.82, p<0.0001; interaction: $F_{(30,90)}$=2.13, p=0.002. Within-region PL ANOVA; main effect of data type: $F_{(1,6)}$=21.28, p=0.02; main effect of time: $F_{(30,180)}$=2.36, p<0.001; interaction: $F_{(30,180)}$=2.59, p<0.001).

The preferred phase was measured for each neuron to determine whether neurons that were phase locked to local oscillations might spike with similar timing on correct trials. We calculated the median angle of the resultant vector and tested for a significant difference in spike phase angle distributions between phase locked neurons using a circular analog of the Kruskal-Wallis Test. For the four neurons that were phase locked to delta oscillations in the ACC (**Figure 3.3E**), we found they shared a statistically similar phase angle of 3.20 rad (p=0.29). In the PL (**Figure 3.3F**), the seven neurons that were phase locked to PL beta oscillations also shared a statistically similar phase angle of 4.98 rad (p=0.2256). Therefore, across animals and neurons, ACC neurons that phase locked to ACC delta oscillations preferred the trough of delta oscillations, whereas PL neurons phase locked to the peak of PL beta oscillations.

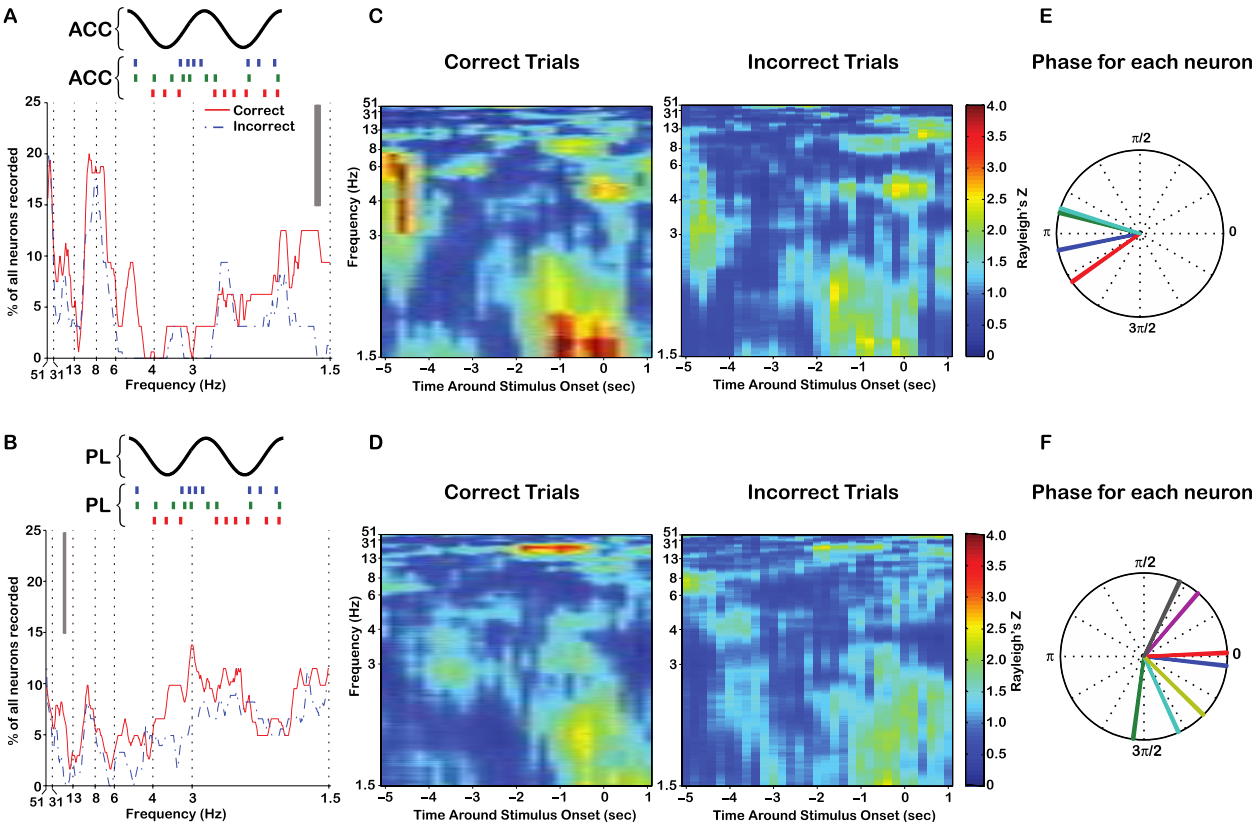

Figure 3.3. Within-region spike-LFP phase locking before stimulus onset.

(A) A schematic illustrating that the top panel (A, C, and E) are data using ACC spikes and ACC field potentials. The proportion of neurons that were significantly (Rayleigh's Test, $p<0.05$) phase locked to frequencies between 1.5 Hz and 50.0 Hz, during -2 to 0 sec before stimulus onset, on correct (red, solid) and incorrect (blue, dotted) trials. The width of the vertical bar indicates frequencies at which there was a reduction in the proportion of phase locked neurons on incorrect trials (Chi-squared test, $p<0.05$). (C) Mean, time-resolved, phase locking strength (Rayleigh's Z) is averaged across ACC neurons that phase locked to ACC delta (1 – 4 Hz) oscillations before stimulus onset. Stimulus onset is at t = 0 sec. Rayleigh's Z was calculated in 2 sec windows that were slid in 200 msec steps. Delta phase locking was evident during correct trials and was not present during incorrect trials. (E) The median phase angle of each ACC neuron illustrates that neurons are all phase locked to the trough of ACC delta oscillations (Circular Analog of Kruskal-Wallis Test, p=n.s. indicating no difference in phase angle distribution between neurons). (B) A schematic illustrating that the bottom panel (B, D, and F) is data using PL spikes and PL LFP. A larger proportion of neurons phase locked to beta (13 – 30 Hz) oscillations on correct trials. (D) These neurons phase locked to beta oscillations during the pre-stimulus period, only on correct trials. (F) The PL neurons phase locked to the peak of PL beta oscillations.

3.4.3 BETWEEN-REGION SPIKE-LFP PHASE LOCKING DURING PREPARATORY ATTENTION

As a measure of communication across PFC areas, we measured between-region spike-LFP phase locking. This analysis correlated spike times from the ACC with LFP phase recorded simultaneously in the PL (**Figure 3.4A - C**) and vice versa (**Figure 3.4D - F**). Across the entire frequency spectrum, significantly more neurons were phase locked on correct trials (**Table 1**) (χ^2=4.27, p=0.068 for ACC spikes locked to PL LFP and χ^2=6.31, p=0.029 for PL spikes locked to ACC LFP).

Four ACC neurons phase locked to PL beta LFP exclusively on correct trials (**Figure 3.4A**). On incorrect trials, there were no phase locked neurons. The reduced proportion of phase locked neurons was centered at 22 Hz. Time-resolved phase locking strength (**Figure 3.4B**) was reduced on incorrect trials (ANOVA; main effect of trial: $F_{(1,3)}$=8.50, p=0.061; main effect of time: $F_{(30,90)}$=4.49, p<0.001; interaction: $F_{(30,90)}$=3.67, p<0.001). The difference between trial types occurred during the 2 sec window prior to the stimulus onset and the window spanning -1.8 sec to 0.2 sec around stimulus onset (t(6)=4.37, p=0.005; t(6)=4.12, p=0.006). The phase locking observed during correct trials was greater than the level of synchrony expected by chance (ANOVA; main effect of trial: $F_{(1,3)}$=11.45, p=0.043; main effect of time: $F_{(30,90)}$=4.43, p<0.0001; interaction: $F_{(30,90)}$=5.73, p<0.0001). Again, these neurons exhibited no change in firing rate over time, and firing rate did not differ between trial types (ANOVA; main effect of trial: $F_{(1,3)}$=0.300, p=0.622; main effect of time: $F_{(39,117)}$=0.892, p=0.651; interaction: $F_{(39,117)}$=0.637, p=0.946). In addition to spike-LFP phase synchrony, we also measured LFP-LFP phase synchrony at 22 Hz as further evidence that the ACC and PL were communicating in the beta frequency range. PLV at 22 Hz was not different between correct and incorrect trials

(**Figure 3.4C**); however, they both were significantly greater than the magnitude of synchrony expected by chance (ANOVA; main effect of trial: $F_{(2,6)}=14.23$, $p=0.005$; main effect of time: $F_{(327,981)}=0.85$, $p=0.965$; interaction: $F_{(654,1962)}=0.90$, $p=0.947$).

Seven PL neurons were phase locked to ACC alpha LFP oscillations on correct trials, whereas none were phase locked on incorrect trials (**Figure 3.4D**). The reduction in the proportion of phase locked neurons was centered at 12 Hz. Time-resolved, phase locking strength was larger on correct trials (**Figure 3.4E**) (ANOVA; main effect of trial: $F_{(1,6)}=3.64$, $p=0.105$; main effect of time: $F_{(30,180)}=3.26$, $p<0.001$; interaction: $F_{(30,180)}=2.99$, $p<0.001$). The difference between trial types occurred during three consecutive windows (from -2 sec to 0.4 sec) around stimulus onset ($t(12)=4.50$, $p<0.001$; $t(12)=4.06$, $p=0.002$; $t(12)=2.26$, $p=0.043$). The phase locking strength on correct trials was not spurious (ANOVA; main effect of trial: $F_{(1,6)}=12.27$, $p=0.007$; main effect of time: $F_{(30,180)}=3.28$, $p<0.0001$; interaction: $F_{(30,180)}=3.01$, $p<0.0001$). These neurons exhibited no change in firing rate over time and firing rate did not differ between trial types (ANOVA; main effect of trial: $F_{(1,6)}=0.776$, $p=0.412$; main effect of time: $F_{(39,234)}=0.655$, $p=0.943$; interaction: $F_{(39,234)}=0.819$, $p=0.770$). The LFP-LFP phase synchrony between brain regions at 12 Hz increased over time before stimulus onset (**Figure 3.4F**). The PLV was not different between correct and incorrect trials, but was higher than expected by chance (ANOVA; main effect of trial: $F_{(2,6)}=67.11$, $p<0.001$; main effect of time: $F_{(170,510)}=2.33$, $p<0.001$; interaction: $F_{(340,1020)}=1.02$, $p=0.406$).

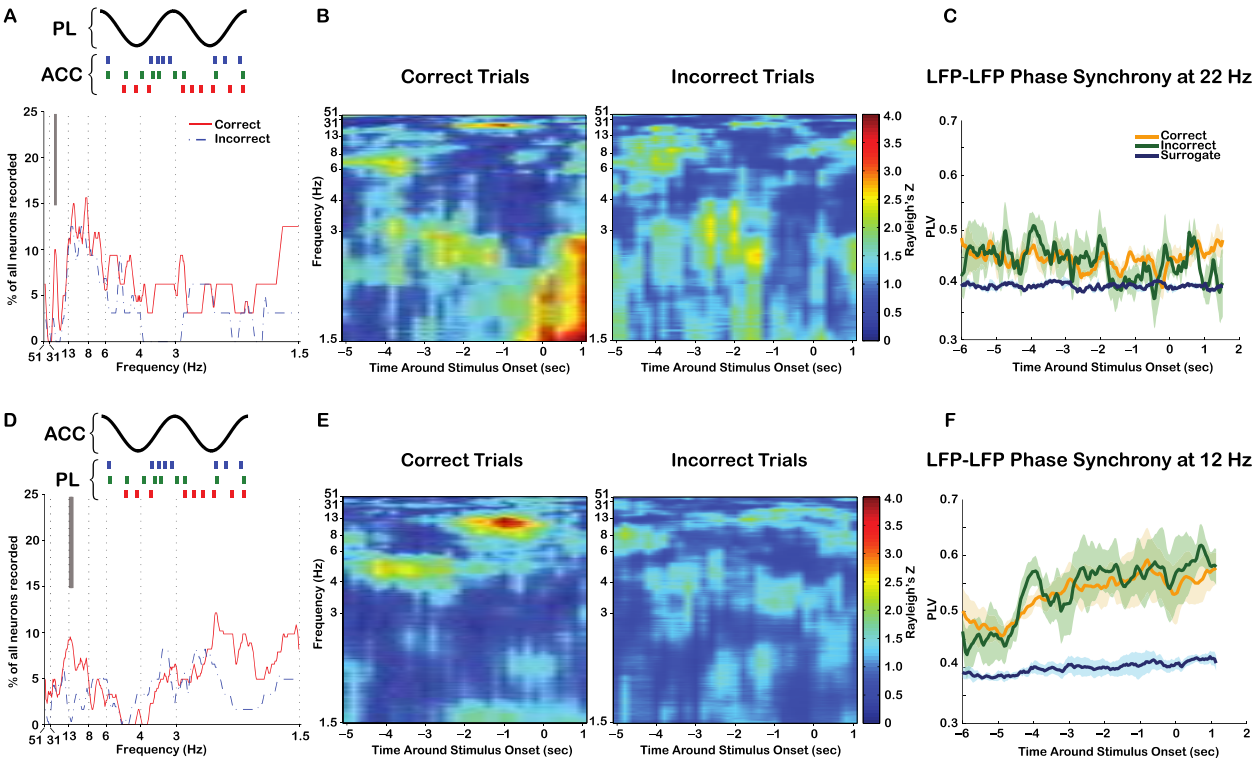

Figure 3.4. Between-region phase locking during the pre-stimulus period.

(A) A schematic illustrating that the top panel (A, B, and C) uses ACC neuron spikes and PL LFP oscillations. The proportion of neurons, between 1.5 Hz and 50.0 Hz, that significantly phase lock to LFP from -2 to 0 sec before stimulus onset on correct (red, solid) and incorrect (blue, dotted) trials. The width of the vertical bar indicates frequencies at which there was a reduction in the proportion of phase locked neurons on incorrect trials (Chi-squared test, p,0.05). (B) Mean, time-resolved phase locking strength (Rayleigh's Z) is averaged across the ACC neurons that phase locked to PL beta (13 – 30 Hz) LFP oscillations before stimulus onset. Stimulus is at t = 0 sec. Rayleigh's Z was calculated in 2 sec windows that were slid in 200 msec steps. Beta phase locking was present on correct trials and was not present on incorrect trials. The between-region spike-field phase locking was centered at 22 Hz. (C) Pre-stimulus phase synchrony between the LFP signals recorded in the ACC and PL at 22 Hz. LFP-LFP phase synchrony was quantified over time using a within trial phase locking value (PLV). Stimulus onset is at t = 0 sec. The mean PLV and its standard error (across rats) is shown for correct trials (orange), incorrect trials (green), and trial shuffled surrogate data (blue). During both correct and incorrect trials, a significantly high (compared to surrogate) level of LFP-LFP phase synchrony exists at 22 Hz before stimulus onset. (D, E, and F) Same as above. (D) A schematic illustrating that the bottom panel uses PL neuron spikes and ACC LFP oscillations. A larger proportion of neurons phase locked to alpha oscillations on correct trials. (E) These PL neurons phase locked to ACC alpha (8 -12 Hz) oscillations on correct trials, rather than incorrect trials, during the pre-stimulus period. The between-region phase locking was centered at 12 Hz. (F) Pre-stimulus LFP-LFP phase synchrony at 12 Hz increases over time on correct (orange) and incorrect (green) trials. In both trial types, a significantly high level of LFP-LFP synchrony occurs at 12 Hz before stimulus onset.

3.4.4 SINGLE ACC NEURONS PHASE LOCK TO DIFFERENT FREQUENCIES DURING PREPARATORY ATTENTION AND ACTION PREPARATION

As shown above, the ACC neurons that exhibited pre-stimulus phase locking to PL beta oscillations exclusively on correct trials also phase locked to delta oscillations after stimulus onset (**Figure 3.4B**). The average response latency (time of nose poke minus time of stimulus onset) on correct trials was 0.74±0.20 sec across all rats. This may indicate that neurons' delta phase locking on correct trials was due to changes in neural activity after stimulus onset and before the instrumental response to the chosen stimulus location. If this is the case, it is possible that these neurons also phase locked to delta oscillations on incorrect trials, but that it was not apparent in these plots because the average response latency on incorrect trials was 1.62±0.20 sec. Therefore, we characterized how this population of pre-stimulus beta phase locked neurons represented motor-related planning and/or motor execution after the stimulus onset.

Neural activity was aligned to the instrumental nose poke action and spike-LFP phase locking was measured before nose poke onset. Preparatory phase locking to PL delta oscillations occurred on both correct and incorrect trials and began less than 1 sec before nose poke onset (**Figure 3.5A**). The phase locking was of similar strength in both trial types; however, it began significantly earlier on correct trials (ANOVA using the mean from 1.5 – 2.4 Hz; main effect of trial: $F_{(1,3)}$=1.89, p=0.263; main effect of time: $F_{(25,75)}$=1.96, p=0.013; interaction: $F_{(25,75)}$=0.75, p=0.781). Furthermore, the observed phase locking was not spurious (ANOVA; main effect of trial (correct and surrogate): $F_{(1,3)}$=1.84, p=0.269; main effect of time: $F_{(25,75)}$=1.64, p=0.054; interaction: $F_{(25,75)}$=1.72, p=0.0376; post-hoc t-test at -500 msec, p=0.038). Although trial

shuffling reduced the average Rayleigh's Z (from -1 to 0 sec before nose poke action) to 1.60, which is below a Z-score indicating 2 standard deviations from the mean, relatively high levels of chance synchrony were found with delta oscillations. There was no change in firing rate before nose poke onset. The phase locking of ACC spikes to PL delta oscillations was accompanied by an increase in PL delta band power that was not significantly different between trial types (**Figure 3.5B**).

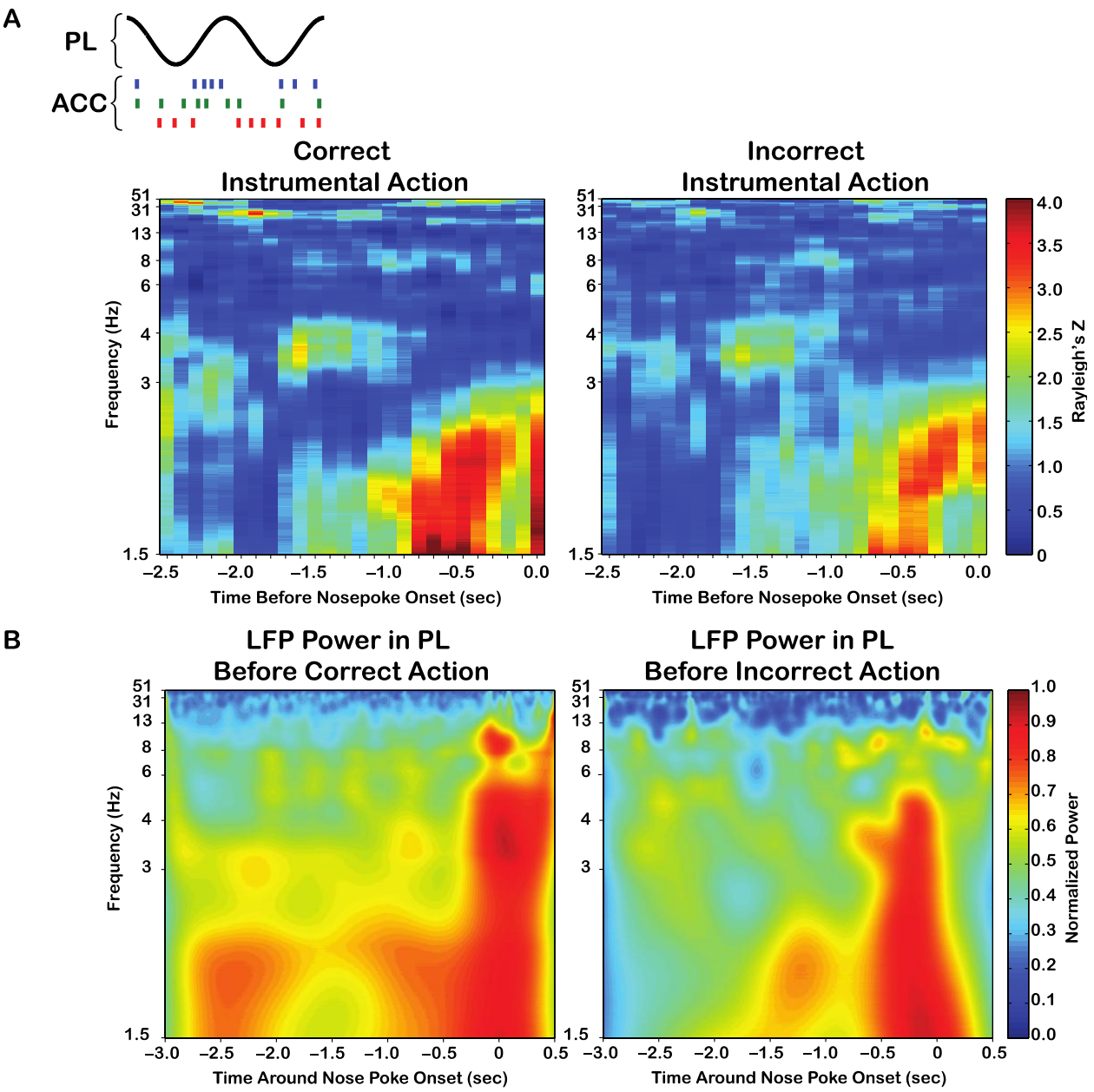

Figure 3.5. Phase locking of ACC units to PL delta oscillations before instrumental response.

(A) A schematic illustrating that the top panel uses spikes from ACC neurons that were phase locked to PL beta oscillations during the pre-stimulus period. Neural activity is aligned to the onset of instrumental action (nose poke) at t = 0 sec. The mean, time-resolved phase locking strength was calculated across these neurons using a 1 sec window, slid in 100 msec steps. Between-region delta oscillation phase locking occurs before the action during both correct and incorrect trials. (B) During the same time period, PL delta power is increased.

3.5 DISCUSSION

3.5.1 WITHIN- AND BETWEEN-REGION PHASE SYNCHRONY DURING PREPARATORY ATTENTION

We investigated synchrony between and within the rat ACC and PL before onset of a behaviorally relevant stimulus. Our analysis was primarily focused on the pre-stimulus period, which is when a preparatory top-down attention signal is generated by the PFC (Egner et al., 2008; Stokes et al., 2009; Summerfield et al., 2006; Chelazzi et al., 1993; Sylvester et al., 2009; Totah et al., 2009) and exerts its effects upon sensory cortex neurons (Fries, 2001; Fries et al., 2008; Roelfsema et al., 1997; Chelazzi et al., 1993; Driver and Frith, 2000). We found that, at certain frequencies, within- and between-region spike-LFP phase locking was reduced on incorrect trials, both in terms of the proportion of phase locked neurons and the strength of phase locking over time.

Within-region spike-LFP phase locked neurons shared a similar phase angle distribution. Given that within-region synchrony aligns multiple spike trains in time as a mechanism for increasing overall post-synaptic output (Fries, 2005; 2009), our data suggest that a population of neurons spike together in a temporal pattern aligned to the dynamics of local LFP oscillations and thus increase their output to downstream targets during top-down attention. These targets could include cortical areas involved in perception of the upcoming behaviorally relevant stimulus. Additionally, spike-LFP phase locking at the beta frequency was shared between both PL and ACC neurons that were phase locked to PL oscillations. Overall, these data support the hypothesis that neurons in the ACC drive beta LFP oscillations within the PL and entrain the

local PL neurons to the beta rhythm. Future studies recording larger populations of neurons within a single subject simultaneously will be necessary to further test this hypothesis.

Another key finding of this study was that spike-LFP phase synchrony occurred across a wide range of frequencies, although at many frequencies the proportion of phase locked neurons was not different between correct and error trials. Direct cortico-cortical projections between the recorded locations in the ACC and contralateral PL exist in the rat (Jones et al., 2005) and could directly mediate this synchrony. The observation that synchrony occurred at many frequencies is consistent with the results of others (Canolty et al., 2010) and supports the hypothesis that oscillation phase synchrony could be used to form multiple neuronal assemblies and bind the relevant neurons together at relevant times (Siegel et al., 2009; Singer 2009). However, given that synchrony at only certain frequencies was predictive of behavioral performance, many of these other synchronous interactions may relate to other PFC dependent processing that occurs at the same time as preparatory attention.

On the other hand, we found that between-region synchrony in the alpha and beta frequency ranges was related to behavioral performance, which suggests a role in the generation of a top-down attention signal. Beta frequency oscillations are associated with top-down attention (Buschman and Miller, 2007; Engel and Fries, 2010; Gross et al., 2006; Liang et al., 2002; Roelfsema et al., 1997). The degree of beta frequency coherence between frontal and parietal cortices during attention varies as a function of stimulus expectancy (Gross et al., 2006). Furthermore, beta frequency coherence between PFC areas and lateral intraparietal area is increased during top-down attention, rather than bottom-up attention (Buschman and Miller, 2007). The finding of increased alpha spike-LFP phase synchrony during top-down attention may seem paradoxical given that the alpha rhythm has been associated with a relaxed eyes

closed state, or "idling", and cognitive disengagement (Pfurtscheller, 2001). However, other behaving animal electrophysiology studies, in addition to our study, have described increased alpha frequency LFP-LFP coherence between multiple visual cortex areas in the cat and increased within-region spike-LFP coherence in the alpha frequency in visual cortex during top-down attention (Fries et al., 2008; Stein et al., 2000). Additionally, human EEG recordings have demonstrated increased alpha phase synchrony between the PFC and visual cortex during attention (Zanto and Gazzaley, 2009; Palva and Palva, 2007). Furthermore, it has been demonstrated that perturbing the PFC by transcranial magnetic stimulation reduces cross-cortical alpha synchrony, thus enhancing distracter-related visual cortex potentials and impairing attention task performance (Zanto and Gazzaley, 2009). Thus although the alpha rhythm has been associated with idling, our data and those of others support the hypothesis that alpha rhythms may be used to suppress the neural representation of distracters (Klimesch et al., 2007). Notably, individuals with schizophrenia and ADHD exhibit increased distractibility and reduced alpha phase synchrony (Bob et al., 2008), which suggests that a reduction in cortical alpha synchrony could move inhibitory executive functions into a dysfunctional state.

In addition to finding between-region spike-LFP phase synchrony during the pre-stimulus period, our study demonstrated that significant levels of between-region LFP-LFP phase synchrony occur during the pre-stimulus period. Although we did not find a difference in LFP-LFP phase synchrony between correct and incorrect trials, it is possible that the LFP signals in two distant cortical regions could synchronize and that local mechanisms govern whether or not local neurons will entrain to a distal rhythm. Alternatively, the phase difference relationship may be consistent over time (high PLV), but the value of the phase difference could differ between

correct and incorrect trials and thus adjust the effectiveness of neural communication between trial types (Tiesinga et al., 2008).

3.5.2 THE SAME NEURONS MAY PARTICIPATE IN SEPARATE NEURAL ASSEMBLIES SUPPORTION ATTENTION AND ACTION

We found that neurons in the ACC, which were phase locked to PL beta oscillations before stimulus onset, switched to delta oscillation phase locking after the stimulus and in preparation for the instrumental action. Previous work has shown that, in anticipation of an instrumental action in a rodent operant task, delta power increases within the rat PFC and LFP-LFP delta frequency coherence increases between the PL and the nucleus accumbens-core (Gruber et al., 2009). We replicate the finding of increased PL delta oscillation power before an instrumental action, but also demonstrate that between-region spike-LFP delta synchrony occurs between the ACC and PL before an instrumental action. In addition, we demonstrate that these same ACC neurons participate in top-down attention. Beta oscillation phase locking before the stimulus was specific to correct trials, whereas the delta oscillation phase locking occurred during both correct and incorrect trials. Therefore, while coordination of neural activity between the ACC and PL may be necessary during top-down attention, coordination also may be needed for action planning and/or execution, regardless of whether or not the action is the correct decision. From a systems perspective, the shift from beta to delta frequency may indicate that the same population of neurons participates in multiple cognitive processes by joining different neuronal assemblies, at different times, for different cognitive functions (Canolty et al., 2010).

3.5.3 GENERAL CONCLUSIONS

These data demonstrate that areas of the PFC dynamically interact during attention and action. Phase synchrony of LFP oscillations may serve as a neurophysiological mechanism by which multiple PFC areas can interact. These neurophysiological changes, which occur before the onset of a sensory stimulus, may serve to prime the neural representation of stimuli within sensory cortex and to improve the accuracy and speed of decision-making and behavior.

The fact that pre-stimulus phase synchrony was reduced during error trials suggests that diminished communication between multiple PFC areas could reflect an impaired cognitive state. Reduced synchrony between cortical regions has been observed in the brains of individuals with top-down attention deficits, such as those with ADHD and schizophrenia (Cubillo et al., 2010; Mazaheri et al., 2010; Murias et al., 2006; Phillips and Silverstein, 2003; Wang et al., 2009; Bob et al., 2008). Therefore, electrophysiological recordings, combined with pharmacological or genetic manipulations during the rodent sustained attention task (Totah et al., 2009), may provide a useful paradigm for studying normal and impaired top-down attention.

4.0 VTA NEURON ACTIVATION AND CORRELATION WITH ANTERIOR CINGULATE CORTEX OSCILLATIONS PREDICTS ATTENTIONAL ACCURACY

4.1 ABSTRACT

Preparatory attention selects upcoming stimuli that will guide behavior. This form of top-down attention is dependent on pre-stimulus activation of prefrontal cortex (PFC) regions, including anterior cingulate cortex (ACC), and is influenced by PFC dopamine neurotransmission, but the nature of this influence is not understood. Here we recorded from the ACC and ventral tegmental area (VTA), which contains PFC projecting dopamine and GABA neurons, during preparatory attention. In correlation with attentional accuracy, firing rate of distinct populations of VTA neurons increased during either the pre-stimulus period or after stimulus onset. VTA neurons synchronized with ACC gamma oscillations during the pre-stimulus period and with beta oscillations after stimulus onset. Event selective activation of distinct populations of VTA neurons and their correlation with different ACC oscillations suggest that VTA and ACC form functional networks that control both attention to a stimulus and the subsequent stimulus-guided behavior.

4.2 INTRODUCTION

Preparatory attention to an upcoming stimulus allows an organism to select sensory stimuli that will guide behavior (Driver and Frith, 2000). Prefrontal cortex (PFC) regions including the anterior cingulate cortex (ACC) are thought to provide a top-down attention signal that selects behaviorally relevant stimuli (Desimone and Duncan, 1995). Prior to the onset of a behaviorally relevant stimulus, preparatory attention selects a stimulus by priming the activity of sensory neurons that will represent the upcoming stimulus (Chelazzi et al., 1993; Luck et al., 1997). In line with this notion, during an attention task, neurons in the ACC increase their firing rate before the onset of a behaviorally relevant stimulus in a manner that correlates with attentional accuracy (Totah et al., 2009).

In addition to the involvement of PFC regions, clinical and basic studies strongly implicate dopamine neurotransmission in the regulation of attentional accuracy. For instance, drugs that increase extra-synaptic dopamine levels in the PFC are effective in treating attention deficit disorders (Swanson et al., 2010) and enhancing attentional accuracy in rats (Berridge et al., 2006). Reduction of dopamine neurotransmission in the PFC by receptor antagonists (Granon et al., 2000) or lesions of dopamine neurons in the ventral tegmental area (VTA), from whence PFC dopamine afferents originate, impair attention (Crofts et al., 2001). It is assumed generally that dopamine modulates the generation of a top-down attention signal in PFC regions (Noudoost and Moore, 2011). The nature of this modulation, however, is not well understood.

We explored the possibility that dopamine neurons in the VTA correlate with the oscillatory structure of ACC during preparatory attention and that this neural activity would correlate with attentional accuracy. Rhythmic gamma band activity in PFC regions has been associated with attention (Gruber et al., 1999; Gregoriou et al., 2009). Furthermore, VTA

neurons may be involved in the generation of gamma oscillations and synchronous neuronal activity in PFC regions (Peters et al., 2004; Bandyopadhyay et al., 2005; Tierney et al., 2008; Fujisawa and Buzsáki, 2011). We recorded single unit activity in the VTA and ACC using an attention task, which allowed for comparing accurate and inaccurate behavioral responses. We analyzed neural activity during two events: the pre-stimulus period when the ACC generates a top-down preparatory attention signal (Totah et al., 2009), and after stimulus onset because VTA neurons have been observed to exhibit a phasic response to the presentation of salient stimuli (Schultz, 1998; Horvitz, 2000). Phase locking between VTA spikes and ACC local field potential (LFP) oscillations, as well as phase locking between the LFP oscillations, in each brain region were compared between correct and incorrect trials. During the pre-stimulus period, firing rate of putative dopamine and GABA neurons in the VTA and the strength of their coupling to ACC gamma oscillations were associated with attentional accuracy. After stimulus onset, the firing rate of VTA neurons and coupling to ACC beta oscillations were associated with attentional accuracy. Our data suggest that dopamine and GABA neurons in the VTA influence the control of preparatory attention and stimulus-guided behavior by PFC regions.

4.3 METHODS

4.3.1 SUBJECTS AND BEHAVIORAL METHODS

Male Sprague-Dawley rats were used (n=20). All rats were housed on a reverse light cycle and tested during their active phase. All animal use procedures were approved by and carried out in compliance with the University of Pittsburgh Institutional Animal Care and Use

Committee (IACUC). The behavioral task has been described in detail in our previous work (Totah et al., 2009). Briefly, rats were trained and tested in operant chambers with a house light on the ceiling, 3 stimulus ports with internal LED lights on one wall, and an illuminated food magazine on the wall opposite from the stimulus ports. Nose pokes into the stimulus ports and the food magazine were registered by photosensors. A correct response, consisting of a nose poke into an illuminated stimulus port, was rewarded with sucrose. An incorrect response into an unlit stimulus port resulted in an extinguished house light. The rat was required to nose poke into a stimulus port within 5 sec after stimulus onset; otherwise, the house light was extinguished (i.e., an omission trial). The rat initiated each trial with a poke into the food magazine, which either contained sucrose pellets or was empty depending on whether the previous trial was correct or an error.

At the start of a trial, an 8 sec pre-stimulus period passed before the stimulus onset. On each trial, one of the 3 stimulus ports would illuminate. The location of the stimulus was selected at random from the three stimulus ports. There was a balanced distribution of the selection of the 3 ports, but the order of presentation was random. Each session lasted 30 minutes. Based on satisfying performance criteria (see previous work for detailed training information (Totah et al., 2009)), the stimulus duration was gradually reduced to 300 msec. Rats were deemed ready for electrode implantation when they met the performance criterion of > 70% accuracy [i.e., # of correct responses / (# of correct responses + # of incorrect responses)] and < 20% omissions (i.e., # of omitted responses / # of total trials) for six consecutive sessions using the 300 msec cue duration. The mean number of sessions needed to complete training was 42 sessions. Rats exhibited attentive behavior, whereby they oriented to the operant chamber wall that contained the stimulus ports and waited for the stimulus. Orientation to the wall of stimulus

ports began approximately 2 sec before stimulus onset and was maintained throughout the pre-stimulus period. It was rare (<1 % of trials across many 30 min sessions) for rats to orient away from the stimulus ports once they had begun orienting. Sessions were videotaped and reviewed in order to eliminate trials on which the rat did not directly face the stimulus ports because those were not stereotypical task behaviors.

4.3.2 ELECTROPHYSIOLOGY PROCEDURE

Rats were implanted under isoflorane anesthesia with microelectrode arrays of 8 Teflon-insulated stainless steel wires with an impedance of 300 – 700 kΩ (NB Labs, Denison, TX). Twelve rats were implanted with one array in the VTA (-5.1 to -6.1 mm posterior to bregma, +0.4 to +0.6 mm lateral to bregma, and -8.0 mm ventral from the dura surface). Another 8 rats were implanted with 2 arrays; one placed in the VTA and the other in the ipsilateral ACC: +1.1 to +2.1 mm anterior to bregma, +0.4 to +0.6 mm lateral to bregma, and -2.1 mm ventral from the dura surface.

After 1 week of recovery, rats were acclimated to the recording cable in the operant box for four 30-min sessions and re-trained to criterion performance. Once performance was stable and above criterion, a 30 min session was recorded. Single units and LFP were recorded via a unity-gain FET headstage and lightweight cabling, which passed through a commutator to allow freedom of movement. Neural activity was amplified using a 1,000X gain and single unit activity was band pass filtered at 300 – 8,000 Hz and LFPs were band pass filtered at 0.7 – 170 Hz. Neural activity was digitized at a rate of 40 kHz and LFPs were down sampled to 1 kHz using Recorder software (Plexon, Inc.). Single unit activity was digitally high-pass filtered at 300 Hz and LFPs were digitally low-pass filtered at 125 Hz. If voltage crossed an experimenter-defined

threshold, the single unit trace was recorded for 500 □sec before and 2500 □sec after threshold crossing, yielding a 3.0 msec duration waveform.

4.3.3 CLASSIFICATION OF SINGLE UNITS INTO GROUPS OF PUTATIVE NEURONS

Spike sorting was performed using Offline Sorter (Plexon, Inc.) using manual sorting methods described previously (Totah et al., 2009). Single units recorded in the VTA were separated into 3 groups: putative dopamine, putative GABA, and "Other" units that could not be classified. Classification was according to previously published methods (Grace and Bunney, 1983; Steffensen et al., 1998; Fiorillo et al., 2003; Ungless et al., 2004; Kim et al., 2010), and based upon baseline firing rate and the waveform duration. Waveform duration was calculated from the average spike waveform across all spikes. Single units that had a firing rate <= 10.0 Hz and a duration of >= 1.5 msec were assigned to the putative dopamine neuron group. Single units that had a firing rate > 10.0 Hz and waveform duration of < 1.5 msec were assigned to the putative GABA neuron group. All other single units were assigned to a group designated as "Other" neurons. The use of these electrophysiological criteria for classifying VTA neurons recorded *in vivo* in the awake rat may permit units that could use glutamate as a neurotransmitter to be classified as putative dopamine neurons (Ungless et al., 2004); however, it is unlikely that they use GABA as a neurotransmitter (Steffensen et al., 1998). Neural activity was analyzed both across all recorded VTA single units and according to these 3 groups of putative neurons.

4.3.4 ELECTROPHYSIOLOGICAL DATA ANALYSIS

Electrophysiological data were analyzed with custom scripts written in MATLAB (Mathworks, Natick, MA). Single unit spiking was aligned to stimulus onset (t = 0 sec) and binned into 250 msec bins for the pre-stimulus period and 20 msec bins for the post-stimulus period. The pre-stimulus period was from -4 sec to 0 sec and the post-stimulus period was from 0 sec to 240 msec (but plotted until 500 msec). The shorter post-stimulus period was chosen to correspond with the characterized duration of the dopamine neuron response to stimuli (Schultz, 1998). Firing rate was averaged across trials within trial type. For normalization (Z-score), we used the -5.75 sec to 4.0 sec as a baseline period to calculate a mean and standard deviation of baseline firing rate. Single units were considered to be responsive (i.e., increase in firing rate from baseline) if there were at least 3 consecutive time bins with Z>2. Incorrect trials were interpreted as being indicative of a preparatory attention signal that was inadequate for selecting the correct stimulus location.

In eight rats that were implanted in both the VTA and ipsilateral ACC, an LFP signal was collected from one electrode on the ACC array. The signal was aligned to the behavioral event of interest and trials with clipping were removed from analysis. In order to study spike-LFP phase synchrony, the LFP signal was convolved with a complex Morlet wavelet, resulting in a complex number, W(f,t), in scale, f, and time, t. The conversion from scale to frequency resulted in plots of frequency space appearing non-uniform because scale resolution is related inversely to frequency. Spike-LFP phase synchrony was calculated in 1 sec time windows slid in 100 msec steps (pre-stimulus period) and in non-overlapping 80 msec time windows (post-stimulus period). Although the post-stimulus time window was small compared to the period of slow (i.e., delta and theta) oscillations, we calculated instantaneous LFP phase for – 8 sec to + 3 sec around

stimulus onset and used the spike times available in the 80 msec post-stimulus window to select the corresponding phase angles. To assess the phase locking characteristics of a neuron, we collected the LFP phase angles that corresponded to the spike times for all spikes within a time window, across all trials. A neuron was considered significantly phase locked if the distribution of spike phase angles departed from a uniform circular distribution (Rayleigh's test for circular uniformity, $p<0.05$). The circular statistics toolbox (MATLAB) was used for statistical analyses of spike-LFP phase synchrony (Berens, 2009). If any time window had <6 spikes, we could not rely on Rayleigh's test (Fisher, 1996) and we chose to remove that neuron from analysis. These criteria left 38 neurons and 22 neurons for phase locking analysis during the pre-stimulus period and post-stimulus period, respectively. The value of Rayleigh's Z statistic for a neuron was used as a measure the strength of spike-LFP phase locking. Rayleigh's Z was calculated by

$$Z = nR^2$$

where R is the mean resultant phase vector length of n spikes. The p-value for Rayleigh's test for circular uniformity is calculated as

$$p = e^{-Z} * (1 + \frac{2Z - Z^2}{4n} - \frac{24Z - 132Z^2 + 76Z^3 - 9Z^4}{228n^2})$$

We controlled for spurious phase locking, while keeping the timing of behavioral events intact, by computing phase locking between spikes from a trial and the LFP signal from a different, randomly selected trial (without replacement). A distribution of the expected spurious phase locking was formed by calculating Rayleigh's Z values on 200 sets of trial shuffled data. For each time-frequency bin, the upper limit of the 95% confidence interval of the distribution was selected as the expected spurious Rayleigh's Z for that particular neuron in that particular time-frequency bin. Rayleigh's Z values were compared between the original data (correct trials) and the shuffled data using a 2-way repeated measures ANOVA (with factors data type and

time). In order to compare phase locking between correct and incorrect trials, while equalizing for any bias due to unequal sample sizes, we employed a resampling procedure. For a given neuron with *x* number of spike times in the correct condition and *y* number of spike times in the incorrect condition (where $x > y$), we removed *y* number of spikes (selected randomly without replacement) from the correct condition and replaced them with all of the *y* number of spikes from the incorrect condition. We calculated Rayleigh's Z for the new group with replaced spike times. We repeated this resampling procedure 5,000 times and calculated Rayleigh's Z on each iteration. We then used the mean of the Z distribution to calculate a p-value for that neuron. Thus, the same number of spikes per neuron is present in both correct and incorrect conditions. Accordingly, conditions labeled as "incorrect" in the phase locking analysis reflect the degree to which the insertion of the spike times from incorrect trials degrades or enhances phase locking observed on correct trials.

Phase synchrony between LFP signals in the VTA and ACC was measured as a phase locking value (PLV) over time in each trial and averaged across trials within animals. PLV was measured for the pre-stimulus time period; however PLV was not calculated for the post-stimulus time period because the small time window of spike-field phase locking (80-160 msec) is much smaller than the time window of 6 – 10 oscillation periods required to accurately measure PLV. The constancy of the difference in phase between the LFP signals at electrodes, *j* and *k*, was calculated as a PLV, such that

$$PLV_{j,k}(f,t) = \frac{1}{N}\left|\sum_{N} e^{i(\varphi_i - \varphi_j)}\right|$$

where N is the number of samples in the time window, φ is phase, and | | is the complex modulus (Lachaux et al., 1999). PLV ranges from 0 to 1 (constant phase difference). Phase angle first was extracted from W(*f*,*t*) using,

$$\theta(f,t) = \tan^{-1}\frac{\Im\{W(f,t)\}}{\Re\{W(f,t)\}}$$

where $\theta(f,t)$ is phase angle at a time and frequency point and $\Im$ and $\Re$ are the imaginary and real components of the wavelet coefficients, respectively. PLV was calculated using a time window consisting of 10 cycles and slid in steps of $1/10^{th}$ of a time window. Because synchrony between two oscillatory signals can occur by chance, we used a surrogate data set to determine if the occurrence of synchrony was greater than expected by chance. We computed a distribution of PLVs that would be expected if the two signals were independent of one another by computing 200 surrogate PLV values with a random trial selected for one of the electrodes (see above references). If the observed PLV was higher than the 95^{th} percentile of the surrogate PLV, then it was considered significant.

4.4 RESULTS

4.4.1 THE FIRING RATE OF VTA UNITS DURING PREPARATORY ATTENTION

Single units in the VTA (123 units from 20 rats) were a heterogeneous population with a variable average firing rate and waveform duration. Across this population, we found that 29 (23.6%) increased their firing rate during the pre-stimulus period on correct trials. On incorrect and omission trials, the proportion of responsive units was reduced to 12 (9.8%) and 8 (6.5%) units, respectively (**Figure 4.1A**). The proportion of activated units was significantly different between correct trials and incorrect trials (χ^2=8.46, p=0.004), as well as between correct trials and omission trials (χ^2=14.03, p<0.0001). Furthermore, the mean increase in firing rate across

pre-stimulus responsive units was associated with attentional accuracy (**Figure 4.1B**). Units were most activated during correct trials, while during incorrect trials the level of activation was significantly reduced and, during omission trials, the firing rate did not change from the baseline rate (ANOVA; interaction, $F_{(46,1288)}=10.27$, $p<0.0001$). The time-course of activation during correct trials was stable and lasted for several seconds (**Figure 4.1C**). Most responsive units became activated during the final 2 sec before stimulus onset, which corresponds with the approximate time of orientation to the wall of stimulus ports (Totah et al., 2009).

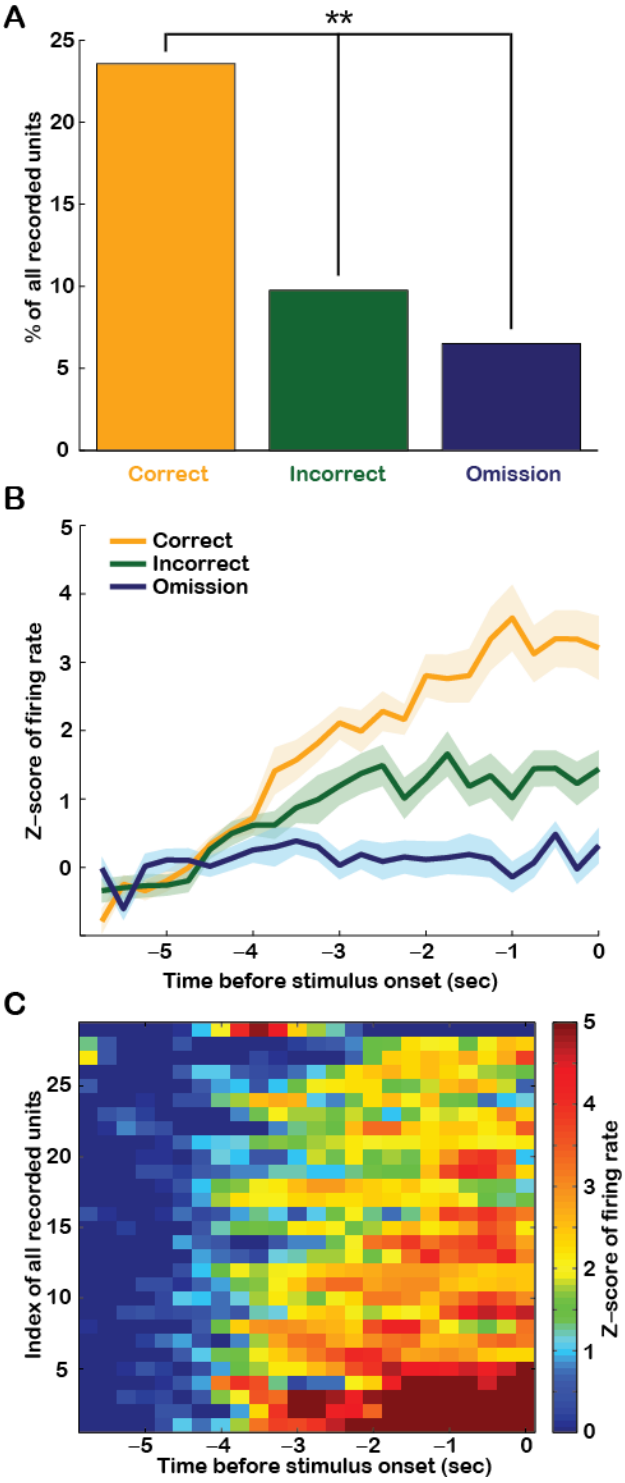

Figure 4.1. VTA units increased firing rate before the stimulus and the number of responsive units and magnitude of activation predicted attentional accuracy.

(A) During correct trials, the largest proportion of units (out of 123 total) was activated, whereas the proportion of activated units was reduced during incorrect and omission trials (**p<0.01). (B) The mean change in normalized

firing rate of units that were significantly activated before the stimulus. Stimulus onset is at t = 0 sec and plotted using 250 msec bins. The magnitude of change was largest during correct trials and reduced during the other trial types (time x trial interaction, $p<0.0001$). During omission trials, the firing rate did not change. (C) The increase in firing rate was stable and lasted for several seconds. The change in normalized firing rate during correct trials is plotted over time (250 msec bins) for each significantly activated unit. Individual units are displayed on the y-axis and time around stimulus onset is displayed on the x-axis. A Z-score >2 (yellow) signified a significant increase in firing rate from each units's baseline firing rate. Most units were activated in the final 2 sec, which corresponded to the approximate time of orientation to the wall of stimulus ports.

We assessed how this stable and sustained activation was represented in different groups of VTA units according to putative neuronal type. The VTA contains neurons that primarily use dopamine or GABA as neurotransmitter (Nair-Roberts et al., 2008). We divided the single units into groups using standard extracellular electrophysiology criteria (see Methods). Given that using these criteria to classify VTA units as dopamine neurons could lead to misclassification (Margolis et al., 2006), we characterized the task-related activity of all recorded VTA single units and, when separating them into putative groups, we also show data for "Other" units that could not be classified using these criteria. **Figure 4.2A** shows representative example waveforms of a putative dopamine neuron and a putative GABA neuron. We recorded 72 putative dopamine neurons (mean and standard deviation of firing rate=3.40±2.31 Hz), 14 putative GABA neurons (mean firing rate=33.38±21.61 Hz), and 37 other neurons (mean firing rate=19.43±20.48 Hz). **Figure 4.2B** is a plot of the firing rate and waveform duration for all recorded single units (N=123). There is a clear separation between high baseline firing rate, short-duration waveform single units (putative GABA neurons) and low baseline firing rate, long-duration waveform single units (putative dopamine neurons).

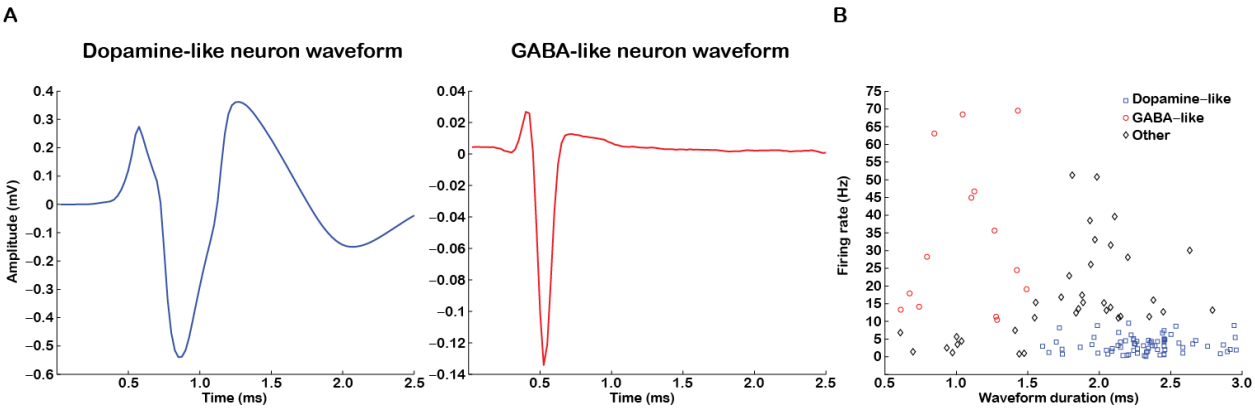

Figure 4.2. VTA single units were classifed as putative dopamine and GABA neurons based upon electrophysiological criteria of firing rate and waveform duration.

(A) Putative dopamine neurons were characterized by long waveform duration, whereas putative GABA neurons were characterized by short waveform duration. The waveform traces are the mean waveform from a single example unit. (B) Using firing rate and waveform duration to classify single units produced 2 groups of units. In order to assess VTA neural activity during attention, we compare VTA unit activity both as a single collection of all recorded units and as separate collections of putative dopamine, GABA, and other neurons that could not be classified.

A similar proportion of each putative neuron group was activated during attention (Chi-squared test, p=n.s.) (**Figure 4.3A**). The magnitude of activation for each group of neurons correlated with attentional accuracy (**Figure 4.3B, 3C, 3D**) (ANOVA; Dopamine group; interaction: $F_{(46,690)}=8.41$, $p<0.0001$; GABA group; interaction: $F_{(46,184)}=3.59$, $p<0.0001$; Other group; interaction: $F_{(46,322)}=1.48$, $p=0.028$). Therefore, putative dopamine and GABA neurons exhibit sustained activation during attention that is predictive of attentional accuracy.

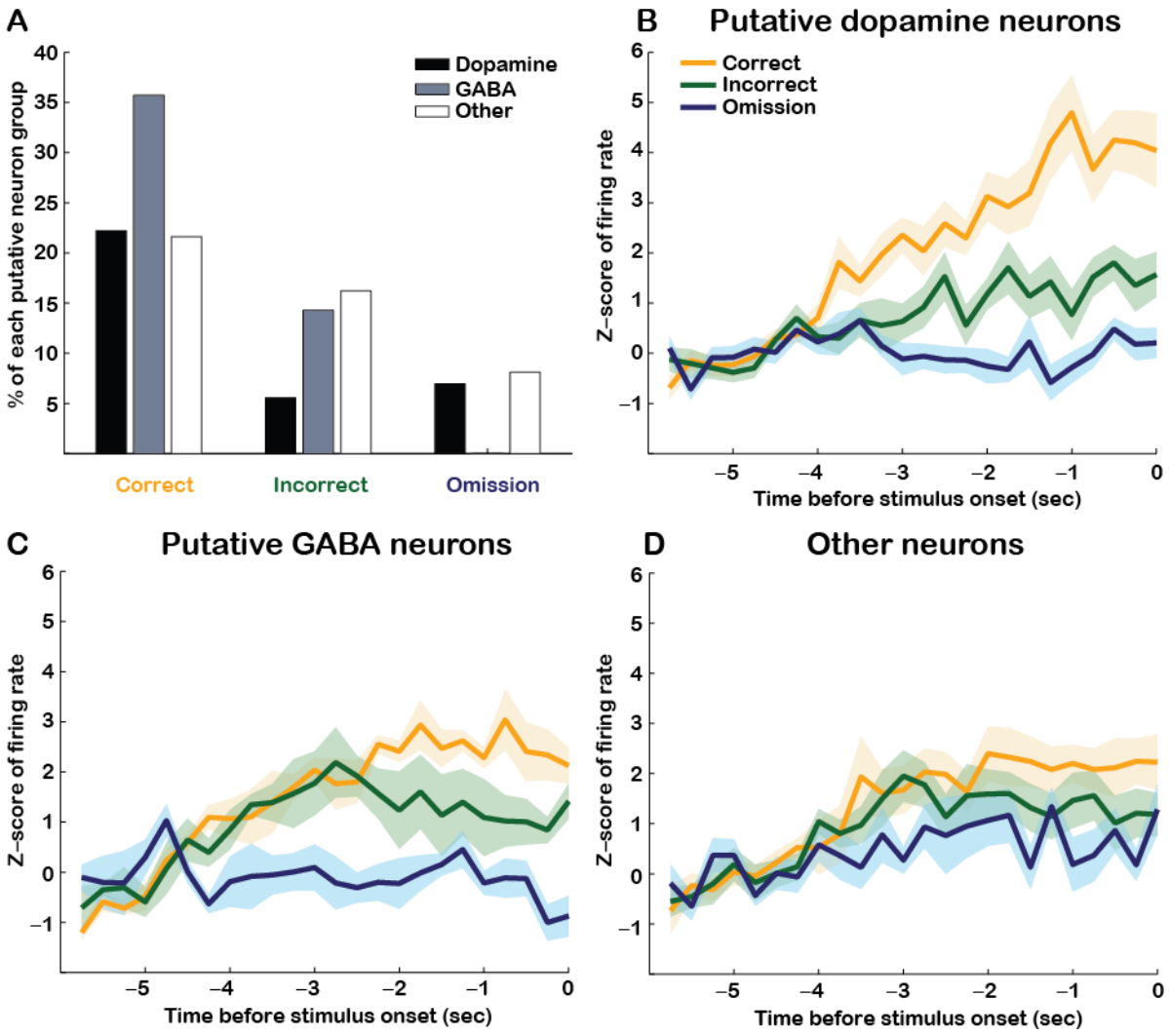

Figure 4.3. The population of VTA units that increased firing rate before the stimulus onset consisted of putative dopamine and GABA neurons.

(A) The population of VTA units that increased firing rate consisted of similar proportions of each putative neuron group. (B, C, D) All three groups of neurons were activated in a manner that predicted attentional accuracy. The highest level of activation was during correct trials (time x trial interaction, dopamine group: $p<0.0001$, GABA group: $p<0.0001$, other group: $p<0.05$).

4.4.2 VTA UNIT SPIKE LOCKING TO ACC GAMMA OSCILLATIONS DURING PREPRATORY ATTENTION

We measured spike-LFP phase locking using 38 VTA single units and ACC LFP oscillations during the 1 sec before stimulus onset (see Methods regarding spike number criteria that led to single unit removal). A schematic representation is shown in **Figure 4.4A**. During this time period, there was prominent phase locking of VTA spikes to theta (~ 6 Hz), alpha (~ 8 – 10 Hz) and gamma (~30 – 50 Hz) LFP oscillations in the ACC. Thirty-three out of 38 single units (86.8%) were phase locked to at least one frequency between 5 and 50 Hz. Correct trials were associated with significantly more units phase locked to gamma oscillations than incorrect trials between 38.7 – 41.1 Hz (denoted by orange marker) (**Figure 4.4B**, Fisher's Exact Test (FET), p=0.005). Within this frequency range (38.7 – 41.1 Hz), seven units were phase locked on correct trials, while none were phase locked during incorrect trials. In order to see how phase locking changed over time, we calculated phase locking in 1 sec windows slid in 100 msec steps around stimulus onset. During correct trials, phase locking was increased before stimulus onset (**Figure 4.4C**). Phase locking was significantly higher than shuffled trial order control (ANOVA; interaction: $F_{(70,420)}=3.191$, $p<0.0001$). On incorrect trials, phase locking was significantly reduced from -1200 msec to +200 msec around stimulus onset (ANOVA; interaction: $F_{(70,420)}=2.97$, $p<0.0001$; all post-hoc t-tests on the 1 sec windows, $p<0.01$) (**Figure 4.4D**). We also measured LFP-LFP phase synchrony between the ACC and VTA averaged across the frequencies at which VTA spikes were phase locked (38.7 – 41.1 Hz) (**Figure 4.4E**). Synchrony was greater than expected by chance (ANOVA; trial: $F_{(2,70)}=14.75$, $p<0.0001$, time: $F_{(297,3564)}=1.16$, $p=0.041$, interaction: $F_{(594,7128)}=0.960$, $p=0.747$). Therefore, the strength of VTA

spike phase locking to ACC gamma oscillations and the number of phase locked units during the pre-stimulus period was predictive of attentional accuracy.

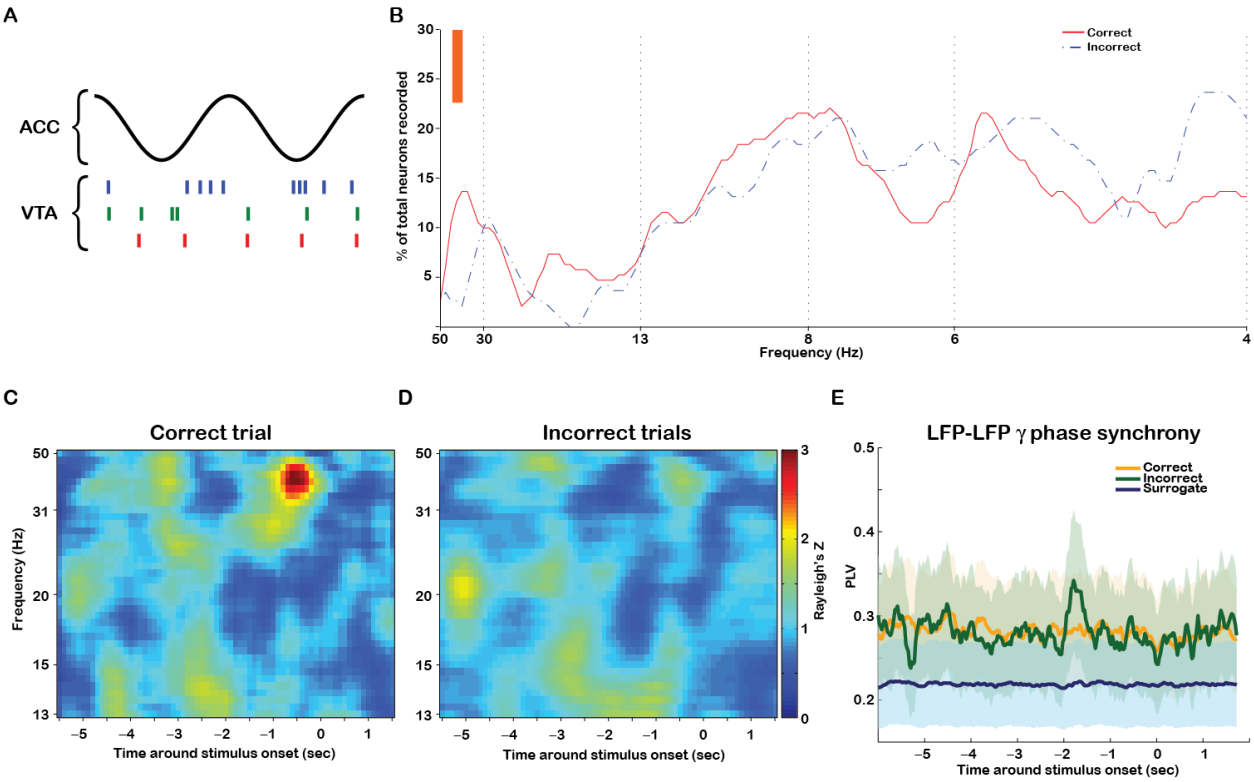

Figure 4.4. VTA units were phase locked to ACC gamma oscillations during the pre-stimulus period in a manner that predicted attentional accuracy.

(A) A schematic demonstrating that we calculated spike-LFP phase locking strength for each VTA neuron in 1 sec windows at frequencies between 1 – 50 Hz. (B) Prominent phase locking was observed in the theta, alpha, and gamma frequency bands. Between 38.7 – 41.1 Hz, significantly more units were phase locked during the correct trials compared to incorrect trials (FET, $p<0.01$, orange bar). (C, D) The mean phase locking strength of gamma locked units was significantly higher during correct trials (C) (time x trial interaction, $p<0.0001$) compared to incorrect trials (D). The increase in gamma phase locking occurred just before stimulus onset (t = 0 sec). (E) The mean LFP-LFP phase synchrony averaged across rats was greater than expected by chance during both correct and incorrect trials; however, it was not different between trial types and did not change over time.

4.4.3 VTA UNIT FIRING RATE RESPONSE AFTER STIMULUS ONSET

A short duration phasic increase in firing rate was observed within 250 msec after the stimulus onset in 21 out of 123 single units (17.1%) during correct trials. Although rats were oriented to the stimulus ports during both correct and incorrect trials, the proportion of responsive units was reduced significantly during incorrect trials and omission trials compared to correct trials (**Figure 4.5A,** FET; $p=0.0006$ for correct versus incorrect trials and $p<0.0001$, for correct versus omission trials). In contrast to the heterogeneous population of putative dopamine and GABA neurons that were activated before stimulus onset (see **Figure 4.3A**), this population of units consisted of primarily putative dopamine neurons (**Figure 4.5B**). During correct trials, 27.8% of the putative dopamine neurons exhibited post-stimulus activation. Twenty out of 72 putative dopamine neurons responded, whereas only 1 out of 14 putative GABA neurons responded. The change in firing rate was reduced during the incorrect and omission trials (**Figure 4.5C**) (ANOVA; interaction: $F_{(48,960)}=11.58$, $p<0.0001$). The population of units that responded during the post-stimulus period of correct trials did not increase firing rate during the pre-stimulus period (**Figure 4.5D**). The phasic response was observed only after onset of the stimulus. Therefore, primarily putative dopamine neurons showed a phasic response after stimulus onset that predicted attentional accuracy.

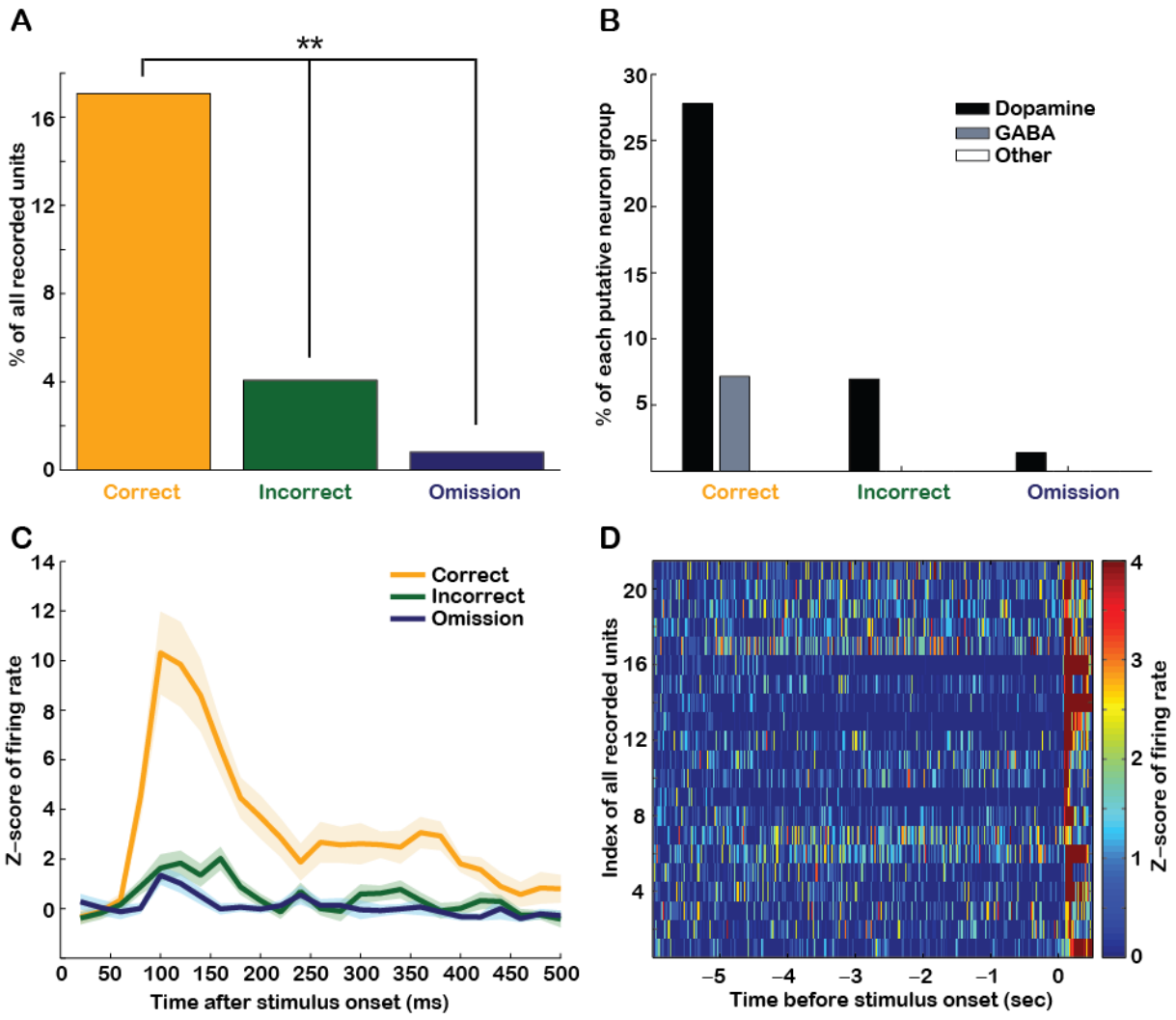

Figure 4.5. VTA units exhibited a post-stimulus activation that reflected the subsequent behavioral response. (A) The proportion of units that had a phasic response after the stimulus was the largest on correct trials and reduced on the other trial types (**p<0.001). (B) The group of units that exhibited a post-stimulus response were putative dopamine neurons. (C) The mean response of the activated neurons (20 msec bins) after stimulus onset (t = 0 sec). The largest activation was on correct trials and the magnitude was reduced during other trials (time x trial interaction, p<0.0001). (D) The normalized change in firing rate for each significantly activated neuron around stimulus onset (t = 0 sec) on correct trials. Individual neurons are displayed on the y-axis and time around stimulus onset is displayed on the x-axis. A Z-score >2 (yellow) signified a significant increase in firing rate from each neuron's baseline firing rate. These neurons did not have a seconds-long activation before the stimulus onset; rather they had a short-duration activation within 250 msec after the stimulus onset.

4.4.4 VTA UNIT SPIKE LOCKING TO ACC BETA OSCILLATIONS AFTER STIMULUS ONSET

Given that putative dopamine neurons had a phasic response during the post-stimulus period that lasted until about 180 msec after stimulus onset, we assessed phase locking of VTA single unit spikes to LFP oscillations in the ACC during the 0 – 180 msec post-stimulus window. During the post-stimulus period, correct trials were associated with significantly more units phase locked to ACC beta oscillations in comparison to incorrect trials between 13.1 and 13.9 Hz (denoted by orange marker) (FET, p=0.053). In this frequency range (13.1 – 13.9 Hz), 4 units (out of 22 VTA units total, see Methods for neurons excluded due to low spike rate) were phase locked to beta oscillations, while none were phase locked on incorrect trials (orange bar, **Figure 4.6A**). Spike-LFP phase locking to ACC beta oscillations occurred in time windows between 20 – 180 msec after stimulus onset during correct trials (**Figure 4.6B**). Note that, while phase locking strength was compared statistically between trial types and the shuffle control until 180 msec after the stimulus, data were plotted until 500 msec post-stimulus. Observed phase locking was significantly greater than the shuffle trial control during the window spanning 100 – 180 msec after stimulus onset (ANOVA; interaction: $F_{(10,30)}=2.57$, p=0.022; post-hoc t-test corresponding to the 100 – 180 msec window, t(6)=6.20, p=0.006). The beta phase locking strength was reduced during incorrect trials in the 100 – 180 msec window (**Figure 4.6C**) (ANOVA; interaction: $F_{(10,30)}=3.97$, p=0.002; post-hoc t-test corresponding to the 100 – 180 msec window, t(6)=5.13, p=0.002).

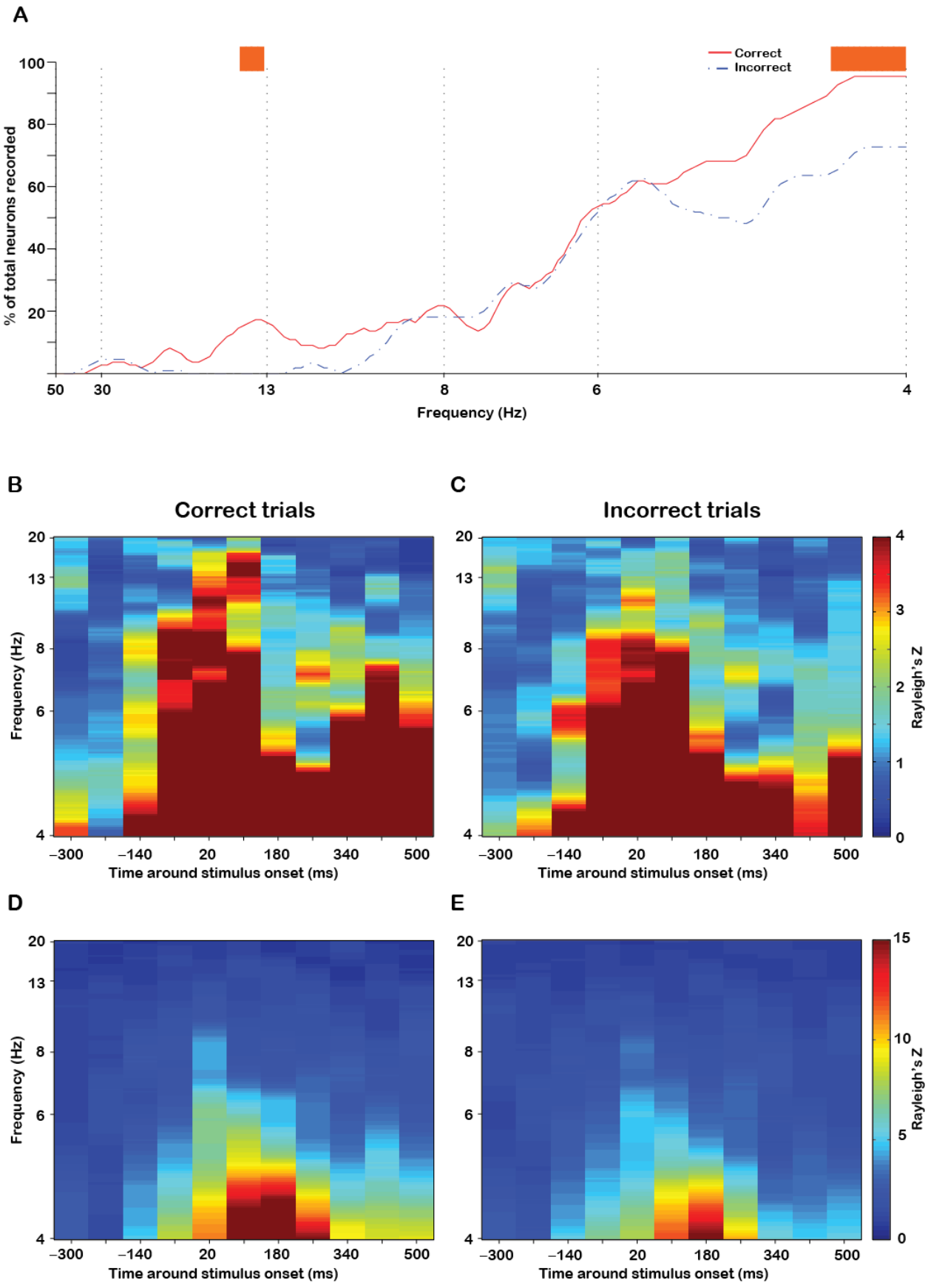
A
Correct
Incorrect
% of total neurons recorded
100
80
60
40
20
50
30
13
8
6
4
Frequency (Hz)
B
Correct trials
C
Incorrect trials
Frequency (Hz)
20
13
8
6
4
−300
−140
20
180
340
500
Time around stimulus onset (ms)
Rayleigh's Z
4
3
2
1
0
D
E
15
10
5

Figure 4.6. VTA units were phase locked to ACC 4 Hz and beta oscillations during the stimulus in a manner that predicted attentional accuracy.

We calculated spike-LFP phase locking strength for each VTA unit in 80 msec windows. (A) After stimulus onset, prominent phase locking was observed in the 4 Hz and beta frequencies. Between 4.0 – 4.4 Hz and between 13.1 – 13.9 Hz, significantly more units were phase locked during the correct trials compared to incorrect trials (FET, $p=0.053$ for beta and $p<0.05$ for ~ 4 Hz, orange bars). (B, C) The mean phase locking strength of beta locked units was significantly higher during correct trials (B) compared to incorrect trials (C) (time x trial interaction, $p<0.0001$). Stimulus onset at t = 0 sec. (D, E) The mean phase locking strength of 4 Hz locked units was significantly higher during correct trials (D) compared to incorrect trials (E) (time x trial interaction, $p=0.001$).

Correct trials also were associated with significantly more units phase locked to ACC 4 Hz oscillations in comparison to incorrect trials between 4.0 and 4.4 Hz (denoted by orange marker, **Figure 4.6A**). In this frequency range (4.0 – 4.4 Hz), 21 units (out of 22 VTA units total) were phase locked to 4 Hz during correct trials and the number was reduced significantly to 16 neurons during incorrect trials (FET, $p=0.021$). Phase locking to ACC 4 Hz oscillations also occurred after stimulus onset (**Figure 4.6D**). However, the phase locking was not different between the observed data and the shuffled trial order control (ANOVA; trial: $F_{(1,20)}=0.04$, $p=0.838$, time: $F_{(10,200)}=7.45$, $p<0.0001$, interaction: $F_{(10,200)}=1.12$, $p=0.351$). Therefore, 4 Hz phase locking was a random correlation, rather than induced by a cognitive process. The 4 Hz phase locking strength was reduced during incorrect trials (**Figure 4.6E**) (ANOVA; interaction: $F_{(10,200)}=3.11$, $p=0.001$), but *post hoc* t-tests did not reveal specific time windows that were significantly different. LFP-LFP synchrony was not measured for these frequencies because the 180 msec time period after the stimulus was not adequate for calculating PLV. During the post-stimulus period, VTA neurons primarily phase locked to ACC beta and 4 Hz oscillations, whereas the phase locking to ACC gamma oscillations that was observed during the pre-stimulus period was no longer observed.

4.5 DISCUSSION

Our results demonstrate that the VTA is activated during attention and that the VTA and ACC may form a network that predicts attentional accuracy. The firing rate of neurons in the VTA with either dopamine-like or GABA-like waveforms correlated with attentional accuracy during the pre-stimulus period when top-down preparatory attention is generated. Neural activity also synchronized with ACC gamma oscillations during this period, providing a potential mechanism by which VTA neurons may assist PFC networks in the generation of a top-down attention signal. This pattern of interaction was selective to the pre-stimulus period. After stimulus onset, a different pattern of activity was observed in which primarily putative dopamine neurons responded and VTA unit activity was coordinated with beta oscillations in the ACC.

4.5.1 DOPAMINE NEURONS MAY STABLIZE ACC ENSEMBLES AGAINST DISTRACTION DURING PREPRATORY ATTENTION

During the pre-stimulus period, VTA neurons maintained a stable enhanced firing rate over a period of seconds. Previous work has demonstrated sustained increases in VTA dopamine neuron firing rate during increasing uncertainty about reward delivery (Fiorillo et al., 2003). Importantly, there is no information about stimulus or reward certainty during the pre-stimulus period of our task. Therefore, a sustained increase of VTA neuron firing was observed even though uncertainty was not modulated. Furthermore, this activation was reduced during incorrect trials, while certainty was the same during correct and incorrect trials. Sustained increases in VTA dopamine neuron firing rate have also been observed before self-initiated movement (Romo and Schultz, 1990). We, however, found that pre-stimulus sustained activity was of

different magnitudes during correct and incorrect trials although both trials required a self-initiated movement.

The sustained increase in dopamine neuron firing rate during the pre-stimulus period could have a tonic, modulatory effect on cortical neurons. This action may stabilize cortical ensembles by synchronizing up-states across neurons (Peters et al., 2004) and limiting PFC inhibitory interneurons to fire within focused time windows (Tierney et al., 2008). In the context of attention, dopamine could strengthen the ACC ensembles that are generating a top-down attention signal against degradation by irrelevant afferent neural activity.

4.5.2 VTA PUTATIVE GABA NEURONS MAY AFFECT ACC GAMMA OSCILLATIONS AND COMMUNICATION OF TOP-DOWN ATTENTION SIGNALS

In addition to putative dopamine neurons, putative GABA neurons in the VTA also are activated during top-down attention. Given that most of our electrodes were placed in the heavily PFC-projecting medial sector of the VTA (Lindvall et al., 1978) and that 60% of the VTA projection to the medial PFC in the rat is GABAergic (Carr and Sesack, 2000a), it is likely that at least a portion of the putative GABA neurons that we recorded were PFC projecting. Our data, therefore, indicate that the GABA projection from the VTA may play a role in regulating communication of the top-down attention signal from the ACC. The activation of GABA neurons could produce suppression of PFC and ACC neuron firing rate, which we have shown predicts attentional accuracy (Totah et al., 2009). The post-synaptic effects of dopamine via metabotropic receptors could be too slow to affect ACC gamma oscillations (although co-release of glutamate release from DA terminals could mediate faster transmission (Koos et al., 2011)), whereas GABA projection neurons could mediate fast effects via ionotropic receptors. Cortical

gamma oscillations require synchronous activation of local inhibitory interneurons (Börgers and Kopell, 2005), which receive synaptic input from GABAergic VTA projection neurons (Carr and Sesack, 2000a). Therefore, VTA GABA neurons projecting to PFC areas, such as the ACC, may affect the generation of local gamma oscillations. Our finding that VTA neurons correlate with ACC gamma oscillation phase is critical because gamma oscillations are used to communicate the top-down attention signal to sensory cortex (Fries, 2009; Gregoriou et al., 2009). By affecting this neural activity, GABA projection neurons may enable the ACC ensembles, which represent behaviorally relevant information, to send their output to sensory cortex. It should be noted, however, that the majority of GABA and dopamine neurons in the VTA project to regions other than the PFC (Fields et al., 2007), suggesting that other regions such as the ventral striatum may be involved in this context.

4.5.3 THE POST-STIMULUS PHASIC RESPONSE OF VTA PUTATIVE DOPAMINE NEURONS REFLECTS SUBSEQUENT THE BEHAVIORAL RESPONSE

The short-duration, phasic increase in firing rate that we observed after stimulus onset was similar to the widely reported dopamine neuron response to salient novel or conditioned stimuli (Schultz, 1998; Horvitz, 2000; Kim et al., 2010). This phasic response, however, was reduced significantly during incorrect and omission trials indicating that the representation of the stimulus reflected the subsequent behavioral response of the rat. One mechanism for a reduced phasic response during incorrect trials is that afferent excitatory drive onto VTA neurons from regions such as primary and associative sensory cortices or the superior colliculcus (Schultz, 1998; Dommett et al., 2005) could be reduced. Alternatively, given that ACC neurons and other PFC regions anticipate the onset of a stimulus earlier (approximately 4 sec before the stimulus)

than VTA neurons (approximately 2 sec before the stimulus) by increasing their firing rate in a manner that correlates with the subsequent decision (Totah et al., 2009), activity in these PFC regions could drive the VTA response to the stimulus. The VTA neurons that responded to the stimulus primarily were putative dopamine neurons. It is noteworthy that the PFC-projecting dopamine neurons, and not GABA neurons, are preferentially innervated by PFC afferents (Carr and Sesack, 2000b; Sesack et al., 2003). Furthermore, microdialysis measurements of PFC dopamine release have suggested that the PFC can control its own dopamine stimulation, presumably via the aforementioned anatomical connections (Takahata and Moghaddam, 1998). Thus, VTA dopamine neurons could be selectively driven by cortical afferents upon stimulus onset resulting in increased cortical dopamine release. Our task used a salient stimulus that was neither novel, nor being learned; rather it was predictable and well learned. Consistent with biased competition models of attention and top-down selection (Desimone and Duncan, 1995; Miller and Cohen, 2001), we propose that in these circumstances of a predictable and well-learned stimulus, PFC and ACC neurons predict the time of an upcoming stimulus and send a top-down control signal to VTA dopamine neurons which elicits a phasic response to the stimulus.

4.5.4 VTA NEURONS MAY AFFECT ACC BETA OSCILLATIONS DURING STIMULUS-GUIDED RESPONSE SELECTION

Top-down control of VTA neurons may provide a mechanism by which the PFC switches itself from a pre-stimulus, focused state to a post-stimulus, flexible state of stimulus-guided behavior. Indeed, as stated above, the PFC can control its own dopamine stimulation, presumably via direct excitation of VTA dopamine neurons projecting back to the PFC

(Takahata and Moghaddam, 1998; Carr and Sesack, 2000b). Phasic activation of dopamine neurons has been proposed to engender a flexible state by increasing PFC neuron sensitivity to afferent input (Durstewitz et al., 2000; Seamans and Yang, 2004). The afferent input could be extrinsic information (i.e., a representation of the sensory stimulus in visual cortex) or intrinsic information (i.e., local pyramidal axon collaterals mediating competition between ensembles). Upon stimulus onset, the ACC may control its own dopamine response so that it can receive feed-forward information about the stimulus from visual cortex and form new ensembles related to making a stimulus-guided response. This mechanism would predict that the observed reduction of a phasic dopamine neuron response during incorrect trials leads to impaired ACC processing of sensory evidence and stimulus-guided response selection. Importantly, we have demonstrated that incorrect trials are associated with longer latencies to make a behavioral choice (Totah et al., 2009), which could be a result of reduced VTA-ACC neural activity.

During this post-stimulus period, when the ACC supports flexible decisions and stimulus-guided behavior, we observed VTA neurons phase locking to ACC beta oscillations. Beta oscillations have been associated with weighting sensory evidence and using it to make a decision in humans (Siegel et al., 2011), as well as flexibly mapping sensory evidence onto a behavioral choice in monkeys (Haegens et al., 2011). Beta rhythms may also be associated with holding a previous stimulus in working memory while a decision is made (Kopell et al., 2011). Thus, top-down control of the VTA and concomitant ACC beta oscillations could provide a mechanism by which the ACC optimizes behavioral selection. Notably, while holding a stimulus in working memory before making a stimulus-guided response, there is a prominent coherence between VTA single units and rat prelimbic cortex 4 Hz LFP oscillations, which are invoked by ongoing cognitive processing (Fujisawa and Buzsáki, 2011). We observed strong phase locking

to 4 Hz LFP oscillations albeit in the ACC; however, in our experiments, shuffling trial order did not reduce phase locking. This suggests that the 4 Hz phase locking may have been a spurious correlation or it could have been evoked by the sensory stimulus.

4.5.5 GENERAL CONCLUSIONS

In conclusion, the current experiments suggest that VTA activity is critical to the ACC neuronal representations that underlie selection of a stimulus by top-down attention and the use of that stimulus to guide response selection. Our results further suggest that different durations of VTA neuronal phasic activity (sustained versus short) and two distinct patterns of coupling with ACC population activity (gamma oscillations versus beta oscillations) could underlie two separate executive functions: attention and action selection. In the context of mental illnesses such as schizophrenia and ADHD that are associated with attentional deficits (Bush, 2010; Luck et al., 2012) and aberrant gamma activity (Uhlhaas and Singer, 2010), distractibility and poor planning and choices could result from a "coordination deficit" of VTA-ACC network activity involving both GABA and dopamine VTA projection neurons.

5.0 GENERAL DISCUSSION

5.1 SUMMARY OF FINDINGS

We demonstrate that neurons in the PL and ACC change firing rate during preparatory attention in a manner that is predictive of attentional accuracy. These changes in firing rate occur as both increases and decreases. We also demonstrate that the PL and ACC interact during preparatory attention across a wide range of frequencies, which may allow for enhanced communication between PL and ACC neurons. Some of these PL-ACC network neurons may participate in both preparatory attention and preparation for a stimulus-guided response.

Using simultaneous recordings in the VTA and ACC, we demonstrate that VTA neurons correlate with ACC gamma oscillations, which are responsible for ensemble formation and enhancing communication of the preparatory attention signal. We also demonstrate that VTA neurons correlate with ACC beta oscillations, which may be used to organize PFC neural activity during decision-making and stimulus-guided behavior. Additionally, we propose that the PFC may provide top-down control to the VTA at stimulus onset. The idea is based on findings that (1) PFC neurons represent the upcoming stimulus before its onset and earlier than dopamine neurons, (2) the PFC pre-stimulus representation is reduced on error trials and would provide less drive to its downstream targets, and (3) the PFC top-down projection to the VTA makes

synaptic contacts with dopamine neurons, which is the group that was primarily responsive to the stimulus.

5.2 PARALLEL VTA DOPAMINE AND GABA PROJECTIONS EFFECT COMMUNICATION OF A TOP-DOWN ATTENTION SIGNAL

Simultaneous activation of GABA and dopamine VTA afferents could provide parallel signals that affect local processing in the deep PFC layers that communicate a top-down attention signal. We found that VTA neuron activity is correlated with cortical gamma oscillations. Based on this, we hypothesize that the VTA GABA neurons could affect cortical gamma activity because of their high firing rate and the presence of ionotropic post-synaptic receptors (Börgers and Kopell, 2005). On the other hand, dopamine neurons could regulate ensemble sensitivity to afferent input via post-synaptic metabotropic receptors effects on ionotropic channels (Seamans and Yang, 2004). While gamma oscillations and ensembles are generated locally, the parallel VTA afferents could regulate these processes, thereby affecting the communication of the top-down attention signal.

We propose a model of VTA modulation of ACC neural activity that depends on parallel activation of both VTA dopamine and GABA neurons (**Figure 5.1**). In this model, ACC gamma oscillations and ensemble formation during the pre-stimulus period could be affected by GABA neurons projecting from the VTA. The GABA neurons could affect cortical gamma activity because of their high firing rate and the presence of ionotropic post-synaptic receptors (Börgers and Kopell, 2005). The pre-stimulus period also is associated with a stable increase in dopamine neuron firing. One particular theory suggests that this dopamine neuron firing would promote

sustained increases in pre-stimulus firing rate and reduce ensemble sensitivity to afferent input and competition between ensembles via post-synaptic metabotropic receptor mediated effects on ionotropic channels (Seamans and Yang, 2004). According to this theory, the reduction in the effectiveness of afferent input could be due to stimulation of extra-synaptic ACC dopamine receptors enhancing NMDA currents (Zheng et al., 1999), but this theory remains to be validated in awake, behaving animals. Therefore, during the pre-stimulus period, the parallel activation of the dopamine and GABA afferents to the ACC may stabilize the representation of the upcoming stimulus and enhance its communication out of the ACC (**Figure 5.1A**). Our data indicates that, upon stimulus onset, PFC networks drive the phasic response of dopamine neurons, some of which may be projecting to the PFC. According to Seamans' and Yang's theory, the subsequent strong stimulation of ACC dopamine receptors would decrease NDMA currents, which would increase neurons' sensitivity to afferent input and competition from other ensembles. The result would be increased responsiveness of ACC neurons to various afferent drives and more flexible representations in the ACC. At the same time, GABA neurons projecting from the VTA also could affect ACC beta oscillations, which have been associated with stimulus-guided response selection (Haegens et al., 2011; Siegel et al., 2011). Thus, during the post-stimulus period, the parallel activation of GABA and dopamine afferents may switch the ACC to a state of flexible stimulus-guided response selection characterized by beta oscillations (**Figure 5.1B**).

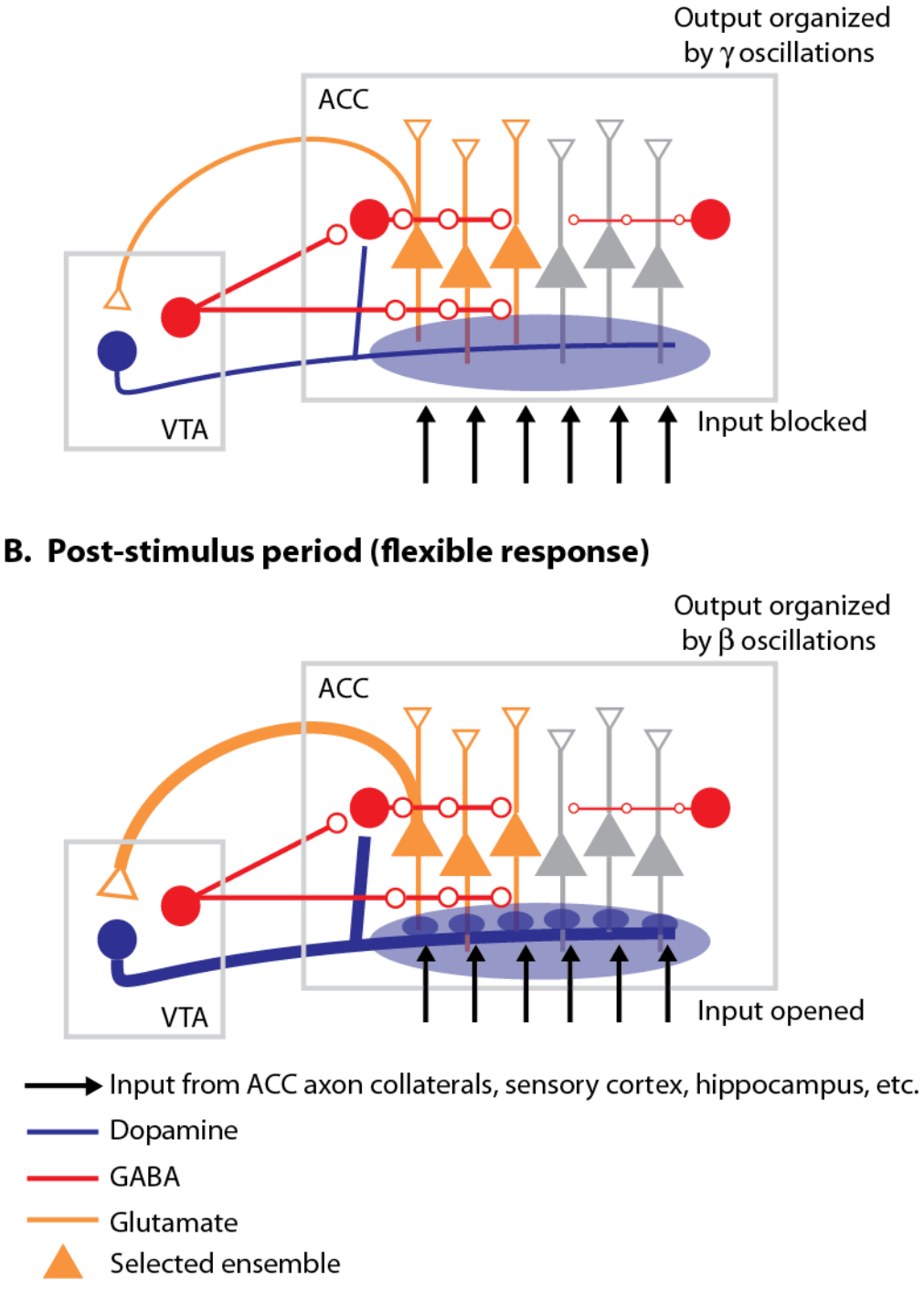

Figure 5.1. A model of coordinated interactions between the VTA and PFC that supports attention and stimulus-guided behavior.

(A) During the pre-stimulus period, the parallel activation of the dopamine and GABA afferents to the ACC may stabilize the representation of the upcoming stimulus and enhance the communication of a top-down attention signal from the ACC to sensory neurons via gamma oscillations. Both dopamine (blue lines) and GABA (red lines)

neurons could support this process via affects on post-synaptic receptors that control formation of an ensemble that represents the upcoming stimulus and reduce competition from task-irrelevant neural activity. (B) Upon stimulus onset, PFC networks (including the ACC) may provide direct excitatory drive (thick orange line) of PFC-projecting dopamine neurons and produce increased dopamine neurotransmission in PFC networks (thick blue line). As a result, new ensembles may form and are responsive to afferent input after stimulus onset. Thus, sensory information can be received by PFC networks and used to guide behavior. The GABA neurons may participate in this process by coordinating activity with PFC beta oscillations, which have been associated with stimulus-guided response selection.

Our model predicts that reduced pre-stimulus levels of dopamine neurotransmission during incorrect trials would allow irrelevant afferent activity to reduce the stability of ACC ensembles and reduce sustained firing rate increases of ACC neurons. We do, indeed, observe a reduction of sustained activity in the ACC and PL during the pre-stimulus period of incorrect trials (Totah et al., 2009). Our model would also predict that, during incorrect trials, (1) fewer ACC neurons would phase lock to local gamma oscillations and/or (2) the same number of neurons would phase lock but the members of the phase locked population would be different between trial types. When we combined neurons from all experiments in this dissertation (N=69 in ACC and N=68 in PL), we found that the population of neurons phase locked to local gamma oscillations contained different member neurons in correct and incorrect trials (**Figure 5.2**). These data suggest that competing ensembles could be activated during incorrect trials. According to our model of VTA-ACC interactions, activation of competing ensembles could occur because of reduced VTA dopamine neuron firing rate during the pre-stimulus period of incorrect trials.

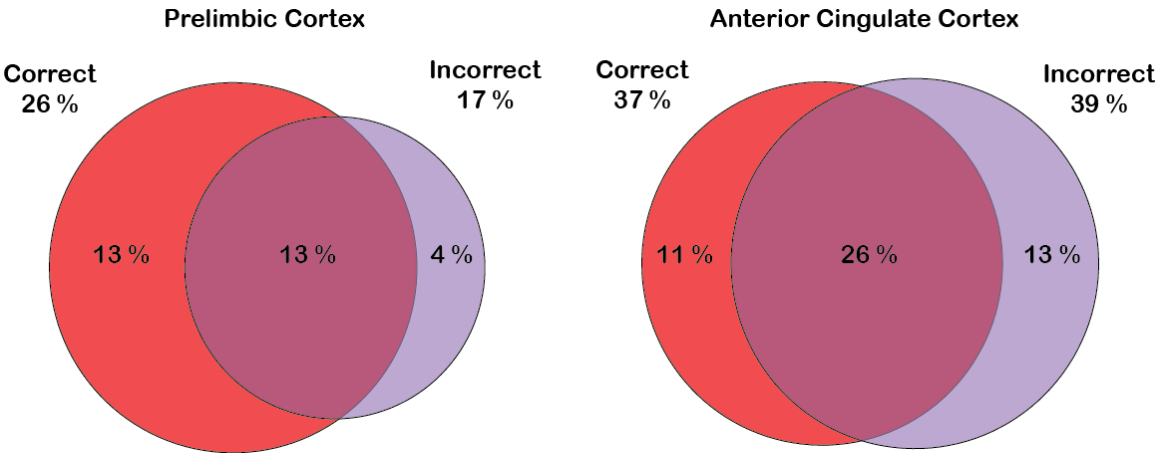

Figure 5.2. The proportion of PL and ACC neurons that are phase locked to local gamma oscillations during correct and incorrect trials.

The numbers above the circles indicate the percentage of total neurons recorded that phase locked to local gamma oscillations in each trial type. The numbers centered inside of the circles indicate the percent of total neurons phase locked on correct trials only (red), incorrect trials only (purple), and both trial types (overlap). The degree to which the circles do not overlap indicate independent populations of neurons that are gamma phase locked on different trial types.

5.3 THE NEUROPHYSIOLOGICAL REPRESENTATION OF A BEHAVIORALLY RELEVANT STIMULUS DURING PREPARATORY ATTENTION

Synchronous oscillations may be used to establish and adjust the capacity of communication channels between groups of neurons (Fries, 2005). A message about stimulus relevance could be communicated to sensory cortices during preparatory attention via a channel aligned to the phase of gamma oscillations (**Section 1.3**). The signal transmitted through these channels could represent what is behaviorally significant to the animal using spike rate (Salinas and Sejnowski, 2000) (**Section 1.1**). During the pre-stimulus period of our behavioral task, the upcoming stimulus may be represented by the stable elevation of PL and ACC neuron firing rate (**Section**

2.4.2). This activation is reduced during incorrect trials suggesting that the stimulus may not be represented strongly enough during error trials. A stable elevation of PFC neuron firing rate is also observed in behavioral tasks that require the subject to represent a past stimulus over a delay. In these tasks, a cue will induce sustained elevations in firing rate over a delay period until the stimulus guides a response (Fuster et al., 1985; Goldman-Rakic, 1995; Rao et al., 1997). Therefore, a stimulus that guides behavior can be remembered from the past or expected in the future and the PFC networks appear to represent stimuli using sustained activity in both situations. I propose that the message represented in sustained activity is selectively routed through a particular communication channel based on its specific cognitive use. Synchrony may be used to communicate the representation of a past stimulus to neurons participating in planning or action preparation, while representation of a future stimulus may be selectively communicated to neurons processing the stimulus.

In the preparatory attention task that we employed, sustained activity was initiated intrinsically, rather than by an external instruction cue. Given that animals develop expectancies and use internal information to control their behavior, allowing the animal to initiate preparatory attention is a more naturalistic approach than using an instruction cue. However, this leads to an important question regarding how the PFC neurons can initiate sustained activity during the pre-stimulus period without a cue. The effects of preparatory attention on sensory cortex activation, as measured by EEG or fMRI, are the same whether the instruction is intrinsic or a cue (Kastner et al., 1999; Doherty et al., 2005). A key direction of investigation for future research should be to understand how sustained pre-stimulus activity is initiated in PFC neurons when behavior is guided internally. Is there a neuronal ensemble that transiently exists as a "cue" to initiate preparatory attention and the representation of the upcoming stimulus? Is this ensemble driven to

become active based on the learned temporal structure of the task? These questions are important because they begin to touch on how internal information—knowledge—allows the brain to organize its activity and give rise to volitional decisions and actions.

5.4 INHIBITION OF NEURONAL FIRING AS SUPRESSION OF IRRELEVANT REPRESENTATIONS

Studies measuring phasic neuronal firing rate changes in the behaving animal have often focused on increases in firing rate, but a number of studies have also demonstrated phasic suppressions of firing rate in PFC networks (**Table 5.1**). Although suppression is detected in a smaller proportion of neurons in comparison to those that increase firing rate, it may be difficult to detect suppression given that PFC have firing rates < 10 Hz) (Connors and Gutnick, 1990). The magnitude of phasic decreases in firing to stimulus onset and during delay periods is correlated with the outcome predicted by the stimulus (Kobayashi et al., 2006; Wallis and Miller, 2003), which suggests that the suppressed neurons are representing behaviorally relevant information.

Table 5.1. The percentage of total recorded units that decreased their firing rate during various behavioral tasks.

No result if cell is blank. References: (Funahashi et al., 1989; Fuster, 1973; Sakagami and Niki, 1994; Kobayashi et al., 2006; Peters et al., 2005; Takenouchi et al., 1999; Bouret and Sara, 2004; Schoenbaum and Eichenbaum, 1995; Chang et al., 2000; Mears et al., 2006; Totah et al., 2009).

Study	Task	Region	Percent of total neurons recorded			
			Cue	Delay	Response	Entire Trial
Fuster (1973)	Delayed response	DLPFC	4.60%	7.60%		
Sakagami et al. (1994)	Go/no-go discrimination	DLPFC	4.00%			
Kobayashi et al. (2006)	Delayed match-to-sample	LPFC		5.61%		
Peters et al. (2005)	Scheduled reinforcement	PL			23%	
Takenouchi et al. (1999)	Pavlovian	PL/ACC	7.20%			
Bouret et al. (2004)	Go/no-go discrimination	PL				29%
Schoenbaum et al. (1995)	Go/no-go discrimination	OFC				13%
Chang et al. (2000)	Drug self administration	PL			6.90%	
Mears et al. (2006)	Inhibitory gating	PL	10.30%			
Funahashi et al. (1989)	Delayed response	DLPFC		13%		
Totah et al. (2009)	Attention	ACC	10.30%			8.50%
Totah et al. (2009)	Attention	PL	7.20%			7.20%

During preparatory attention, firing rates of neurons in the PL and the ACC are decreased throughout the pre-stimulus period (**Section 2.4.2**). Instances of maintained suppression of firing rate have also been observed when a past stimulus is remembered over a delay (Funahashi et al., 1989; Fuster, 1973; Kobayashi et al., 2006; Sakagami and Niki, 1994). In the previous section, I stated that sustained activity might be used to represent a past or future stimulus; these representations can apparently be either increases or decreases in firing rate. However, it is important to understand if the neurons that maintain an increased firing rate during preparatory attention are representing different information compared to those that maintain a decreased firing rate. An important demonstration of what these two neuronal populations may represent can be garnered from the experiments by Lennart and colleagues (Lennert and Martinez-Trujillo, 2011). In these experiments, monkeys were trained to sustain attention on two stimuli of moving dot patterns, which are presented on either side of a fixation cross. The color of the dots was used to define one stimulus as irrelevant and one as the target. The subject had to detect a change in the dot motion of the target stimulus. Neurons would respond to stimuli with a location preference, meaning they would respond more to a stimulus on either the left or right side of the display. If the target stimulus was displayed on a neuron's preferred side, it increased its firing

rate upon dot motion change. On the other hand, if the irrelevant stimulus was displayed, the neuron's firing rate was suppressed. Critically, the degree of suppression correlated with attentional accuracy as measured by correct behavior and faster reaction time. In other words, PFC neurons filtered irrelevant stimuli by suppressing their firing rate and, as task difficulty increased, suppression was reduced and attentional accuracy was impaired. Our experiments demonstrate a similar result during preparatory attention. The magnitude of sustained activity during the pre-stimulus period (increased or decreased) was reduced as behavioral performance worsened.

Accordingly, I propose that the suppression of firing rate is not a representation of the future stimulus. Instead, while the sustained increase in firing rate represents the upcoming stimulus, the sustained decrease in firing rate represents the suppression of irrelevant stimuli that could interfere with the representation of the future stimulus. During error trials, the upcoming stimulus may not be represented strongly enough and irrelevant stimuli may not be suppressed enough. Future analysis could assess, on a trial-by-trial basis, if errors are associated with a lack of activation, a lack of suppression, or a combination of both.

5.5 REPRESENTATION AND COMMUNICATION OF A STIMULUS DURING PREPARATORY ATTENTION: RELEVANCE TO DISEASE

Our work suggests that PFC neurons represent an expected stimulus using sustained activation. Individuals with schizophrenia exhibit PFC hyperactivity, abnormal gamma oscillations, and reduced PFC dopamine neurotransmission (Jackson et al., 2004; Uhlhaas and Singer, 2010; Arnsten, 2011b). This scenario could result in communication of an abnormally strong

preparatory attention signal that could activate sensory neurons to the level observed during stimulus perception, without the presence of a stimulus. Increased drive of sensory neurons could be due to 1) PFC representations being too strong due to PFC hyperactivity and 2) increased communication of the signal due to abnormal gamma oscillations resulting from reduced PFC dopamine.

Therefore, the hallucinations reported by individuals with schizophrenia could be due to an overactive preparatory attention system (Driver and Frith, 2000; Collerton et al., 2005; Fletcher and Frith, 2008). Increased activity of this system could also lead to distortions of existing stimuli during top-down attentional search. For instance, when viewing a face, attention is directed to the eyes and mouth; if top-down attention drives sensory neurons too strongly, it could result in the typical distortion of others' faces to schizophrenics consisting of "stretched lips…grinning…and stretched eyes [with] big circles under them" (Santhouse et al., 2000). In humans, preparatory attention is associated with mental imagery of the upcoming stimulus (Driver and Frith, 2000) and both imagery and preparatory attention activate sensory cortex (Driver and Frith, 2000; Kastner et al., 1999). If the representation of stimuli in preparatory attention control areas is overly elevated, then simply imagining something could make it seem as though it actually existed. Our data provide support for this explanation of some of the positive symptoms of schizophrenia by demonstrating that neurons in PFC networks represent behaviorally relevant stimuli using increases in firing rate and that the VTA-ACC network is associated with cortical gamma oscillations.

BIBLIOGRAPHY

Arnsten, A. F. T. (2011a). Catecholamine Influences on Dorsolateral Prefrontal Cortical Networks. BPS *69*, e89–e99.

Arnsten, A. F. T. (2011b). Prefrontal cortical network connections: key site of vulnerability in stress and schizophrenia. International Journal of Developmental Neuroscience *29*, 215–223.

Asaad, W. F., Rainer, G., and Miller, E. K. (1998). Neural activity in the primate prefrontal cortex during associative learning. Neuron *21*, 1399–1407.

Azouz, R., and Gray, C. M. (2000). Dynamic spike threshold reveals a mechanism for synaptic coincidence detection in cortical neurons in vivo. Proc. Natl. Acad. Sci. U.S.A. *97*, 8110–8115.

Bandyopadhyay, S., Gonzalez-Islas, C., and Hablitz, J. J. (2005). Dopamine enhances spatiotemporal spread of activity in rat prefrontal cortex. Journal of Neurophysiology *93*, 864–872.

Berens, P. (2009). CircStat: a MATLAB toolbox for circular statistics. Journal of Statistical Software.

Berger, B., Thierry, A. M., Tassin, J. P., and Moyne, M. A. (1976). Dopaminergic innervation of the rat prefrontal cortex: a fluorescence histochemical study. Brain Research *106*, 133–145.

Berridge, C. W., Devilbiss, D. M., Andrzejewski, M. E., Arnsten, A. F. T., Kelley, A. E., Schmeichel, B., Hamilton, C., and Spencer, R. C. (2006). Methylphenidate Preferentially Increases Catecholamine Neurotransmission within the Prefrontal Cortex at Low Doses that Enhance Cognitive Function. Biological Psychiatry *60*, 1111–1120.

Bob, P., Palus, M., Susta, M., and Glaslova, K. (2008). EEG phase synchronization in patients with paranoid schizophrenia. Neuroscience Letters *447*, 73–77.

Botvinick, M. M., Cohen, J. D., and Carter, C. S. (2004). Conflict monitoring and anterior cingulate cortex: an update. Trends in Cognitive Sciences *8*, 539–546.

Bouret, S., and Sara, S. J. (2004). Reward expectation, orientation of attention and locus coeruleus-medial frontal cortex interplay during learning. European Journal of Neuroscience *20*, 791–802.

Börgers, C., and Kopell, N. (2005). Effects of noisy drive on rhythms in networks of excitatory and inhibitory neurons. Neural Comput *17*, 557–608.

Börgers, C., Epstein, S., and Kopell, N. J. (2005). Background gamma rhythmicity and attention in cortical local circuits: a computational study. Proc. Natl. Acad. Sci. U.S.A. *102*, 7002–7007.

Bressler, S. L., Tang, W., Sylvester, C. M., Shulman, G. L., and Corbetta, M. (2008). Top-Down Control of Human Visual Cortex by Frontal and Parietal Cortex in Anticipatory Visual Spatial Attention. J. Neurosci. *28*, 10056–10061.

Buffalo, E. A., Fries, P., Landman, R., Liang, H., and Desimone, R. (2010). A backward progression of attentional effects in the ventral stream. Proceedings of the National Academy of Sciences *107*, 361–365.

Buschman, T. J., and Miller, E. K. (2007). Top-Down Versus Bottom-Up Control of Attention in the Prefrontal and Posterior Parietal Cortices. Science *315*, 1860–1862.

Bush, G. (2010). Attention-deficit/hyperactivity disorder and attention networks. Neuropsychopharmacology *35*, 278–300.

Buzsaki, G. (2004). Neuronal Oscillations in Cortical Networks. Science *304*, 1926–1929.

Buzsaki, G., and Chrobak, J. J. (1995). Temporal structure in spatially organized neuronal ensembles: a role for interneuronal networks. Current Opinion in Neurobiology *5*, 504–510.

Canolty, R. T., Ganguly, K., Kennerley, S. W., Cadieu, C. F., Koepsell, K., Wallis, J. D., and Carmena, J. M. (2010). Oscillatory phase coupling coordinates anatomically dispersed functional cell assemblies. Proceedings of the National Academy of Sciences *107*, 17356–17361.

Carli, M., Robbins, T. W., Evenden, J. L., and Everitt, B. J. (1983). Effects of lesions to ascending noradrenergic neurones on performance of a 5-choice serial reaction task in rats; implications for theories of dorsal noradrenergic bundle function based on selective attention and arousal. Behavioural Brain Research *9*, 361–380.

Carr, D. B., and Sesack, S. R. (2000a). GABA-containing neurons in the rat ventral tegmental area project to the prefrontal cortex. Synapse *38*, 114–123.

Carr, D. B., and Sesack, S. R. (2000b). Projections from the rat prefrontal cortex to the ventral tegmental area: target specificity in the synaptic associations with mesoaccumbens and mesocortical neurons. J. Neurosci. *20*, 3864–3873.

Chang, J. Y., Janak, P. H., and Woodward, D. J. (2000). Neuronal and behavioral correlations in the medial prefrontal cortex and nucleus accumbens during cocaine self-administration by rats. Neuroscience *99*, 433–443.

Chawla, D., Lumer, E. D., and Friston, K. J. (2000). Relating macroscopic measures of brain

activity to fast, dynamic neuronal interactions. Neural Comput *12*, 2805–2821.

Chawla, D., Rees, G., and Friston, K. J. (1999). The physiological basis of attentional modulation in extrastriate visual areas. Nat Neurosci *2*, 671–676.

Chelazzi, L., Miller, E. K., Duncan, J., and Desimone, R. (1993). A neural basis for visual search in inferior temporal cortex. Nature *363*, 345–347.

Chudasama, Y., Passetti, F., Rhodes, S. E. V., Lopian, D., Desai, A., and Robbins, T. W. (2003). Dissociable aspects of performance on the 5-choice serial reaction time task following lesions of the dorsal anterior cingulate, infralimbic and orbitofrontal cortex in the rat: differential effects on selectivity, impulsivity and compulsivity. Behavioural Brain Research *146*, 105–119.

Chuhma, N., Zhang, H., Masson, J., Zhuang, X., Sulzer, D., Hen, R., and Rayport, S. (2004). Dopamine neurons mediate a fast excitatory signal via their glutamatergic synapses. Journal of Neuroscience *24*, 972–981.

Collerton, D., Perry, E., and McKeith, I. (2005). Why people see things that are not there: a novel Perception and Attention Deficit model for recurrent complex visual hallucinations. Behav Brain Sci *28*, 737–57; discussion 757–94.

Connors, B. W., and Gutnick, M. J. (1990). Intrinsic firing patterns of diverse neocortical neurons. Trends in Neurosciences *13*, 99–104.

Corbit, L. H., and Balleine, B. W. (2003). The role of prelimbic cortex in instrumental conditioning. Behavioural Brain Research *146*, 145–157.

Coull, J. T., Frith, C. D., Büchel, C., and Nobre, A. C. (2000). Orienting attention in time: behavioural and neuroanatomical distinction between exogenous and endogenous shifts. Neuropsychologia *38*, 808–819.

Crofts, H. S., Dalley, J. W., Collins, P., Van Denderen, J. C., Everitt, B. J., Robbins, T. W., and Roberts, A. C. (2001). Differential effects of 6-OHDA lesions of the frontal cortex and caudate nucleus on the ability to acquire an attentional set. Cereb. Cortex *11*, 1015–1026.

Cubillo, A., Halari, R., Ecker, C., Giampietro, V., Taylor, E., and Rubia, K. (2010). Reduced activation and inter-regional functional connectivity of fronto-striatal networks in adults with childhood Attention-Deficit Hyperactivity Disorder (ADHD) and persisting symptoms during tasks of motor inhibition and cognitive switching. Journal of Psychiatric Research *44*, 629–639.

Dale, C. L., Simpson, G. V., Foxe, J. J., Luks, T. L., and Worden, M. S. (2008). ERP correlates of anticipatory attention: spatial and non-spatial specificity and relation to subsequent selective attention. Exp Brain Res *188*, 45–62.

Descarries, L., Lemay, B., Doucet, G., and Berger, B. (1987). Regional and laminar density of the dopamine innervation in adult rat cerebral cortex. Neuroscience *21*, 807–824.

Desimone, R., and Duncan, J. (1995). Neural mechanisms of selective visual attention. Annu. Rev. Neurosci. *18*, 193–222.

Doherty, J. R., Rao, A., Mesulam, M. M., and Nobre, A. C. (2005). Synergistic effect of combined temporal and spatial expectations on visual attention. Journal of Neuroscience *25*, 8259–8266.

Dommett, E., Coizet, V., Blaha, C. D., Martindale, J., Lefebvre, V., Walton, N., Mayhew, J. E. W., Overton, P. G., and Redgrave, P. (2005). How visual stimuli activate dopaminergic neurons at short latency. Science *307*, 1476–1479.

Driver, J., and Frith, C. D. (2000). Shifting baselines in attention research. Nat Rev Neurosci *1*, 147–148.

Duncan, J. (2001). An adaptive coding model of neural function in prefrontal cortex. Nat Rev Neurosci *2*, 820–829.

Durstewitz, D., Seamans, J. K., and Sejnowski, T. J. (2000). Dopamine-mediated stabilization of delay-period activity in a network model of prefrontal cortex. Journal of Neurophysiology *83*, 1733–1750.

Egner, T., Monti, J. M. P., Trittschuh, E. H., Wieneke, C. A., Hirsch, J., and Mesulam, M. M. (2008). Neural Integration of Top-Down Spatial and Feature-Based Information in Visual Search. J. Neurosci. *28*, 6141–6151.

Engel, A. K., and Fries, P. (2010). Beta-band oscillations--signalling the status quo? Current Opinion in Neurobiology *20*, 156–165.

Everling, S., Tinsley, C. J., Gaffan, D., and Duncan, J. (2006). Selective representation of task-relevant objects and locations in the monkey prefrontal cortex. European Journal of Neuroscience *23*, 2197–2214.

Felleman, D. J., and Van Essen, D. C. (1991). Distributed hierarchical processing in the primate cerebral cortex. Cereb. Cortex *1*, 1–47.

Ferrera, V. P., Rudolph, K. K., and Maunsell, J. H. (1994). Responses of neurons in the parietal and temporal visual pathways during a motion task. J. Neurosci. *14*, 6171–6186.

Fields, H. L., Hjelmstad, G. O., Margolis, E. B., and Nicola, S. M. (2007). Ventral Tegmental Area Neurons in Learned Appetitive Behavior and Positive Reinforcement. Annu. Rev. Neurosci. *30*, 289–316.

Fiorillo, C. D., Tobler, P. N., and Schultz, W. (2003). Discrete coding of reward probability and uncertainty by dopamine neurons. Science *299*, 1898–1902.

Fisher, N. (1996). Statistical analysis of circular data (Cambridge Univ Pr).

Fletcher, P. C., and Frith, C. D. (2008). Perceiving is believing: a Bayesian approach to

explaining the positive symptoms of schizophrenia. Nat Rev Neurosci *10*, 48–58.

Ford, J. M., Krystal, J. H., and Mathalon, D. H. (2007). Neural synchrony in schizophrenia: from networks to new treatments. Schizophr Bull *33*, 848–852.

Freedman, D. J., Riesenhuber, M., Poggio, T., and Miller, E. K. (2001). Categorical representation of visual stimuli in the primate prefrontal cortex. Science *291*, 312–316.

Fries, P. (2005). A mechanism for cognitive dynamics: neuronal communication through neuronal coherence. Trends in Cognitive Sciences *9*, 474–480.

Fries, P. (2001). Modulation of Oscillatory Neuronal Synchronization by Selective Visual Attention. Science *291*, 1560–1563.

Fries, P. (2009). Neuronal Gamma-Band Synchronization as a Fundamental Process in Cortical Computation. Annu. Rev. Neurosci. *32*, 209–224.

Fries, P., Womelsdorf, T., Oostenveld, R., and Desimone, R. (2008). The Effects of Visual Stimulation and Selective Visual Attention on Rhythmic Neuronal Synchronization in Macaque Area V4. J. Neurosci. *28*, 4823–4835.

Fujisawa, S., Amarasingham, A., Harrison, M. T., and Buzsáki, G. (2008). Behavior-dependent short-term assembly dynamics in the medial prefrontal cortex. Nat Neurosci *11*, 823–833.

Fujisawa, S., and Buzsáki, G. (2011). A 4 Hz Oscillation Adaptively Synchronizes Prefrontal, VTA, and Hippocampal Activities. Neuron *72*, 153–165.

Funahashi, S., Bruce, C. J., and Goldman-Rakic, P. S. (1989). Mnemonic coding of visual space in the monkey's dorsolateral prefrontal cortex. Journal of Neurophysiology *61*, 331–349.

Fuster, J. M. (2001). The prefrontal cortex--an update: time is of the essence. Neuron *30*, 319–333.

Fuster, J. M. (1973). Unit activity in prefrontal cortex during delayed-response performance: neuronal correlates of transient memory. Journal of Neurophysiology *36*, 61–78.

Fuster, J. M., Bauer, R. H., and Jervey, J. P. (1985). Functional interactions between inferotemporal and prefrontal cortex in a cognitive task. Brain Research *330*, 299–307.

Ghose, G. M., and Maunsell, J. H. R. (2002). Attentional modulation in visual cortex depends on task timing. Nature *419*, 616–620.

Goldman-Rakic, P. S. (1995). Cellular basis of working memory. Neuron *14*, 477–485.

Granon, S., Passetti, F., Thomas, K. L., Dalley, J. W., Everitt, B. J., and Robbins, T. W. (2000). Enhanced and impaired attentional performance after infusion of D1 dopaminergic receptor agents into rat prefrontal cortex. Journal of Neuroscience *20*, 1208–1215.

Gregoriou, G. G., Gotts, S. J., Zhou, H., and Desimone, R. (2009). High-frequency, long-range

coupling between prefrontal and visual cortex during attention. Science *324*, 1207–1210.

Gross, J., Schmitz, F., Schnitzler, I., Kessler, K., Shapiro, K., Hommel, B., and Schnitzler, A. (2006). Anticipatory control of long-range phase synchronization. European Journal of Neuroscience *24*, 2057–2060.

Gruber, A. J., Hussain, R. J., and O'Donnell, P. (2009). The nucleus accumbens: a switchboard for goal-directed behaviors. PLoS ONE *4*, e5062.

Gruber, T., Müller, M. M., Keil, A., and Elbert, T. (1999). Selective visual-spatial attention alters induced gamma band responses in the human EEG. Clin Neurophysiol *110*, 2074–2085.

Haegens, S., Nácher, V., Hernández, A., Luna, R., Jensen, O., and Romo, R. (2011). Beta oscillations in the monkey sensorimotor network reflect somatosensory decision making. Proceedings of the National Academy of Sciences *108*, 10708–10713.

Horvitz, J. C. (2000). Mesolimbocortical and nigrostriatal dopamine responses to salient non-reward events. Neuroscience *96*, 651–656.

Hussar, C. R., and Pasternak, T. (2009). Flexibility of Sensory Representations in Prefrontal Cortex Depends on Cell Type. Neuron *64*, 730–743.

Ito, S., Stuphorn, V., Brown, J. W., and Schall, J. D. (2003). Performance monitoring by the anterior cingulate cortex during saccade countermanding. Science *302*, 120–122.

Jackson, M. E., Homayoun, H., and Moghaddam, B. (2004). NMDA receptor hypofunction produces concomitant firing rate potentiation and burst activity reduction in the prefrontal cortex. Proc. Natl. Acad. Sci. U.S.A. *101*, 8467–8472.

Johnston, K., Levin, H. M., Koval, M. J., and Everling, S. (2007). Top-Down Control-Signal Dynamics in Anterior Cingulate and Prefrontal Cortex Neurons following Task Switching. Neuron *53*, 453–462.

Jones, B. F., Groenewegen, H. J., and Witter, M. P. (2005). Intrinsic connections of the cingulate cortex in the rat suggest the existence of multiple functionally segregated networks. Neuroscience *133*, 193–207.

Kastner, S., Pinsk, M. A., De Weerd, P., Desimone, R., and Ungerleider, L. G. (1999). Increased activity in human visual cortex during directed attention in the absence of visual stimulation. Neuron *22*, 751–761.

Kim, Y. B., Matthews, M., and Moghaddam, B. (2010). Putative γ-aminobutyric acid neurons in the ventral tegmental area have a similar pattern of plasticity as dopamine neurons during appetitive and aversive learning. European Journal of Neuroscience *32*, 1564–1572.

Kiyatkin, E. A., and Rebec, G. V. (1998). Heterogeneity of ventral tegmental area neurons: single-unit recording and iontophoresis in awake, unrestrained rats. Neuroscience *85*, 1285–1309.

Klimesch, W., Sauseng, P., and Hanslmayr, S. (2007). EEG alpha oscillations: The inhibition–timing hypothesis. Brain Research Reviews *53*, 63–88.

Kobayashi, S., Nomoto, K., Watanabe, M., Hikosaka, O., Schultz, W., and Sakagami, M. (2006). Influences of Rewarding and Aversive Outcomes on Activity in Macaque Lateral Prefrontal Cortex. Neuron *51*, 861–870.

Kopell, N., Whittington, M. A., and Kramer, M. A. (2011). Neuronal assembly dynamics in the beta1 frequency range permits short-term memory. Proceedings of the National Academy of Sciences *108*, 3779–3784.

Koyama, T., Kato, K., Tanaka, Y. Z., and Mikami, A. (2001). Anterior cingulate activity during pain-avoidance and reward tasks in monkeys. Neurosci. Res. *39*, 421–430.

LaBerge, D. (1995). Attentional processing.

Lachaux, J. P., Rodriguez, E., Martinerie, J., and Varela, F. J. (1999). Measuring phase synchrony in brain signals. Hum. Brain Mapp. *8*, 194–208.

Lavin, A., Nogueira, L., Lapish, C. C., Wightman, R. M., Phillips, P. E. M., and Seamans, J. K. (2005). Mesocortical dopamine neurons operate in distinct temporal domains using multimodal signaling. Journal of Neuroscience *25*, 5013–5023.

Le Van Quyen, M., and Bragin, A. (2007). Analysis of dynamic brain oscillations: methodological advances. Trends in Neurosciences *30*, 365–373.

Lebedev, M. A., Messinger, A., Kralik, J. D., and Wise, S. P. (2004). Representation of Attended Versus Remembered Locations in Prefrontal Cortex. PLoS Biol *2*, e365.

Lennert, T., and Martinez-Trujillo, J. (2011). Strength of Response Suppression to Distracter Stimuli Determines Attentional-Filtering Performance in Primate Prefrontal Neurons. Neuron *70*, 141–152.

Lewis, D. A., Glantz, L. A., Pierri, J. N., and Sweet, R. A. (2003). Altered cortical glutamate neurotransmission in schizophrenia: evidence from morphological studies of pyramidal neurons. Annals of the New York Academy of Sciences *1003*, 102–112.

Liang, H., Bressler, S. L., Ding, M., Truccolo, W. A., and Nakamura, R. (2002). Synchronized activity in prefrontal cortex during anticipation of visuomotor processing. Neuroreport *13*, 2011–2015.

Lindvall, O., Björklund, A., and Divac, I. (1978). Organization of catecholamine neurons projecting to the frontal cortex in the rat. Brain Research *142*, 1–24.

Linkenkaer-Hansen, K., Nikouline, V. V., Palva, J. M., and Ilmoniemi, R. J. (2001). Long-range temporal correlations and scaling behavior in human brain oscillations. Journal of Neuroscience *21*, 1370–1377.

Linkenkaer-Hansen, K., Nikulin, V. V., Palva, S., Ilmoniemi, R. J., and Palva, J. M. (2004). Prestimulus oscillations enhance psychophysical performance in humans. Journal of Neuroscience *24*, 10186–10190.

Lodge, D. J. (2011). The Medial Prefrontal and Orbitofrontal Cortices Differentially Regulate Dopamine System Function. Neuropsychopharmacology *36*, 1227–1236.

Luck, S. J., Chelazzi, L., Hillyard, S. A., and Desimone, R. (1997). Neural mechanisms of spatial selective attention in areas V1, V2, and V4 of macaque visual cortex. Journal of Neurophysiology *77*, 24–42.

Luks, T. L., and Simpson, G. V. (2004). Preparatory deployment of attention to motion activates higher-order motion-processing brain regions. NeuroImage *22*, 1515–1522.

Margolis, E. B., Lock, H., Hjelmstad, G. O., and Fields, H. L. (2006). The ventral tegmental area revisited: is there an electrophysiological marker for dopaminergic neurons? The Journal of Physiology *577*, 907–924.

Matsumoto, M., and Hikosaka, O. (2009). Two types of dopamine neuron distinctly convey positive and negative motivational signals. Nature *459*, 837–841.

Mauritz, K. H., and Wise, S. P. (1986). Premotor cortex of the rhesus monkey: neuronal activity in anticipation of predictable environmental events. Exp Brain Res *61*, 229–244.

Mazaheri, A., Coffey-Corina, S., Mangun, G. R., Bekker, E. M., Berry, A. S., and Corbett, B. A. (2010). Functional disconnection of frontal cortex and visual cortex in attention-deficit/hyperactivity disorder. Biological Psychiatry *67*, 617–623.

Mears, R. P., Klein, A. C., and Cromwell, H. C. (2006). Auditory inhibitory gating in medial prefrontal cortex: Single unit and local field potential analysis. Neuroscience *141*, 47–65.

Mehta, A. D., Ulbert, I., and Schroeder, C. E. (2000a). Intermodal selective attention in monkeys. I: distribution and timing of effects across visual areas. Cereb. Cortex *10*, 343–358.

Mehta, A. D., Ulbert, I., and Schroeder, C. E. (2000b). Intermodal selective attention in monkeys. II: physiological mechanisms of modulation. Cereb. Cortex *10*, 359–370.

Mesulam, M. M. (1981). A cortical network for directed attention and unilateral neglect. Ann. Neurol. *10*, 309–325.

Miller, E. K., and Cohen, J. D. (2001). An integrative theory of prefrontal cortex function. Annu. Rev. Neurosci. *24*, 167–202.

Moghaddam, B., and Homayoun, H. (2007). Divergent Plasticity of Prefrontal Cortex Networks. Neuropsychopharmacology *33*, 42–55.

Montemurro, M. A., Rasch, M. J., Murayama, Y., Logothetis, N. K., and Panzeri, S. (2008).

Phase-of-Firing Coding of Natural Visual Stimuli in Primary Visual Cortex. Current Biology *18*, 375–380.

Morishima, Y., Akaishi, R., Yamada, Y., Okuda, J., Toma, K., and Sakai, K. (2009). Task-specific signal transmission from prefrontal cortex in visual selective attention. Nat Neurosci *12*, 85–91.

Mountcastle, V. B. (1997). The columnar organization of the neocortex. Brain *120 (Pt 4)*, 701–722.

Muir, J. L., Everitt, B. J., and Robbins, T. W. (1996). The cerebral cortex of the rat and visual attentional function: dissociable effects of mediofrontal, cingulate, anterior dorsolateral, and parietal cortex lesions on a five-choice serial reaction time task. Cereb. Cortex *6*, 470–481.

Mumford, D. (1992). On the computational architecture of the neocortex. II. The role of cortico-cortical loops. Biol Cybern *66*, 241–251.

Murias, M., Swanson, J. M., and Srinivasan, R. (2006). Functional Connectivity of Frontal Cortex in Healthy and ADHD Children Reflected in EEG Coherence. Cerebral Cortex *17*, 1788–1799.

Nair-Roberts, R. G., Chatelain-Badie, S. D., Benson, E., White-Cooper, H., Bolam, J. P., and Ungless, M. A. (2008). Stereological estimates of dopaminergic, GABAergic and glutamatergic neurons in the ventral tegmental area, substantia nigra and retrorubral field in the rat. Neuroscience *152*, 1024–1031.

Narayanan, N. S., and Laubach, M. (2009). Delay Activity in Rodent Frontal Cortex During a Simple Reaction Time Task. Journal of Neurophysiology *101*, 2859–2871.

Narayanan, N. S., and Laubach, M. (2006). Top-Down Control of Motor Cortex Ensembles by Dorsomedial Prefrontal Cortex. Neuron *52*, 921–931.

Ng, C.-W., Noblejas, M. I., Rodefer, J. S., Smith, C. B., and Poremba, A. (2007). Double dissociation of attentional resources: prefrontal versus cingulate cortices. Journal of Neuroscience *27*, 12123–12131.

Nieoullon, A. (2002). Dopamine and the regulation of cognition and attention. Progress in Neurobiology *67*, 53–83.

Nieuwenhuis, S., Holroyd, C. B., Mol, N., and Coles, M. G. H. (2004). Reinforcement-related brain potentials from medial frontal cortex: origins and functional significance. Neuroscience & Biobehavioral Reviews *28*, 441–448.

Niki, H., and Watanabe, M. (1979). Prefrontal and cingulate unit activity during timing behavior in the monkey. Brain Research *171*, 213–224.

Nobre, A. C. (2001). Orienting attention to instants in time. Neuropsychologia *39*, 1317–1328.

Noudoost, B., and Moore, T. (2011a). Control of visual cortical signals by prefrontal dopamine. Nature, 1–4.

Noudoost, B., and Moore, T. (2011b). The role of neuromodulators in selective attention. Trends in Cognitive Sciences, 1–7.

Noudoost, B., Chang, M. H., Steinmetz, N. A., and Moore, T. (2010). Top-down control of visual attention. Current Opinion in Neurobiology *20*, 183–190.

O'Donnell, P. (2003). Dopamine gating of forebrain neural ensembles. European Journal of Neuroscience *17*, 429–435.

O'Keefe, J., and Recce, M. L. (1993). Phase relationship between hippocampal place units and the EEG theta rhythm. Hippocampus *3*, 317–330.

Olson, C. R. (2001). Object-based vision and attention in primates. Current Opinion in Neurobiology *11*, 171–179.

Orr, J. M., and Weissman, D. H. (2009). Anterior Cingulate Cortex Makes 2 Contributions to Minimizing Distraction. Cerebral Cortex *19*, 703–711.

Ostlund, S. B., and Balleine, B. W. (2005). Lesions of medial prefrontal cortex disrupt the acquisition but not the expression of goal-directed learning. Journal of Neuroscience *25*, 7763–7770.

Padilla, M. L., Wood, R. A., Hale, L. A., and Knight, R. T. (2006). Lapses in a prefrontal-extrastriate preparatory attention network predict mistakes. J Cogn Neurosci *18*, 1477–1487.

Palva, S., and Palva, J. M. (2007). New vistas for α-frequency band oscillations. Trends in Neurosciences *30*, 150–158.

Passetti, F., Chudasama, Y., and Robbins, T. W. (2002). The frontal cortex of the rat and visual attentional performance: dissociable functions of distinct medial prefrontal subregions. Cereb. Cortex *12*, 1254–1268.

Passingham, R. E., Toni, I., and Rushworth, M. F. S. (2000). Specialisation within the prefrontal cortex: the ventral prefrontal cortex and associative learning. Exp Brain Res *133*, 103–113.

Peters, Y. M., O'Donnell, P., and Carelli, R. M. (2005). Prefrontal cortical cell firing during maintenance, extinction, and reinstatement of goal-directed behavior for natural reward. Synapse *56*, 74–83.

Peters, Y., Barnhardt, N. E., and O'Donnell, P. (2004). Prefrontal cortical up states are synchronized with ventral tegmental area activity. Synapse *52*, 143–152.

Pfurtscheller, G. (2001). Functional brain imaging based on ERD/ERS. Vision Research *41*, 1257–1260.

Phillips, W. A., and Silverstein, S. M. (2003). Convergence of biological and psychological perspectives on cognitive coordination in schizophrenia. Behav Brain Sci *26*, 65–82; discussion 82–137.

Posner, M. I., and Petersen, S. E. (1990). The attention system of the human brain. Annu. Rev. Neurosci. *13*, 25–42.

Pragay, E. B., Mirsky, A. F., and Nakamura, R. K. (1987). Attention-related unit activity in the frontal association cortex during a go/no-go visual discrimination task. Exp. Neurol. *96*, 481–500.

Quilodran, R., Rothé, M., and Procyk, E. (2008). Behavioral shifts and action valuation in the anterior cingulate cortex. Neuron *57*, 314–325.

Quintana, J., and Fuster, J. M. (1992). Mnemonic and predictive functions of cortical neurons in a memory task. Neuroreport *3*, 721–724.

Rainer, G., Asaad, W. F., and Miller, E. K. (1998). Selective representation of relevant information by neurons in the primate prefrontal cortex. Nature *393*, 577–579.

Rainer, G., Rao, S. C., and Miller, E. K. (1999). Prospective coding for objects in primate prefrontal cortex. J. Neurosci. *19*, 5493–5505.

Rao, S. C., Rainer, G., and Miller, E. K. (1997). Integration of what and where in the primate prefrontal cortex. Science *276*, 821–824.

Ress, D., Backus, B. T., and Heeger, D. J. (2000). Activity in primary visual cortex predicts performance in a visual detection task. Nat Neurosci *3*, 940–945.

Reynolds, J. H., and Heeger, D. J. (2009). The Normalization Model of Attention. Neuron *61*, 168–185.

Rodriguez, E., George, N., Lachaux, J. P., Martinerie, J., Renault, B., and Varela, F. J. (1999). Perception's shadow: long-distance synchronization of human brain activity. Nature *397*, 430–433.

Roelfsema, P. R., Engel, A. K., König, P., and Singer, W. (1997). Visuomotor integration is associated with zero time-lag synchronization among cortical areas. Nature *385*, 157–161.

Roelofs, A., van Turennout, M., and Coles, M. G. H. (2006). Anterior cingulate cortex activity can be independent of response conflict in Stroop-like tasks. Proc. Natl. Acad. Sci. U.S.A. *103*, 13884–13889.

Rossi, A. F., Bichot, N. P., Desimone, R., and Ungerleider, L. G. (2007). Top Down Attentional Deficits in Macaques with Lesions of Lateral Prefrontal Cortex. Journal of Neuroscience *27*, 11306–11314.

Rotaru, D. C., Barrionuevo, G., and Sesack, S. R. (2005). Mediodorsal thalamic afferents to layer

III of the rat prefrontal cortex: synaptic relationships to subclasses of interneurons. J. Comp. Neurol. *490*, 220–238.

Ruchsow, M., Grothe, J., Spitzer, M., and Kiefer, M. (2002). Human anterior cingulate cortex is activated by negative feedback: evidence from event-related potentials in a guessing task. Neuroscience Letters *325*, 203–206.

Sakagami, M., and Niki, H. (1994). Encoding of behavioral significance of visual stimuli by primate prefrontal neurons: relation to relevant task conditions. Exp Brain Res *97*, 423–436.

Salinas, E., and Sejnowski, T. J. (2000). CORRELATED NEURONAL ACTIVITY AND THE FLOW OF NEURAL INFORMATION. 1–12.

Santhouse, A. M., Howard, R. J., and ffytche, D. H. (2000). Visual hallucinatory syndromes and the anatomy of the visual brain. Brain *123 (Pt 10)*, 2055–2064.

Sarter, M., Gehring, W. J., and Kozak, R. (2006). More attention must be paid: the neurobiology of attentional effort. Brain Research Reviews *51*, 145–160.

Schoenbaum, G., and Eichenbaum, H. (1995). Information coding in the rodent prefrontal cortex. I. Single-neuron activity in orbitofrontal cortex compared with that in pyriform cortex. Journal of Neurophysiology *74*, 733–750.

Schroeder, C. E., Mehta, A. D., and Foxe, J. J. (2001). Determinants and mechanisms of attentional modulation of neural processing. Front. Biosci. *6*, D672–84.

Schultz, W. (2007). Multiple Dopamine Functions at Different Time Courses. Annu. Rev. Neurosci. *30*, 259–288.

Schultz, W. (1998). Predictive reward signal of dopamine neurons. Journal of Neurophysiology *80*, 1–27.

Seamans, J. K., and Yang, C. R. (2004). The principal features and mechanisms of dopamine modulation in the prefrontal cortex. Progress in Neurobiology *74*, 1–58.

Sesack, S. (2002). Synaptology of dopamine neurons. Handbook of experimental pharmacology.

Sesack, S. R., Carr, D. B., Omelchenko, N., and Pinto, A. (2003). Anatomical substrates for glutamate-dopamine interactions: evidence for specificity of connections and extrasynaptic actions. Annals of the New York Academy of Sciences *1003*, 36–52.

Shidara, M., and Richmond, B. J. (2002). Anterior cingulate: single neuronal signals related to degree of reward expectancy. Science *296*, 1709–1711.

Siapas, A. G., Lubenov, E. V., and Wilson, M. A. (2005). Prefrontal Phase Locking to Hippocampal Theta Oscillations. Neuron *46*, 141–151.

Siegel, M., Donner, T. H., Oostenveld, R., Fries, P., and Engel, A. K. (2008). Neuronal

Synchronization along the Dorsal Visual Pathway Reflects the Focus of Spatial Attention. Neuron *60*, 709–719.

Siegel, M., Engel, A. K., and Donner, T. H. (2011). Cortical network dynamics of perceptual decision-making in the human brain. Front. Hum. Neurosci. *5*, 21.

Siegel, M., Warden, M. R., and Miller, E. K. (2009). Phase-dependent neuronal coding of objects in short-term memory. Proceedings of the National Academy of Sciences *106*, 21341–21346.

Singer, W. (2009). Distributed processing and temporal codes in neuronal networks. Cogn Neurodyn *3*, 189–196.

Sirota, A., Montgomery, S., Fujisawa, S., Isomura, Y., Zugaro, M., and Buzsáki, G. (2008). Entrainment of Neocortical Neurons and Gamma Oscillations by the Hippocampal Theta Rhythm. Neuron *60*, 683–697.

Steffensen, S. C., Svingos, A. L., Pickel, V. M., and Henriksen, S. J. (1998). Electrophysiological characterization of GABAergic neurons in the ventral tegmental area. J. Neurosci. *18*, 8003–8015.

Stein, von, A., Chiang, C., and König, P. (2000). Top-down processing mediated by interareal synchronization. Proc. Natl. Acad. Sci. U.S.A. *97*, 14748–14753.

Stokes, M., Thompson, R., Nobre, A. C., and Duncan, J. (2009). Shape-specific preparatory activity mediates attention to targets in human visual cortex. Proceedings of the National Academy of Sciences *106*, 19569–19574.

Summerfield, C., Egner, T., Greene, M., Koechlin, E., Mangels, J., and Hirsch, J. (2006). Predictive Codes for Forthcoming Perception in the Frontal Cortex. Science *314*, 1311–1314.

Swanson, J., Baler, R. D., and Volkow, N. D. (2010). Understanding the Effects of Stimulant Medications on Cognition in Individuals with Attention-Deficit Hyperactivity Disorder: A Decade of Progress. Neuropsychopharmacology *36*, 207–226.

Sylvester, C. M., Shulman, G. L., Jack, A. I., and Corbetta, M. (2009). Anticipatory and Stimulus-Evoked Blood Oxygenation Level-Dependent Modulations Related to Spatial Attention Reflect a Common Additive Signal. J. Neurosci. *29*, 10671–10682.

Takahata, R., and Moghaddam, B. (1998). Glutamatergic regulation of basal and stimulus-activated dopamine release in the prefrontal cortex. J. Neurochem. *71*, 1443–1449.

Takenouchi, K., Nishijo, H., Uwano, T., Tamura, R., Takigawa, M., and Ono, T. (1999). Emotional and behavioral correlates of the anterior cingulate cortex during associative learning in rats. Neuroscience *93*, 1271–1287.

Tierney, P. L., Thierry, A. M., Glowinski, J., Deniau, J. M., and Gioanni, Y. (2008). Dopamine Modulates Temporal Dynamics of Feedforward Inhibition in Rat Prefrontal Cortex In Vivo.

Cerebral Cortex *18*, 2251–2262.

Tiesinga, P., Fellous, J.-M., and Sejnowski, T. J. (2008). Regulation of spike timing in visual cortical circuits. Nat Rev Neurosci *9*, 97–107.

Totah, N. K. B., Kim, Y. B., Homayoun, H., and Moghaddam, B. (2009). Anterior cingulate neurons represent errors and preparatory attention within the same behavioral sequence. J. Neurosci. *29*, 6418–6426.

Uhlhaas, P. J., and Singer, W. (2010). Abnormal neural oscillations and synchrony in schizophrenia. Nat Rev Neurosci *11*, 100–113.

Uylings, H. B. M., Groenewegen, H. J., and Kolb, B. (2003). Do rats have a prefrontal cortex? Behavioural Brain Research *146*, 3–17.

Varela, F., Lachaux, J. P., Rodriguez, E., and Martinerie, J. (2001). The brainweb: phase synchronization and large-scale integration. Nat Rev Neurosci *2*, 229–239.

Wallis, J. D., and Miller, E. K. (2003). Neuronal activity in primate dorsolateral and orbital prefrontal cortex during performance of a reward preference task. European Journal of Neuroscience *18*, 2069–2081.

Wang, L., Zhu, C., He, Y., Zang, Y., Cao, Q., Zhang, H., Zhong, Q., and Wang, Y. (2009). Altered small-world brain functional networks in children with attention-deficit/hyperactivity disorder. Hum. Brain Mapp. *30*, 638–649.

Weissman, D. H., Gopalakrishnan, A., Hazlett, C. J., and Woldorff, M. G. (2005). Dorsal anterior cingulate cortex resolves conflict from distracting stimuli by boosting attention toward relevant events. Cereb. Cortex *15*, 229–237.

Whittington, M. A., Traub, R. D., Kopell, N., Ermentrout, B., and Buhl, E. H. (2000). Inhibition-based rhythms: experimental and mathematical observations on network dynamics. Int J Psychophysiol *38*, 315–336.

Williams, G. V., and Goldman-Rakic, P. S. (1995). Modulation of memory fields by dopamine D1 receptors in prefrontal cortex. Nature *376*, 572–575.

Woldorff, M. G., Hazlett, C. J., Fichtenholtz, H. M., Weissman, D. H., Dale, A. M., and Song, A. W. (2004). Functional parcellation of attentional control regions of the brain. J Cogn Neurosci *16*, 149–165.

Womelsdorf, T., Schoffelen, J. M., Oostenveld, R., Singer, W., Desimone, R., Engel, A. K., and Fries, P. (2007). Modulation of Neuronal Interactions Through Neuronal Synchronization. Science *316*, 1609–1612.

Woods, D. L., and Knight, R. T. (1986). Electrophysiologic evidence of increased distractibility after dorsolateral prefrontal lesions. Neurology *36*, 212–216.

Zanto, T. P., and Gazzaley, A. (2009). Neural Suppression of Irrelevant Information Underlies Optimal Working Memory Performance. J. Neurosci. *29*, 3059–3066.

Zanto, T. P., Rubens, M. T., Thangavel, A., and Gazzaley, A. (2011). Causal role of the prefrontal cortex in top-down modulation of visual processing and working memory. Nature Publishing Group *14*, 656–661.

Zheng, P., Zhang, X. X., Bunney, B. S., and Shi, W. X. (1999). Opposite modulation of cortical N-methyl-D-aspartate receptor-mediated responses by low and high concentrations of dopamine. Neuroscience *91*, 527–535.